SunStone
29-4-2025

Investigating structures at the local scale via X-ray Absorption Spectroscopy

E. Fonda

Synchrotron SOLEIL

What are we talking about today?

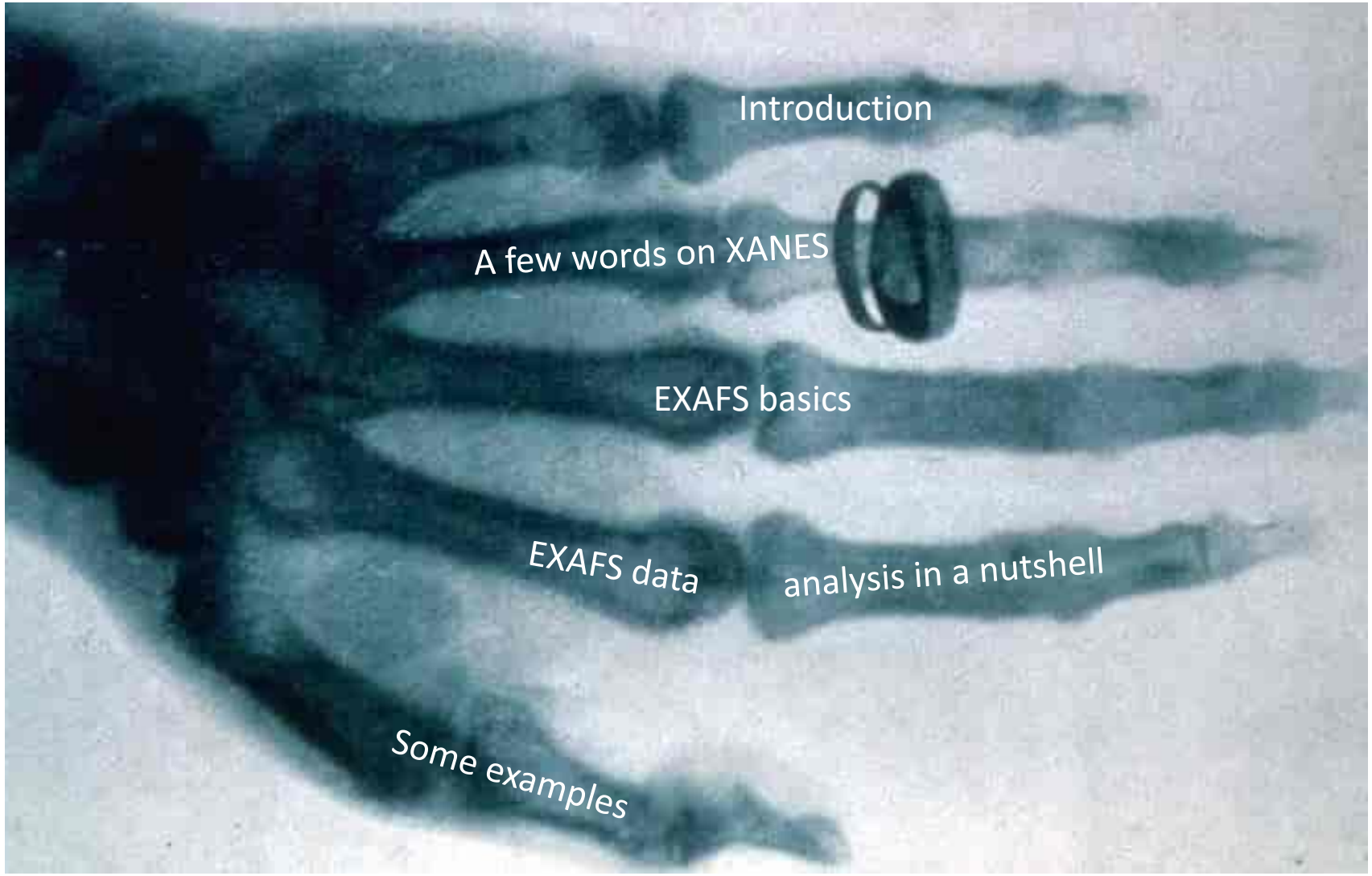

X-rays absorption

$$K_{\max} = h\left(\nu - \nu_o\right).$$

A. Einstein "On a Heuristic Viewpoint Concerning the Production and Transformation of Light" Annalen der Physik (1905)

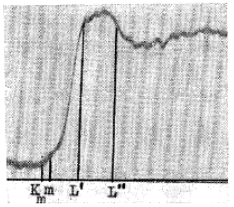

Fig. 6.

Titanium.

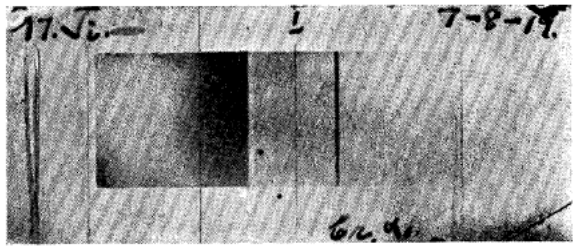

Fig. 10.

Titanium.

HUGO FRICKE

PHYSICAL REVIEW, VOL. XVI., SECOND SERIES.
September, 1920.

My EXAFS Family Tree.

Röntgen (1895)	Discovered X-rays
Maurice de Broglie (1913)	Measured first absorption edge
World War I (1914–1918)	
Fricke (1920)	Observed first fine structure
Kossel (1920)	First theory of XANES
Hanawalt (1931)	EXAFS in gases, temperature effect
Kronig (1931)	First theory of EXAFS
Cauchois (1932)	Curved crystal transmission spectrograph
Hayasi (1936, 1949)	Theory of EXAFS
World War II (1941–1945)	
Sawada (1955)	Amorphous/crystalline polymorphs
Shiraiwa (1958)	Improved theory
Kostarev (1939, 1946)	Theory and measured EXAFS in single crystals
Kozlenkov (1960)	Improved theory
Van Nordstrand (1960)	Instrumentation, fingerprint ID, used XAS to characterize catalysts
Lytle (14 July 1960)	Starts work at Boeing (BSRL)
Krogstad (1960)	Personal communication
Lytle (1962)	Particle-in-a-box model
Prins (1964)	Helped name EXAFS
Parratt (1965)	Personal communication; *Rev. Mod. Phys.* (1959). **31**, 616
Sayers, Stern, Lytle (1968–1971)	Modern theory, Fourier transform of EXAFS
Sayers, Stern, Lytle (1974)	First trip to synchrotron (SSRL)

Lytle, F. (1999). Journal of Synchrotron Radiation **6**(3): 123-134.

X-rays absorption spectroscopy

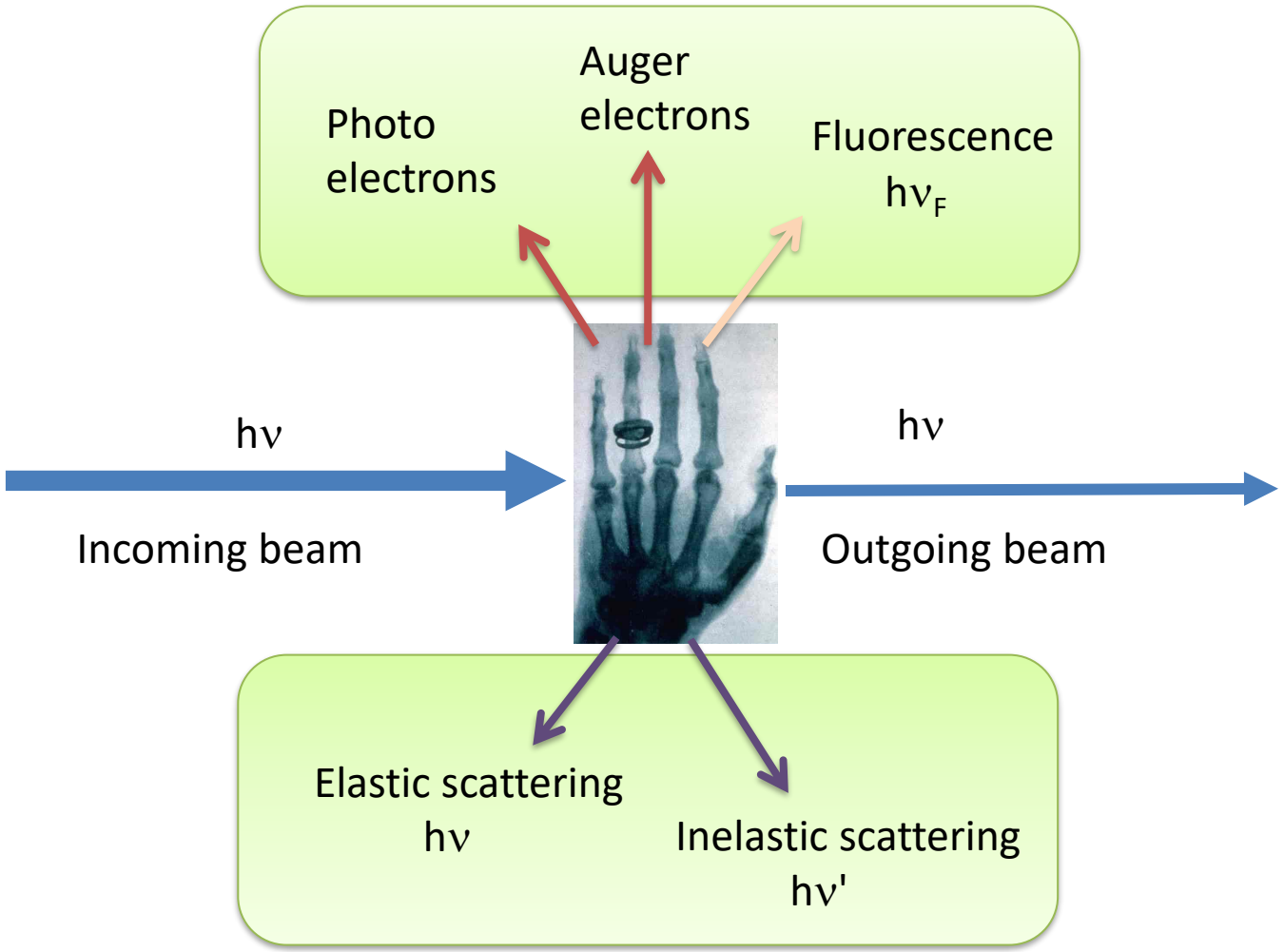

Lambert-Beer :

$$\frac{dI}{I} = -\mu dx$$

$$I = I_0 \exp(-\mu x)$$

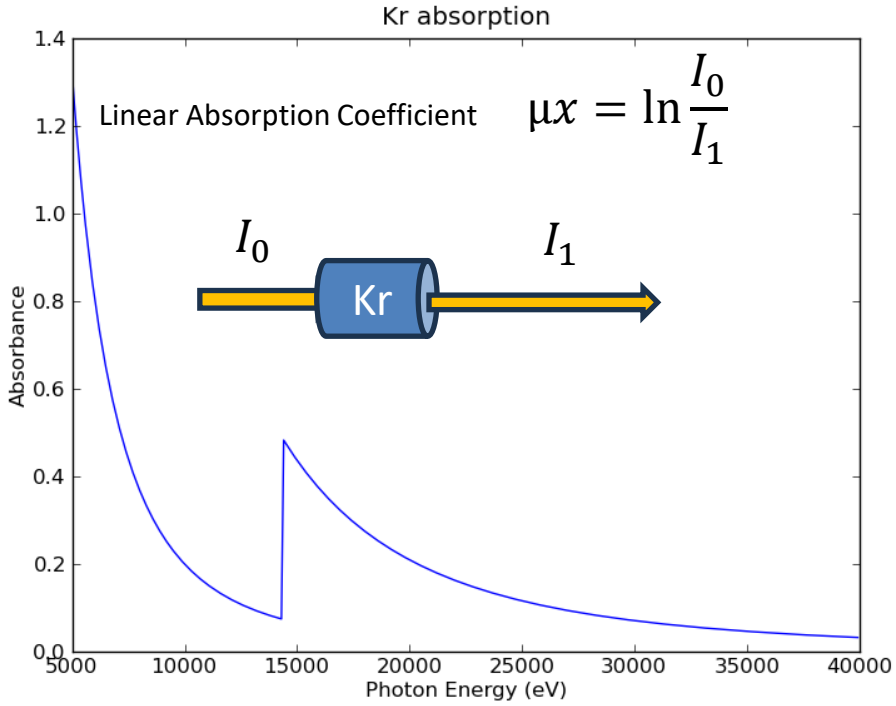

$$\mu \simeq \frac{\rho Z^4}{AE^3}$$

A = atomic mass
Z= atomic number
E = Energy
ρ = mass density

Hard X-rays energies are in the range of core electrons excitations

Electric dipole approximation

Selection rules

$$\Delta\ell = \pm 1 \qquad \Delta s = 0$$

$$\Delta j = 0,\pm 1, \qquad \Delta m = 0,\pm 1$$

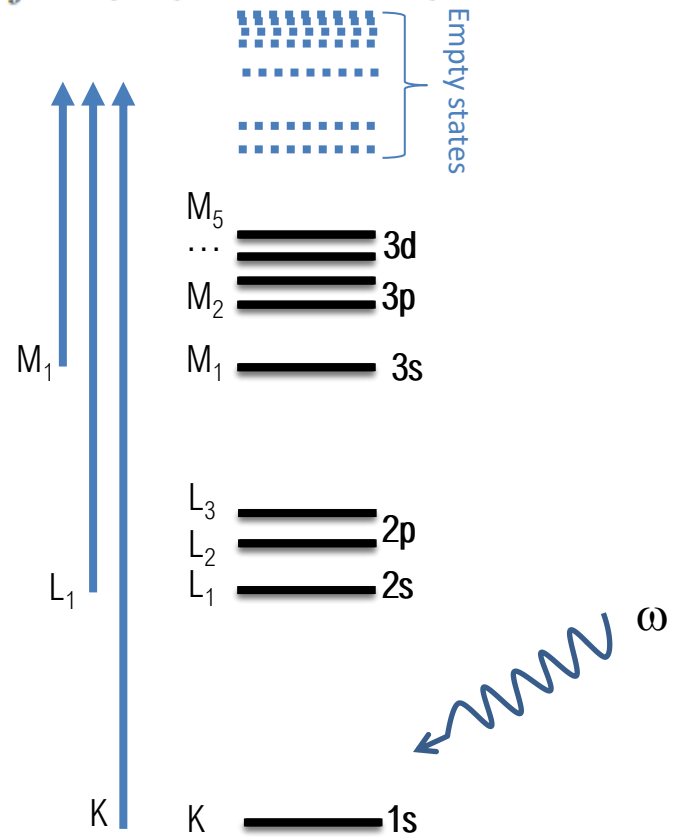

$$\mu(\omega) = \frac{Ne^2\omega\pi}{\hbar c\varepsilon_0}\sum_f \left|\langle f|\vec{\varepsilon}\,\vec{r}|i\rangle\right|^2 \delta(\omega-\omega_0)$$

Each « edge » is identified by n,l,j (e.g. n=2 l=1 j=1-½ gives $2p_{½}$ or L_2)

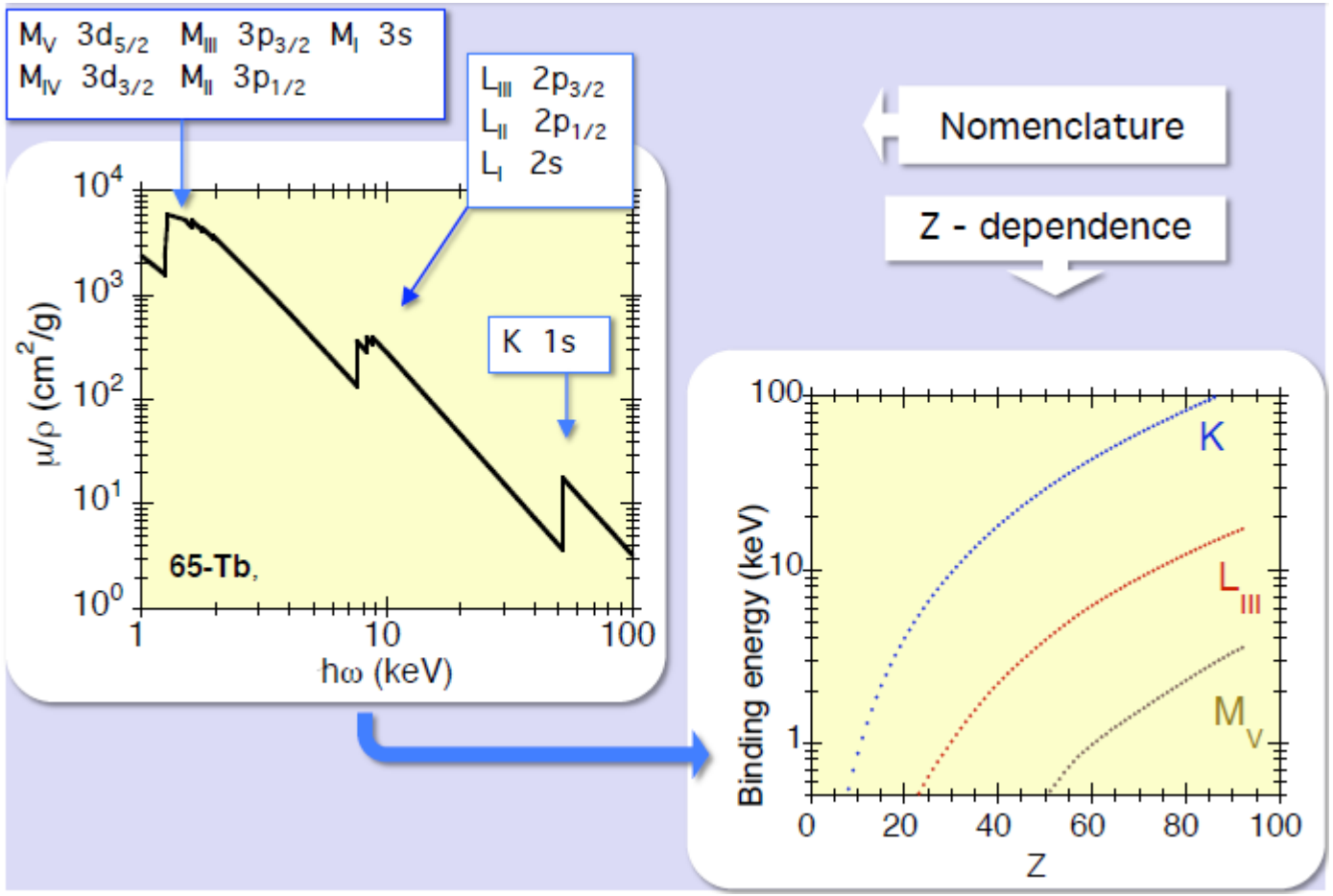

In hard X-ray region edges of one element and of different elements are far apart, i.e. much more than 100eV

➔ strong chemical selectivity

How to practically measure absorption ?

Lambert-Beer : $\frac{dI}{I} = -\mu dx$ $\mu x = \ln\left(\frac{I_0}{I_1}\right)$

$I = I_0 \exp(-\mu x)$

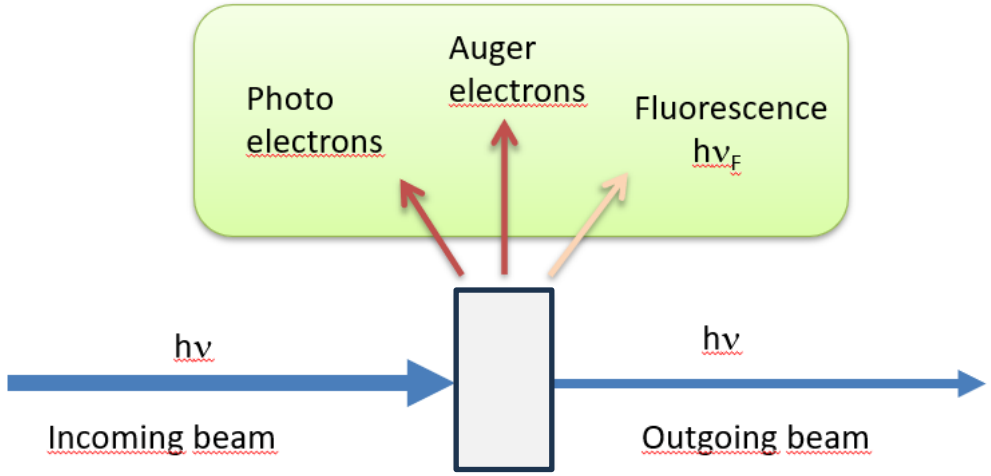

Polychromatic X-ray source

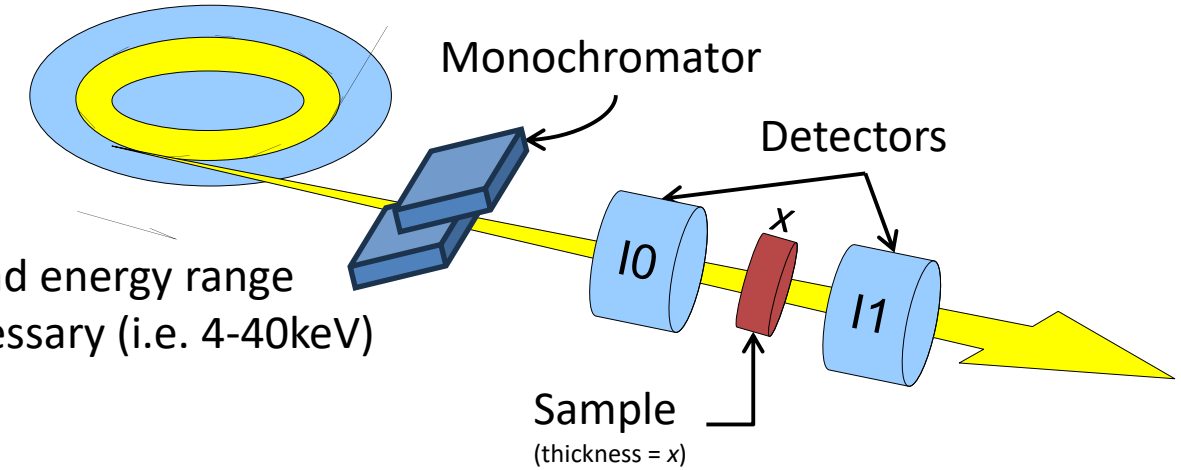

Broad energy range necessary (i.e. 4-40keV)

Characteristic X-ray emission:

De-excitation processes

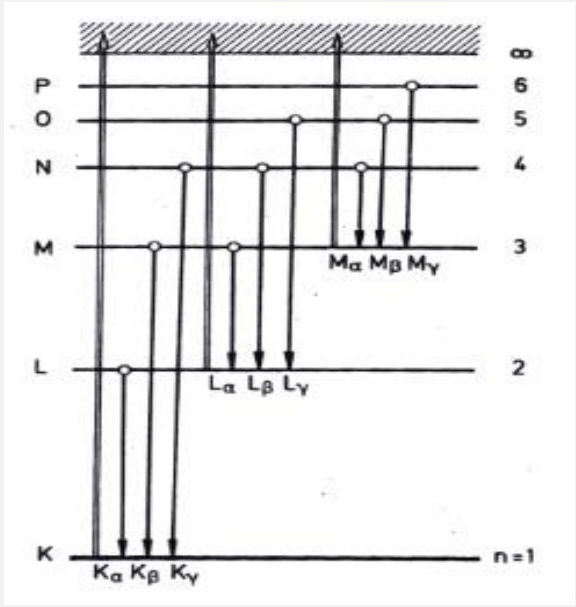

Sample emits fluorescence or electrons proportionally to absorption

➔ indirect measurement of μ is possible.

XAFS: X-ray Absorption Fine Structure

We create a photelectron: $E_p = h\nu - E_0$

Electron Mean Free Path λ(E)

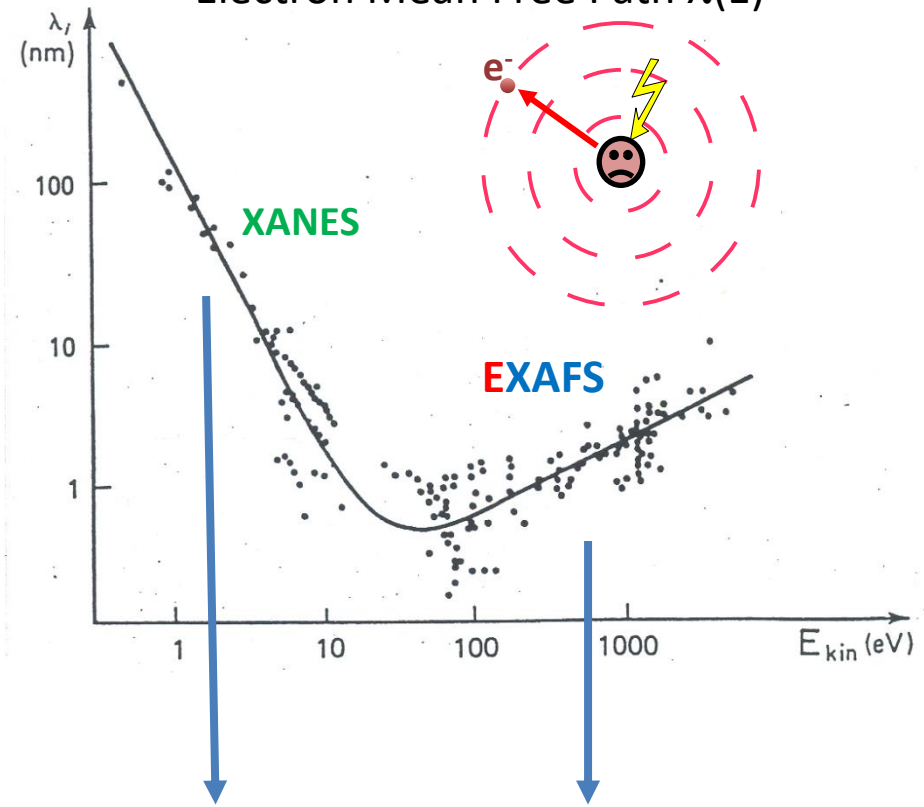

No analytical formula
Direct and complex calculations

Series expansion
analytical formulation

XANES
X-ray Absorption Near Edge Structure

μ : linear absorption coefficient
χ : EXAFS signal

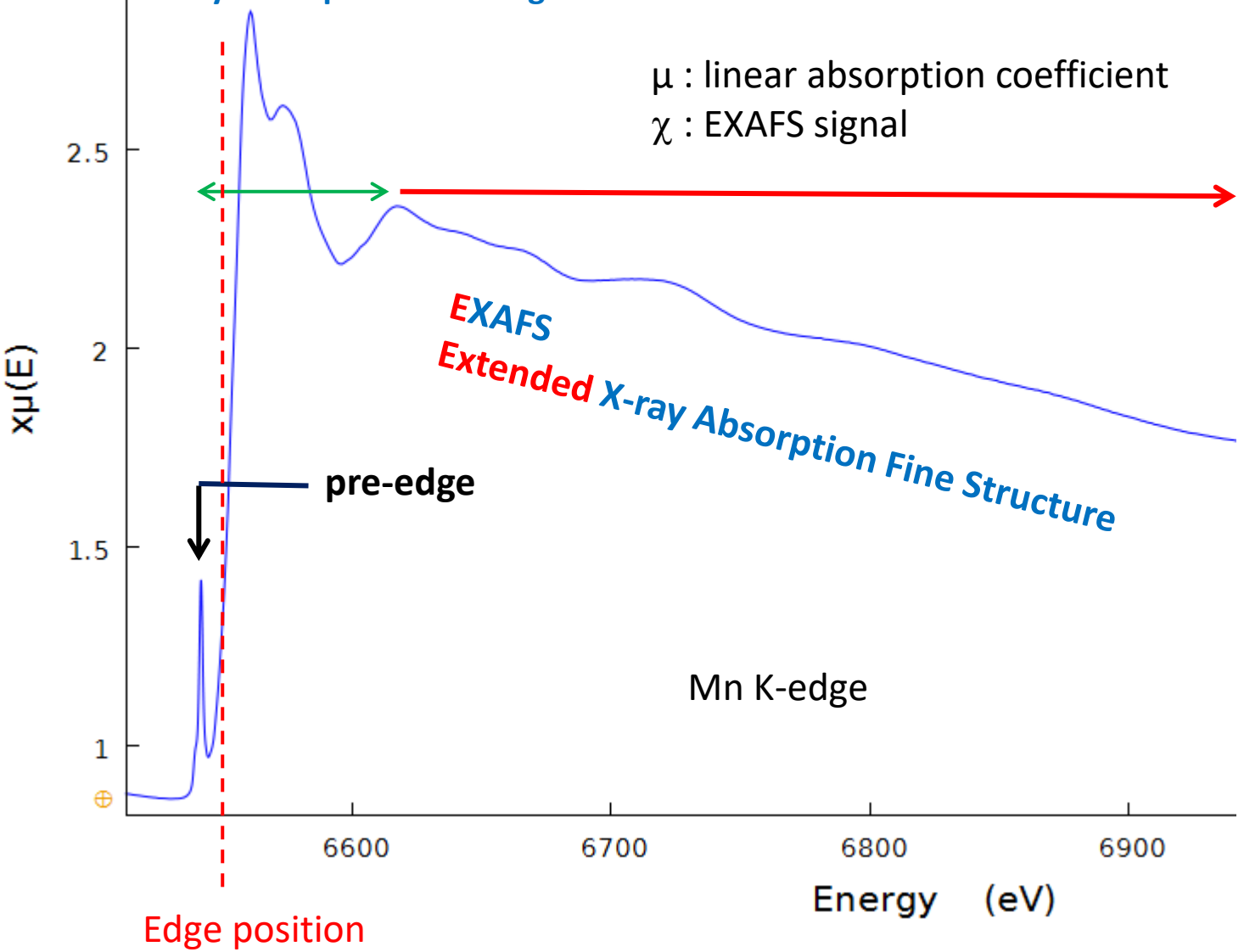

XAFS: X-ray Absorption Fine Structure

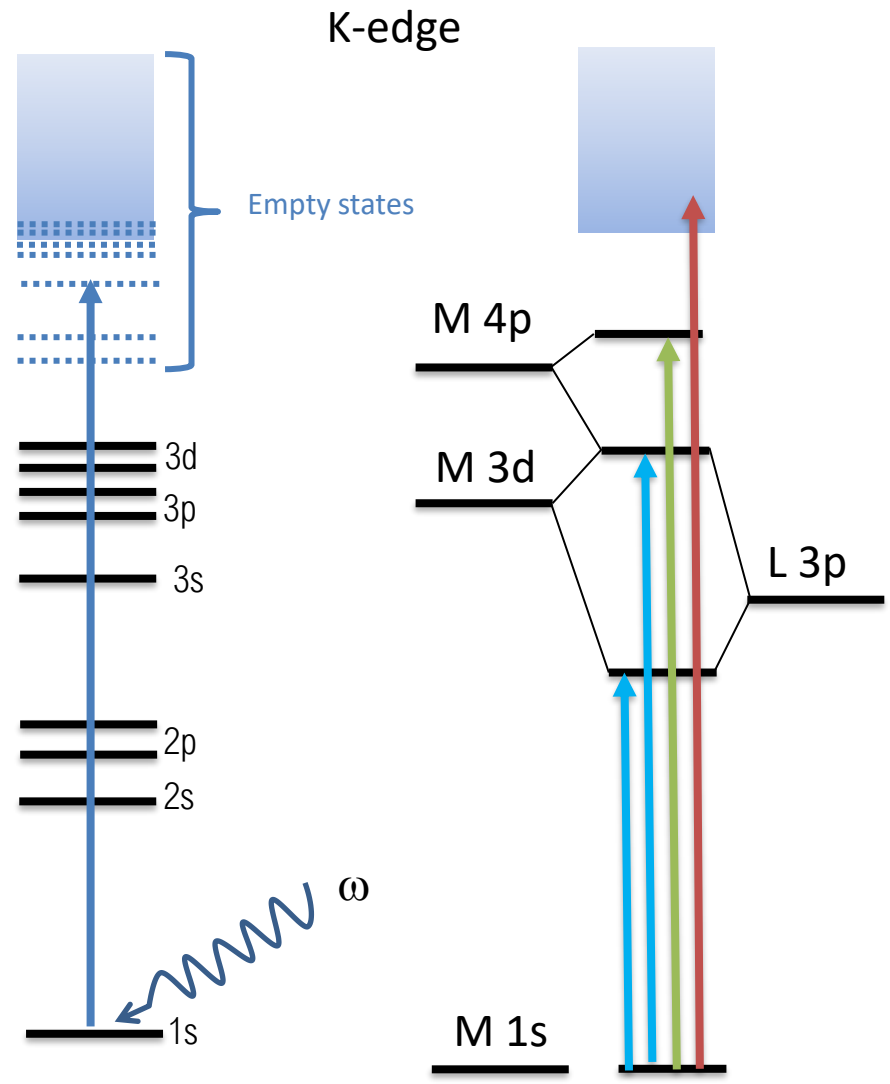

X-ray Absorption Near Edge Structure

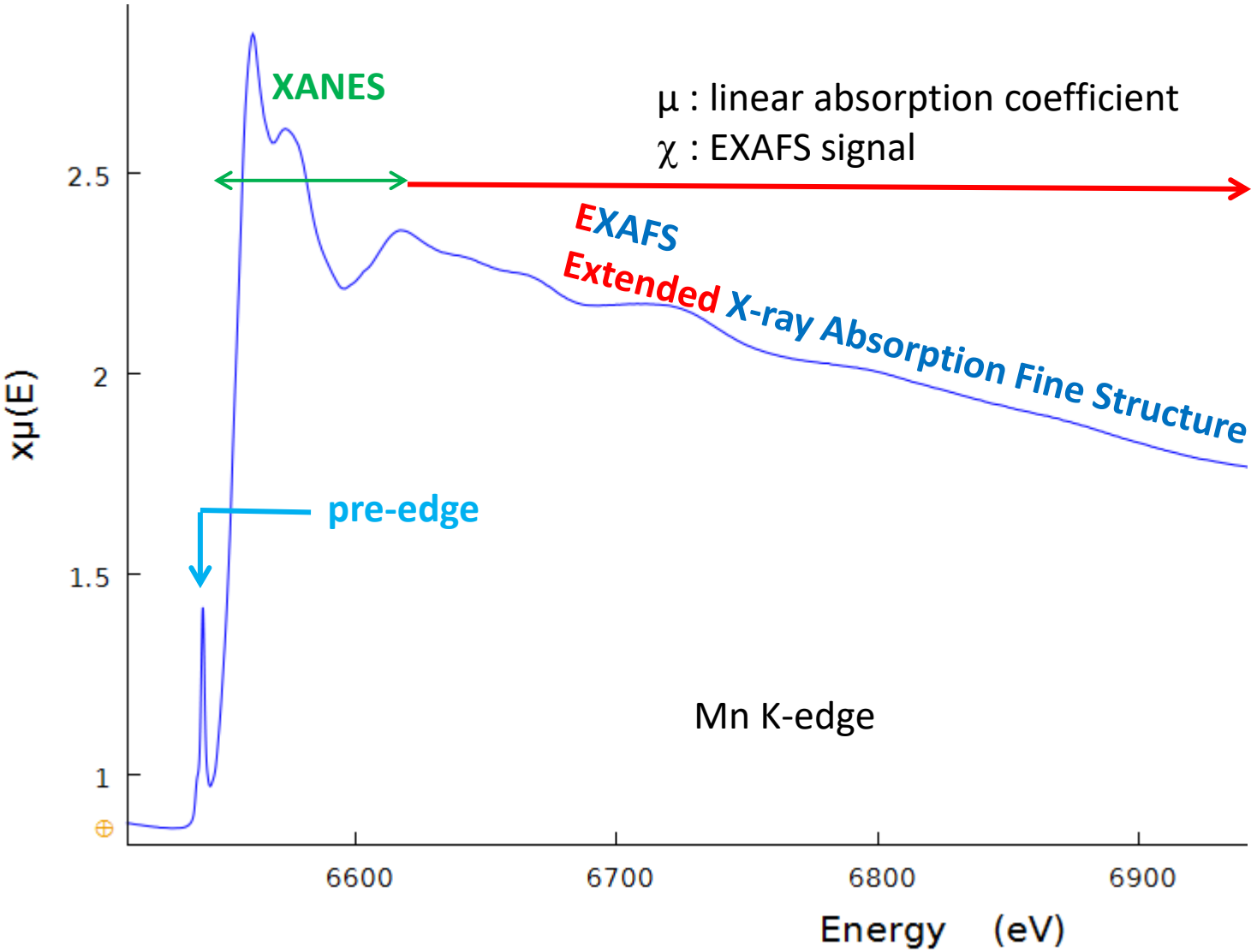

Transitions in pre edge have several origins. Dipole allowed (a1) are stronger.
The pd ligand/absorber hybridization modulates the character of final states => geometry impacts intensity

XANES pre edge and coordination geometry

Ti K edge: only coordination changes

1s→4p + 3pd hybridization, d are more localized →sharp pre edge
Geometrical information can be obtained via p/d mixing

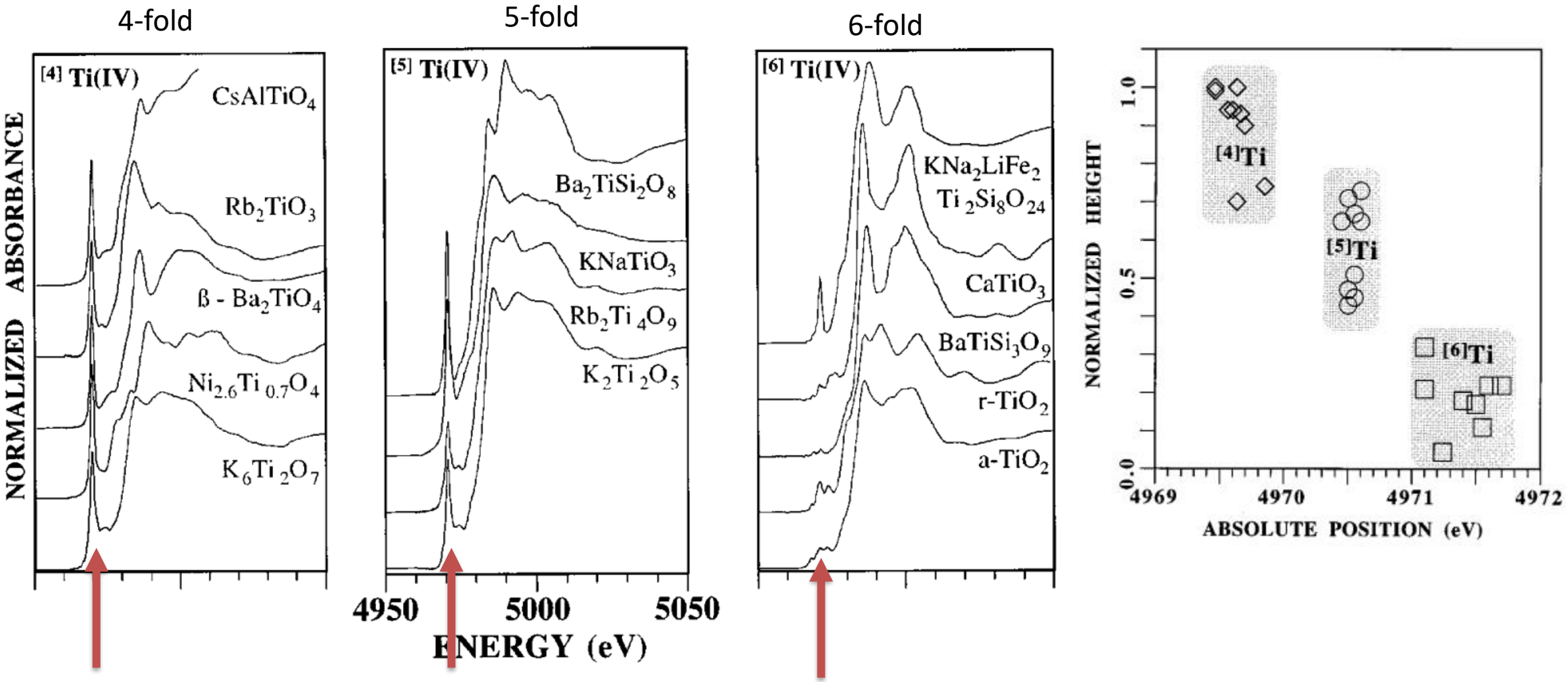

Farges, F., G. E. Brown and J. J. Rehr (1997). Physical Review B **56**(4): 1809-1819.

XANES pre edge: Fe K coordination AND valence

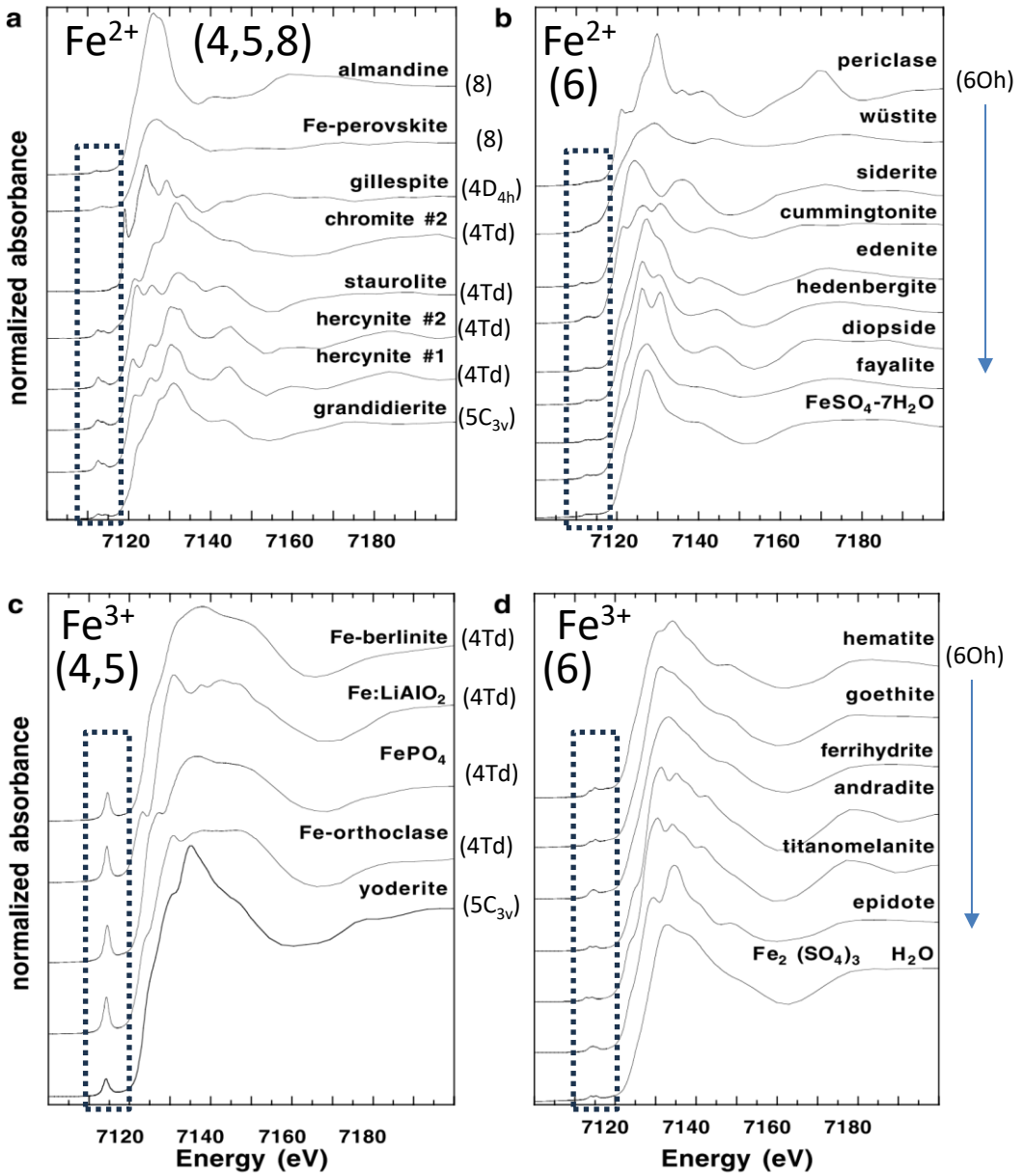

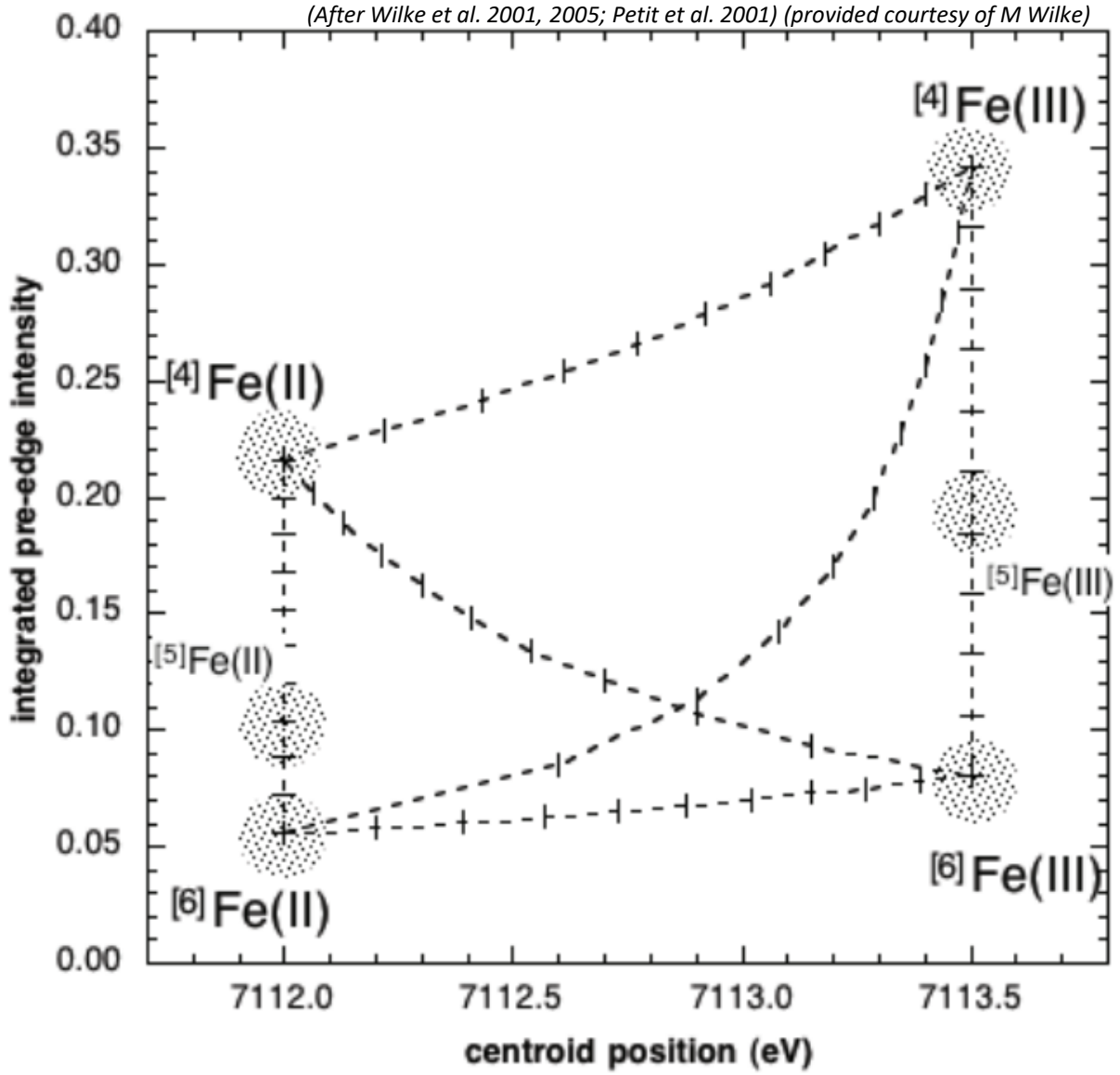

Figure 2 and 6 from Wilke, M., F. Farges, P.-E. Petit, G. E. Brown and F. Martin (2001). American Mineralogist **86**(5-6): 714-730

XANES and oxidation state

K edge: 1s→*n* p

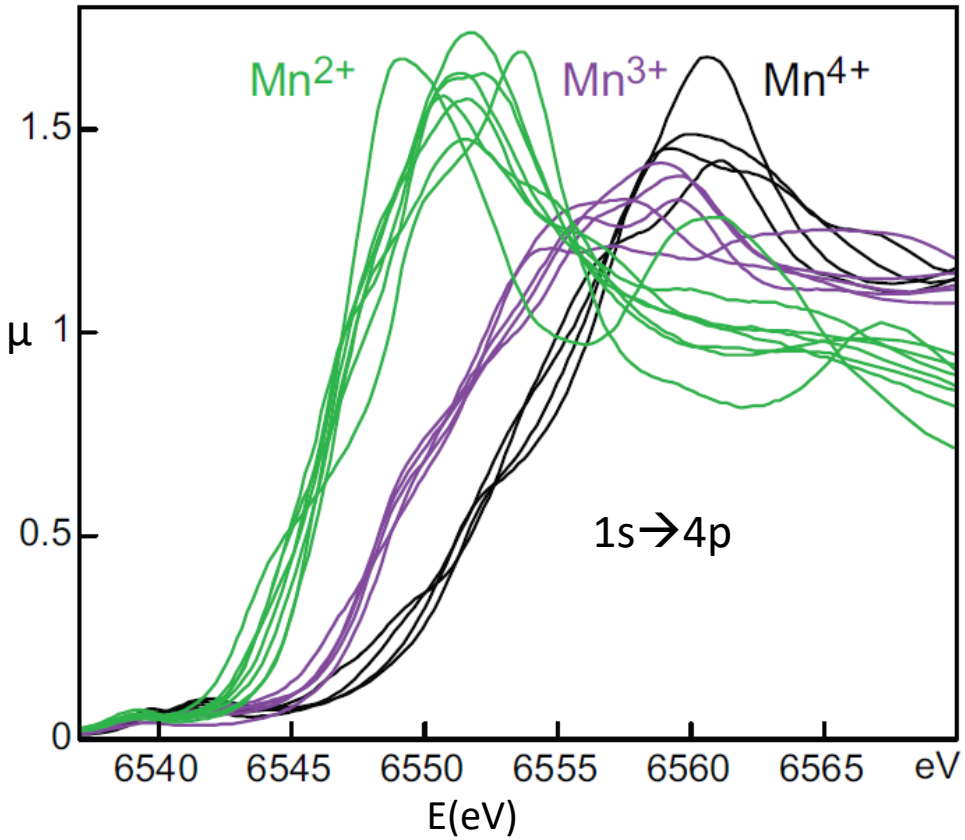

Edge position sensitive to oxidation state

Manceau, A., M. A. Marcus and S. Grangeon (2012) Am. Mineralogist 97

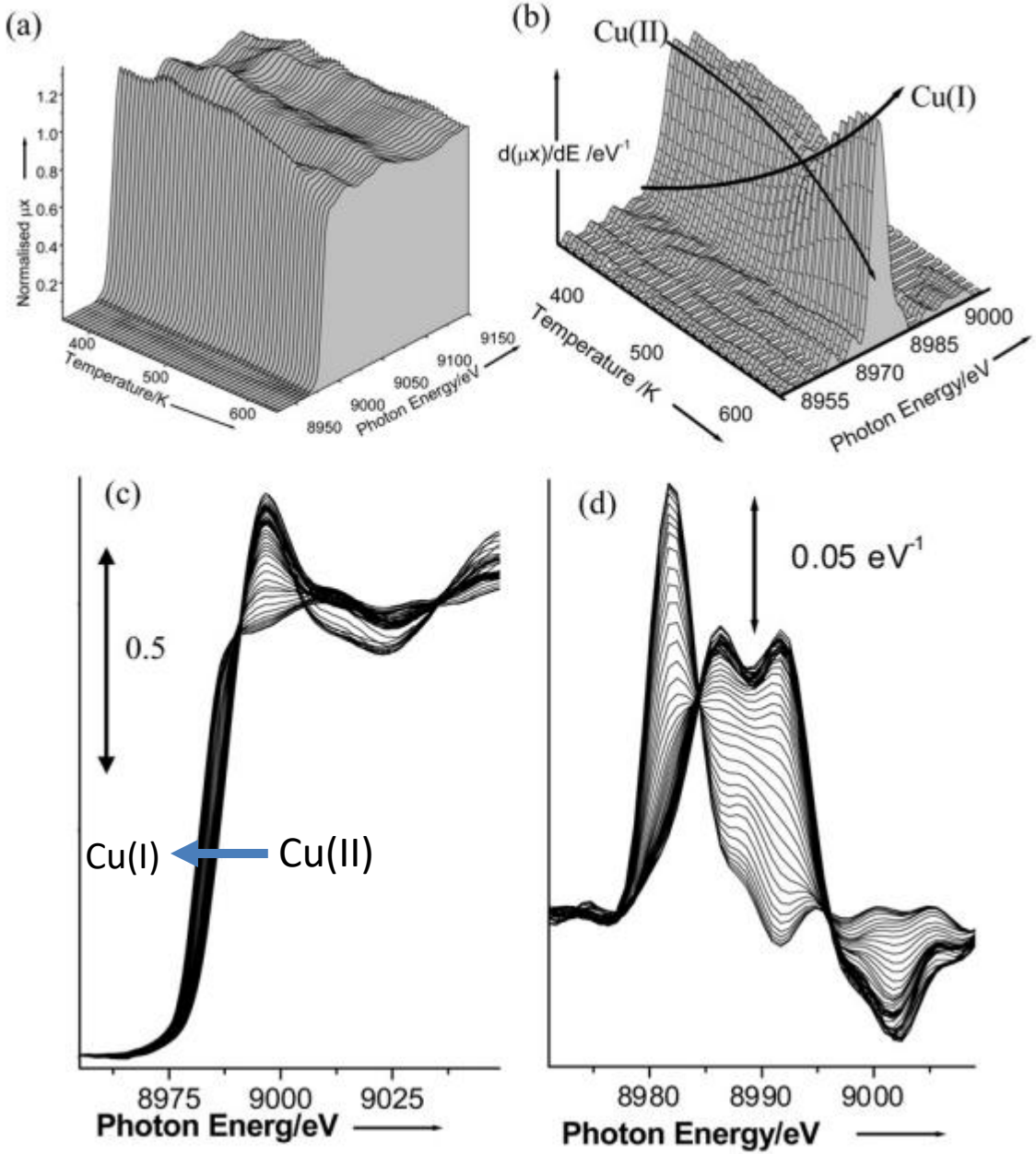

Lamberti, C., S. Bordiga, F. Bonino, C. Prestipino, G. Berlier, L. Capello, F. D'Acapito, F. X. Llabrés i Xamena and A. Zecchina (2003Phys. Chem. Chem. Phys. **5**(20): 4502-4509.

XANES and oxidation state: life is not always that easy

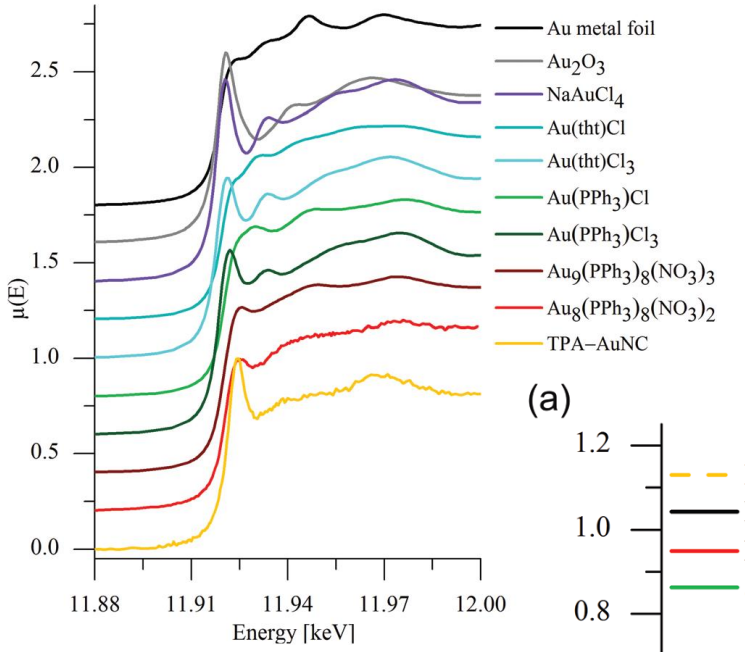

L_3 edge: p→d. Bound and continuum transitions overlap.

No evident correlation of position and oxidation state → ■

Fit to disentangle 2p→5d and 2p→continuum → ■

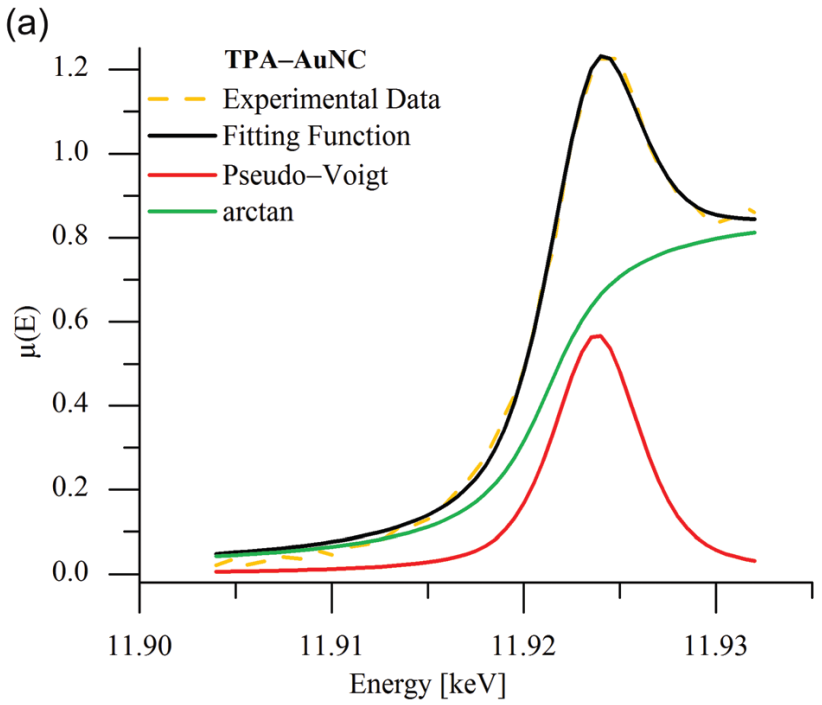

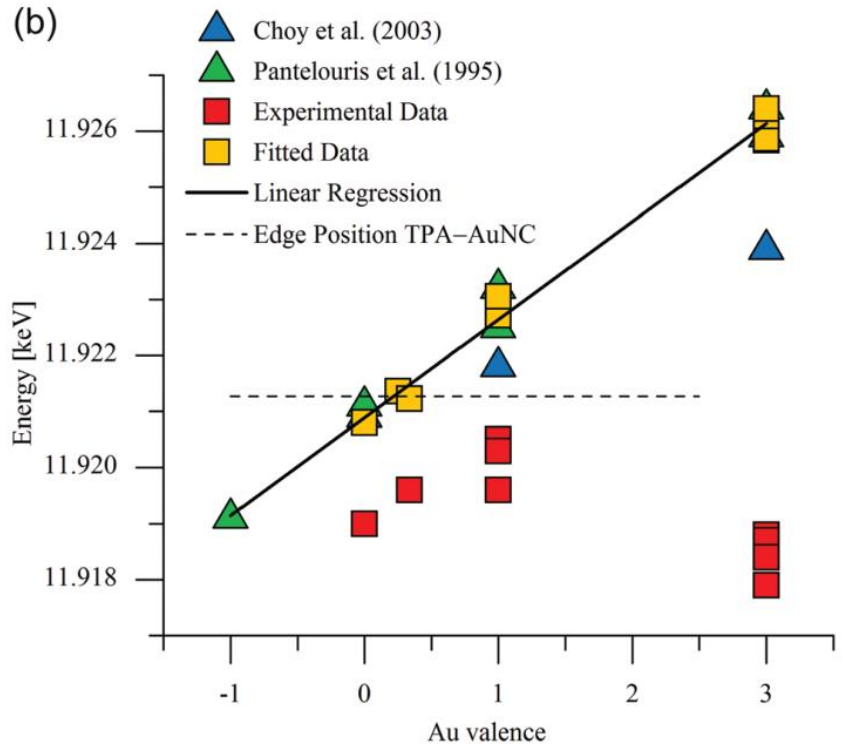

Helmbrecht, C., D. Lutzenkirchen-Hecht and W. Frank (2015). Nanoscale **7**(11): 4978-4983.

XANES take away messages

Information provided by XANES and advantages

- Strong signal = easy to measure

- Information available (minimum):
  - Geometry
  - Oxidation state

Disadvantages

- Geometry AND oxidation state information are often entangled
- There is not a universal method to obtain the information
- Theory is complex and different approaches tackle different problems

Perspectives

- A good playground for machine learning?

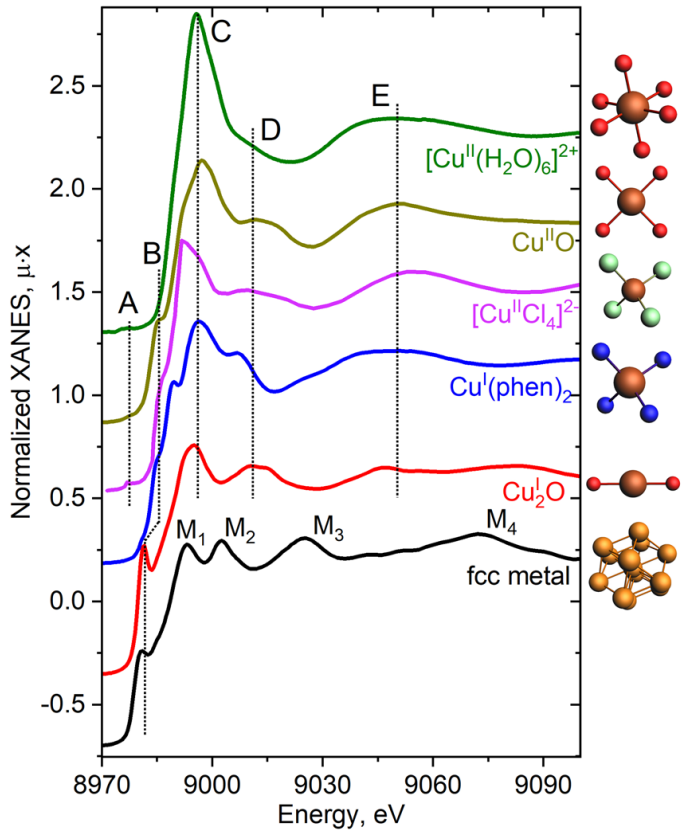

Guda et al. (2021). "Understanding X-ray absorption spectra by means of descriptors and machine learning algorithms." npj Computational Materials **7**(1).

EXAFS: Extended X-ray Absorption Fine Structure

Electron Mean Free Path λ(E)

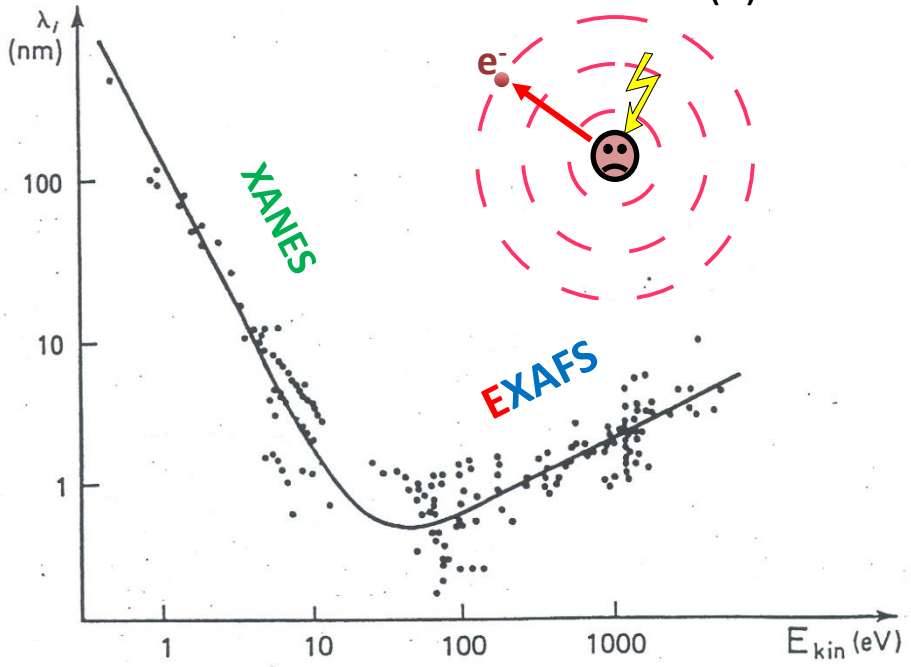

XANES
X-ray Absorption Near Edge Structure

μ : linear absorption coefficient
χ : EXAFS signal

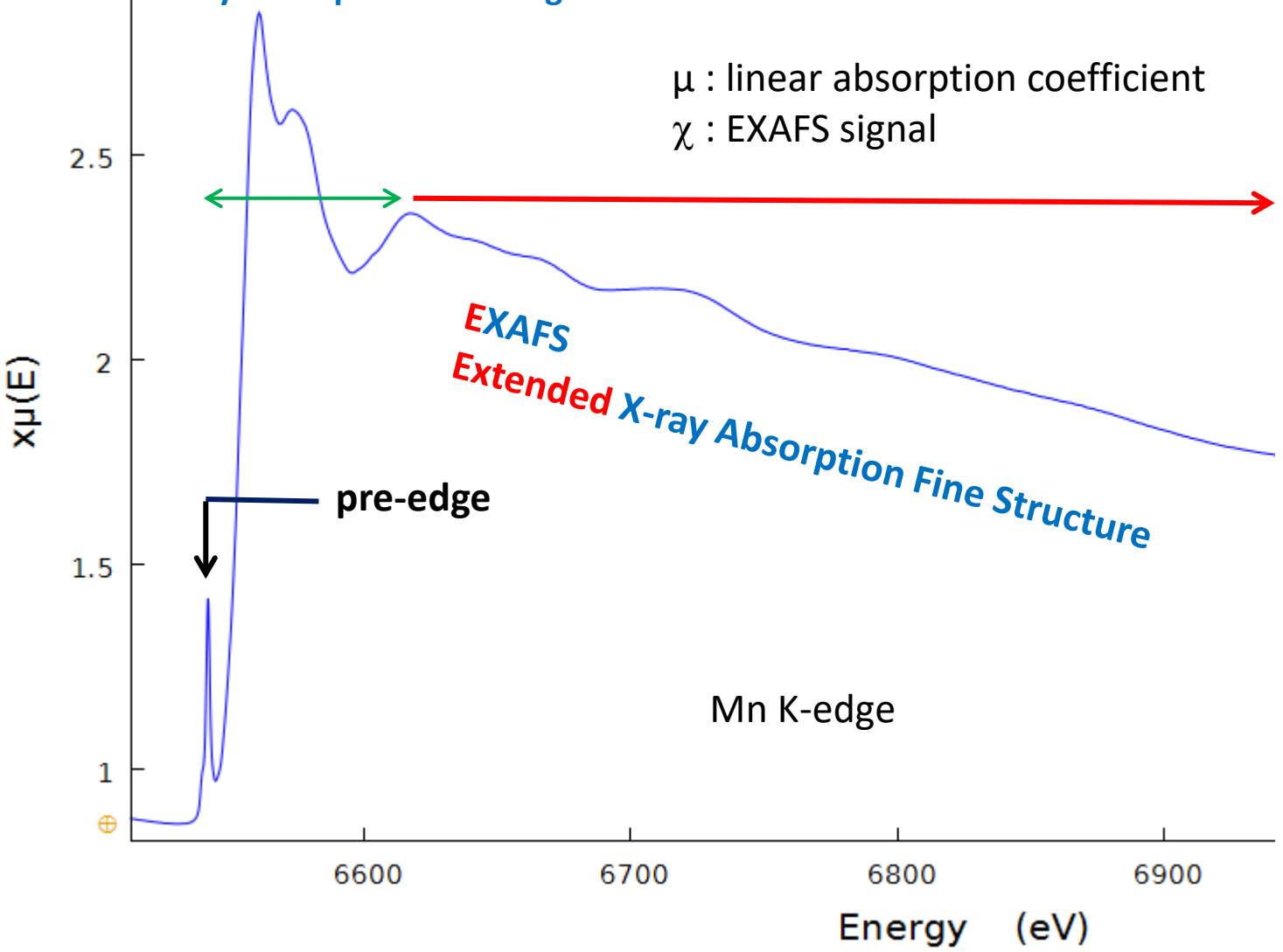

EXAFS explained in a single figure

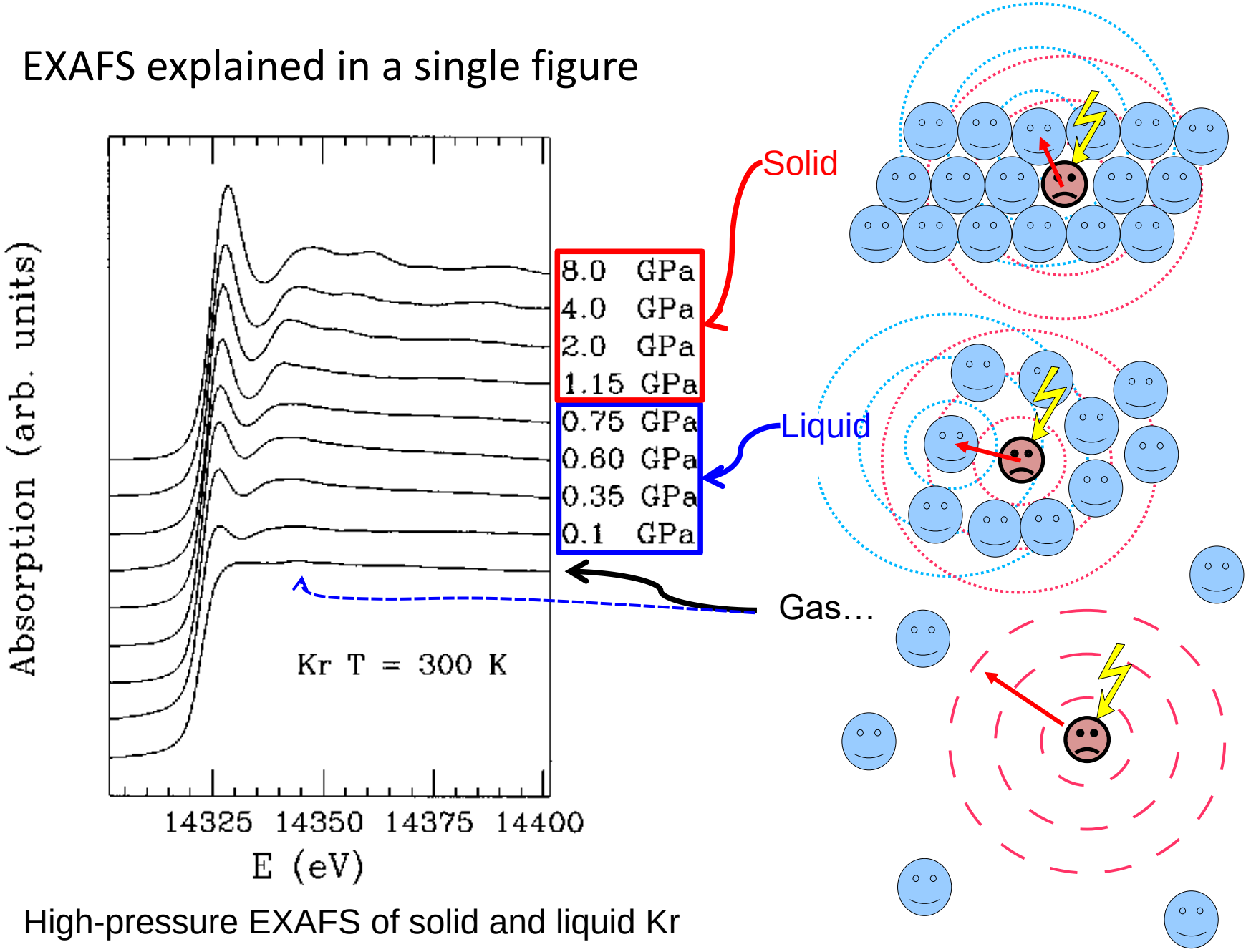

High-pressure EXAFS of solid and liquid Kr

A. Di Cicco, A. Filipponi, J. P. Itié and A. Polian, Phys. Rev. B 54 (1996) 9086-9098

Excitation

Propagation

Back scattering

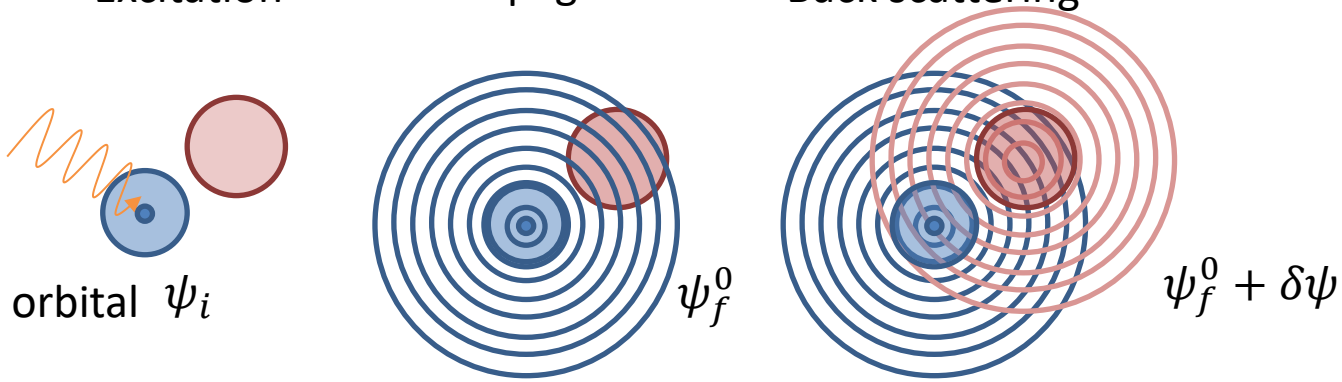

Core orbital ψ_i

ψ_f^0

$\psi_f^0 + \delta\psi$

Photoelectron wavenumber:

$$|\vec{k}| = \frac{2\pi}{\lambda} = \sqrt{\frac{m}{\hbar^2}(E - E_0)}$$

$$\mu(\omega) \propto \left|\langle \psi_f^0 + \delta\psi | \hat{\eta} \cdot \vec{r} | \psi_i \rangle\right|^2$$

Projection over core orbital

As the wave travels, it's shifted by absorber, scatterer and again absorber potentials.

It's backscattered (angle= π) with effective amplitude *f*

$$\boldsymbol{\delta\psi_f} \propto \psi_f^0 i \frac{1}{2k} e^{i\delta} \frac{e^{ikR}}{R} f(k,\pi) \frac{e^{ikR}}{R} e^{i\delta}$$

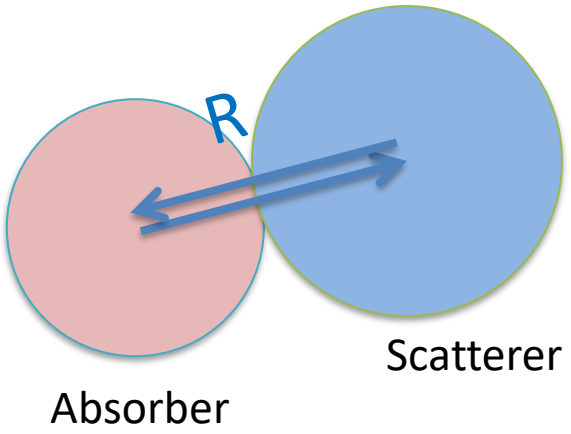

EXAFS equation

$$\chi(k) = 3\left|\hat{\eta}\cdot\hat{R}\right|^2 \frac{1}{kR^2}\left|f(k,\pi)\right|\sin(2Rk+\Phi(k))$$

Polarization

Simplifies to 1 in the following if anysotropy can be neglected

Spherical wave

$\chi(k)$ oscillates with Frequency = 2 R

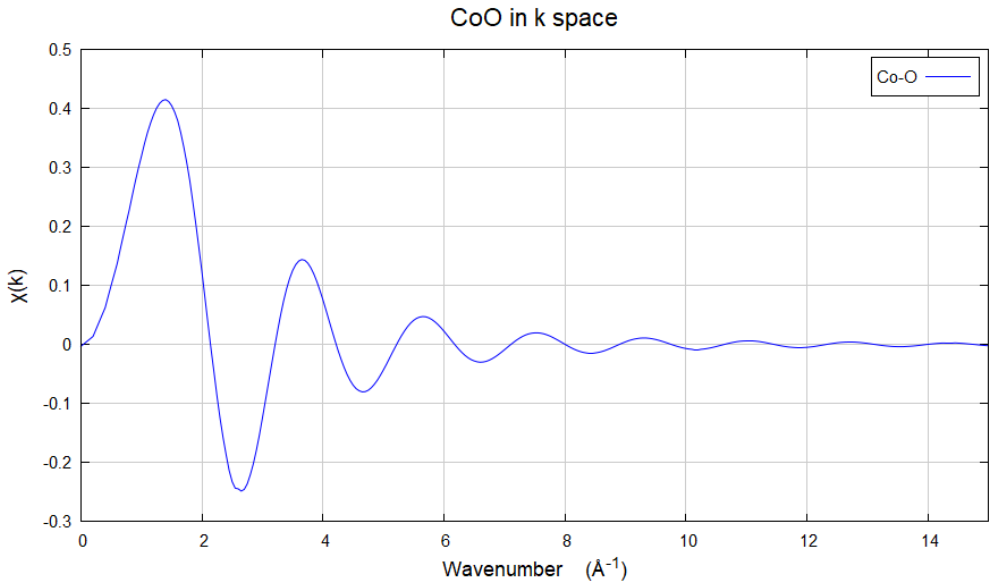

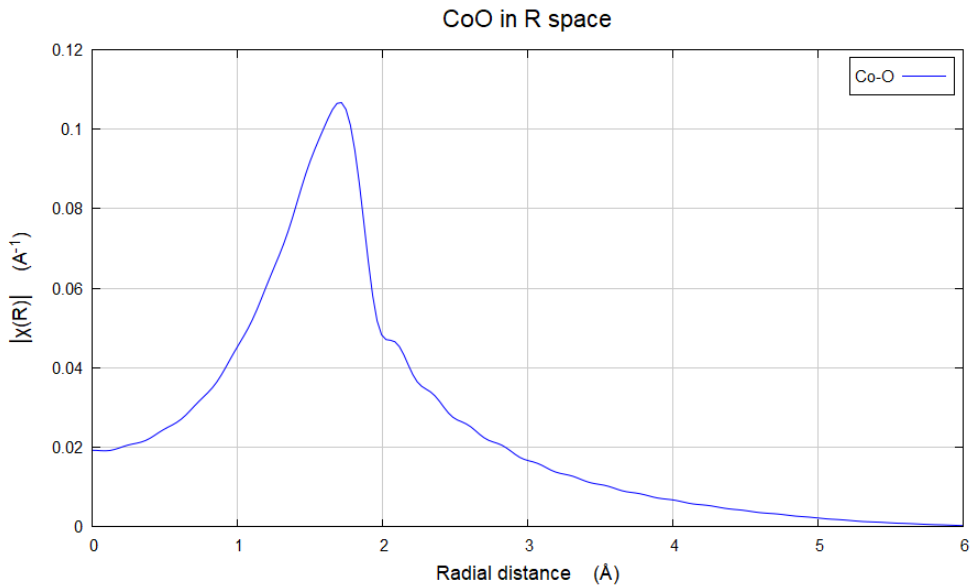

$$k\chi(k) = \frac{1}{kR^2}\,|f(k,\pi)|\,\sin(2Rk + \Phi(k))$$

Spherical wave

$\chi(k)$ oscillates with
Frequency = 2 R

Cu-O

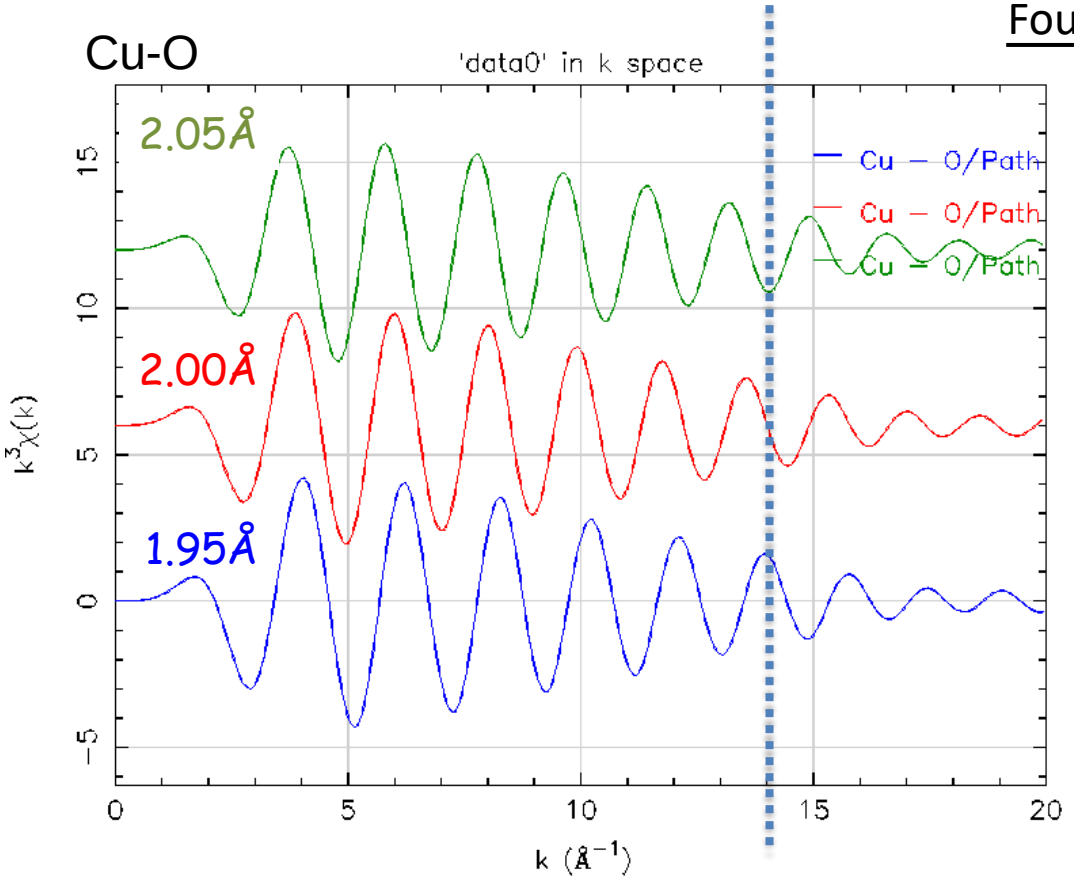

Fourier Transform

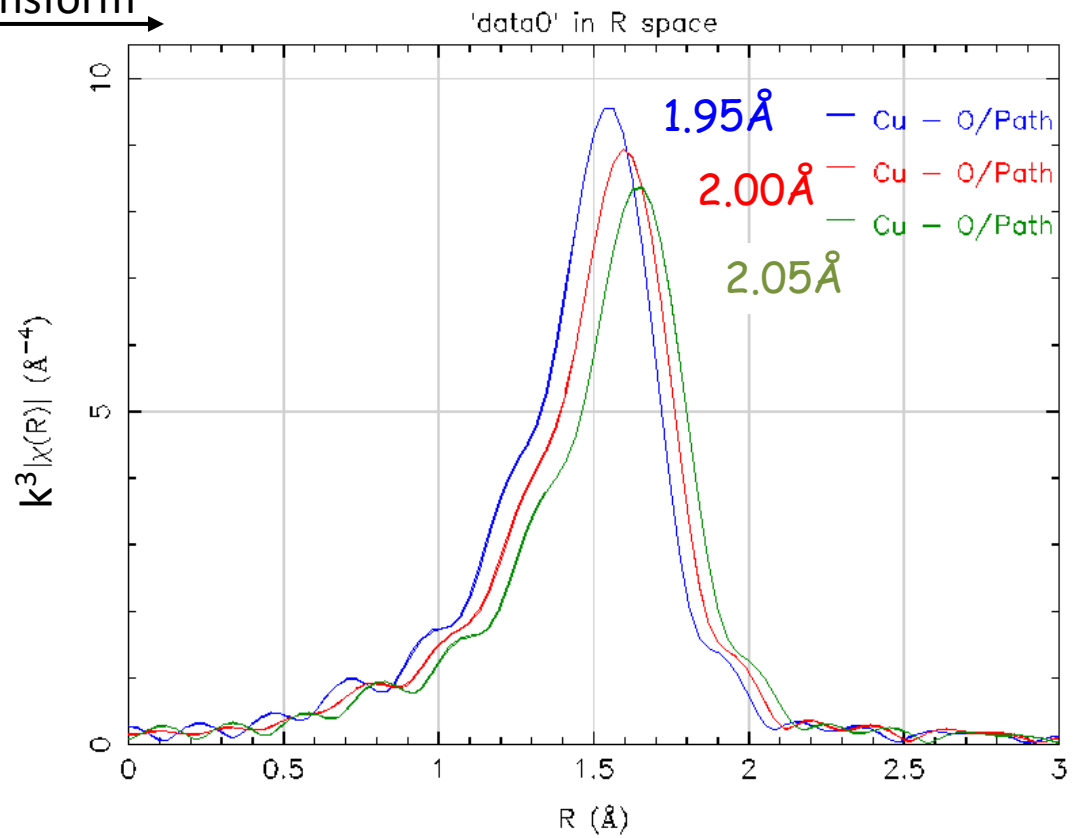

$$k\chi(k) = \frac{1}{R^2}|f(k,\pi)|\sin(2Rk + \Phi(k))$$

Absorbing Atom | **Scattering Atom**

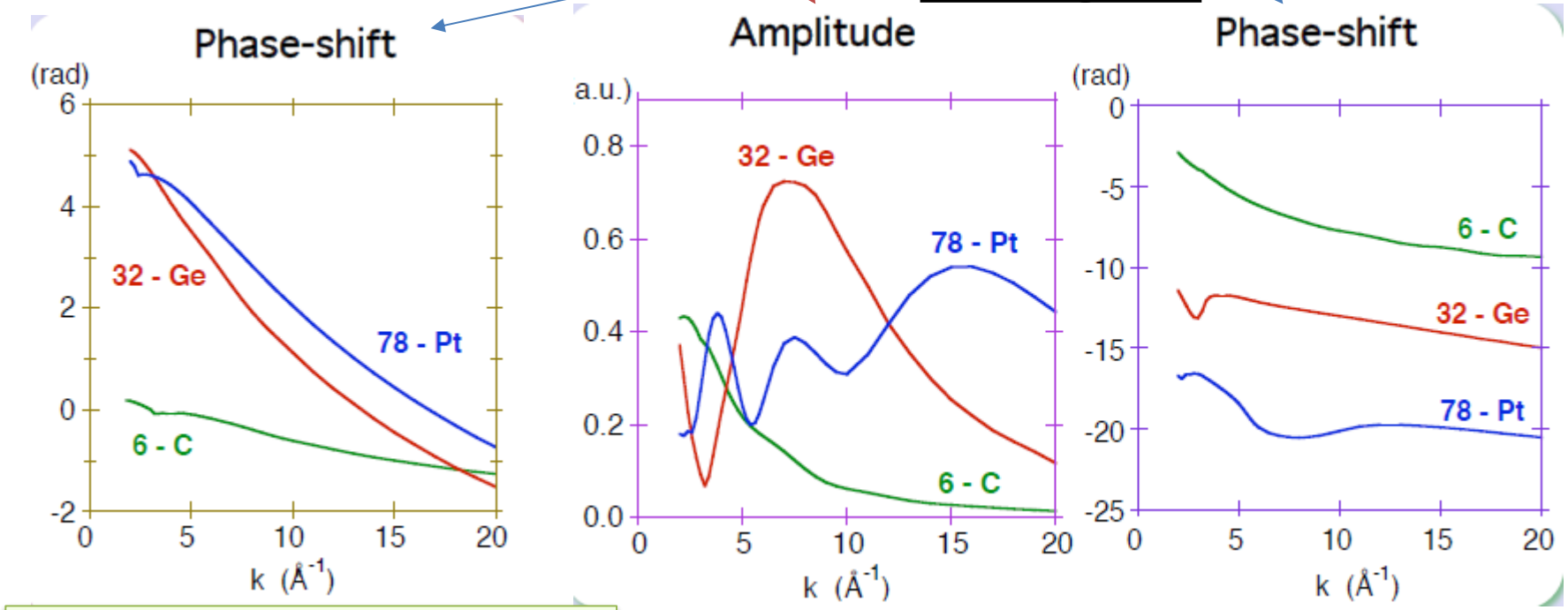

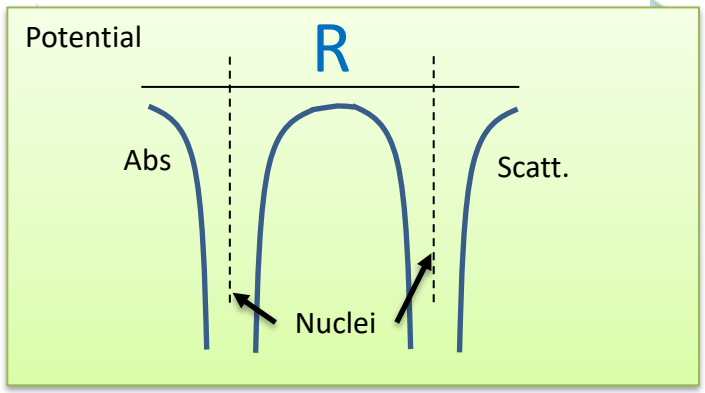

Different neighbors have different phases and scattering amplitudes.
Higher Z higher |f| at higher |k| values

Pair distance distribution :

- Picture of thermal motion, EXAFS depends on T

Damping term: « Debye Waller factor like»

$$k\chi(k) = \frac{1}{R^2}|f(k,\pi)|\,e^{-2\sigma^2 k^2}\sin(2Rk + \Phi(k))$$

Temperature effect

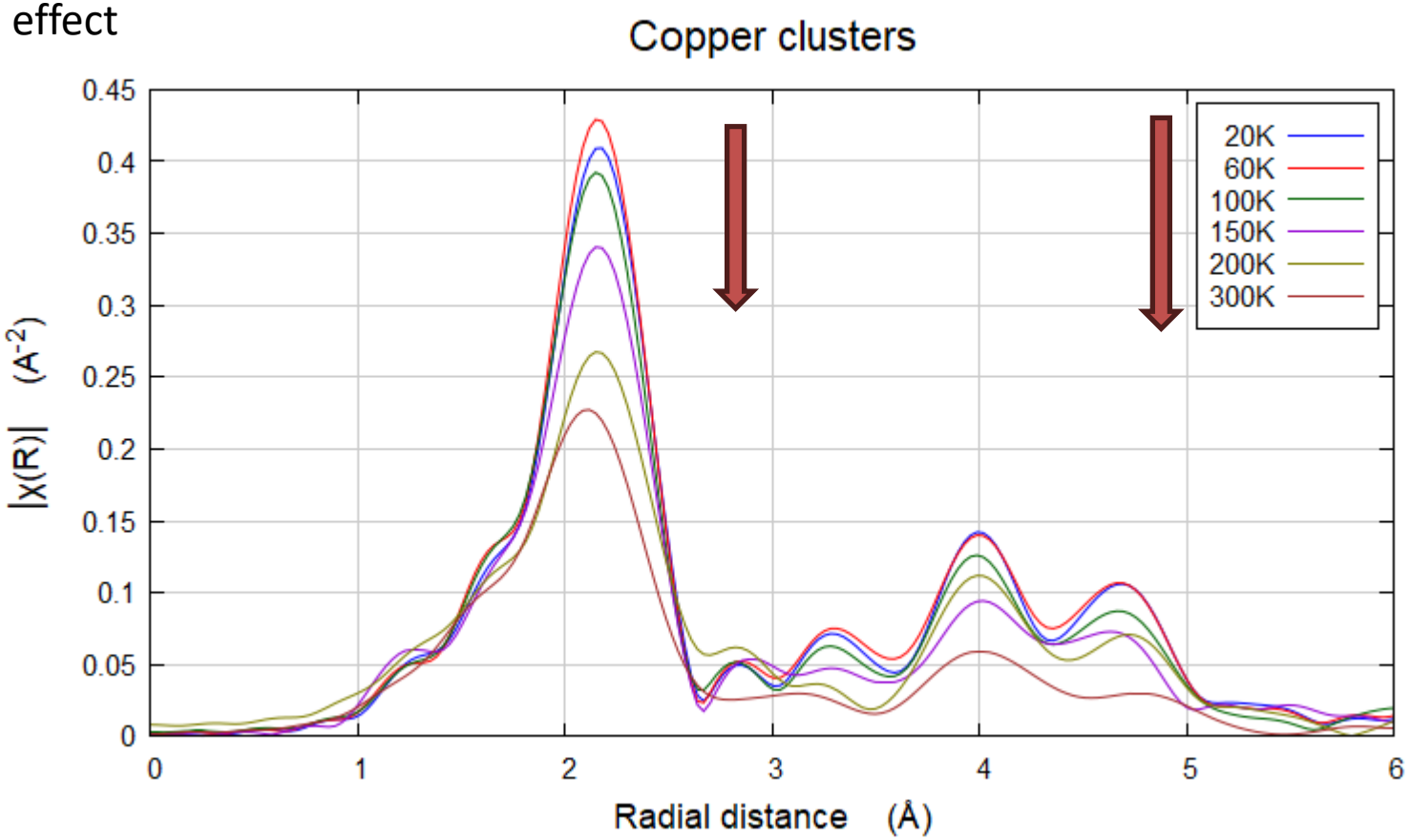

Pair distance distribution :

- Picture of thermal motion, EXAFS depends on T

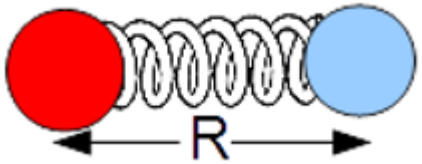

Damping term: « Debye Waller factor like»

$$k\chi(k) = \frac{1}{R^2}|f(k,\pi)|\boxed{e^{-2\sigma^2 k^2}}\sin(2Rk + \Phi(k))$$

- Structural average + structural disorder

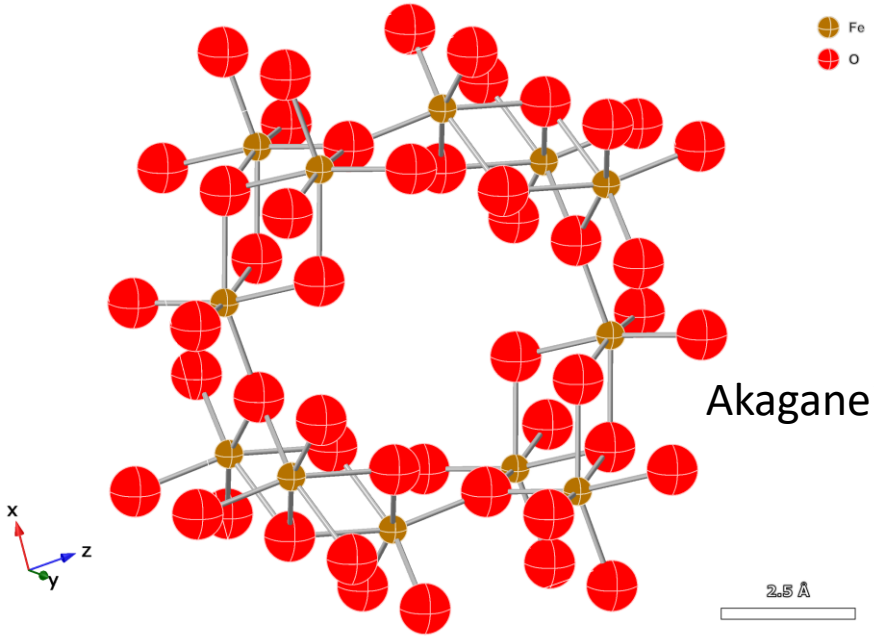

Akaganeite

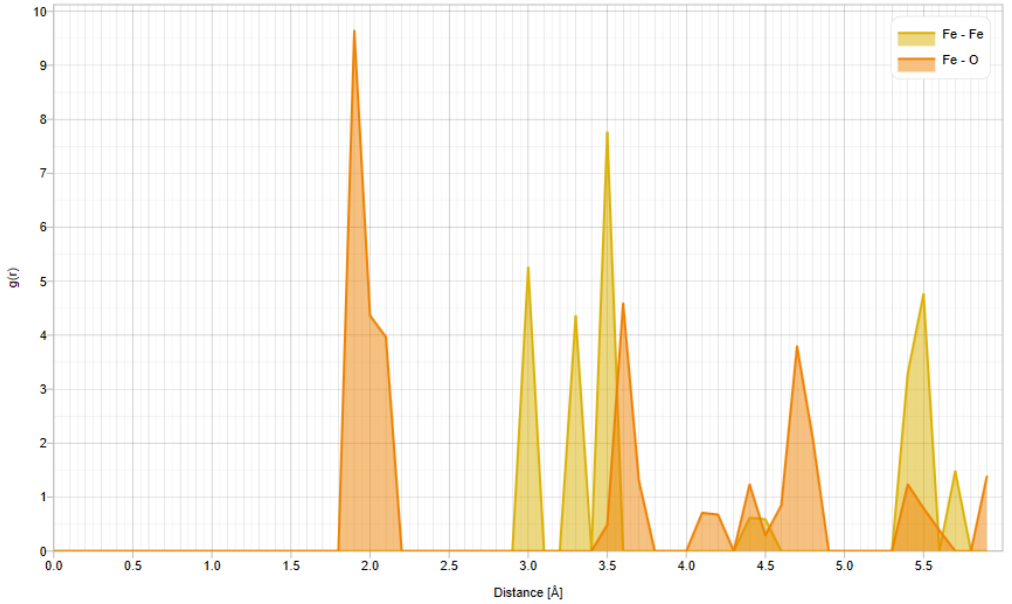

Adding up more atoms

$$k\chi(k) = \sum_i 3\cos^2(\theta_i)\, N_i \frac{1}{R_i^2} |f_i(k,\pi)|\, e^{-2\sigma_i^2 k^2} \sin(2R_i k + \Phi_i(k))$$

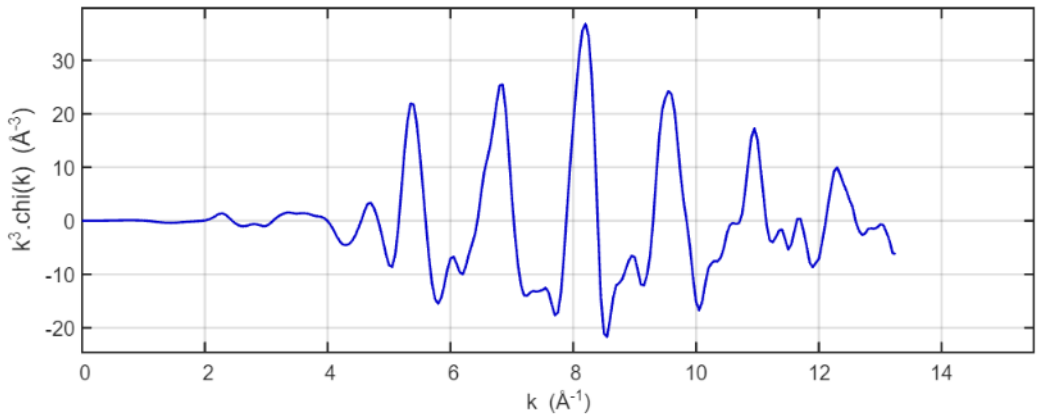

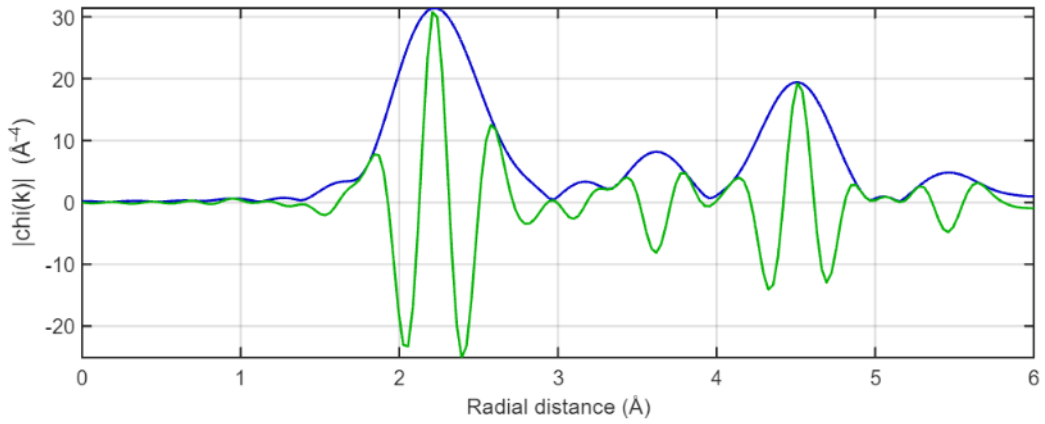

bcc Fe

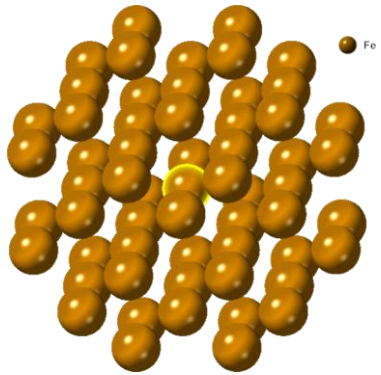

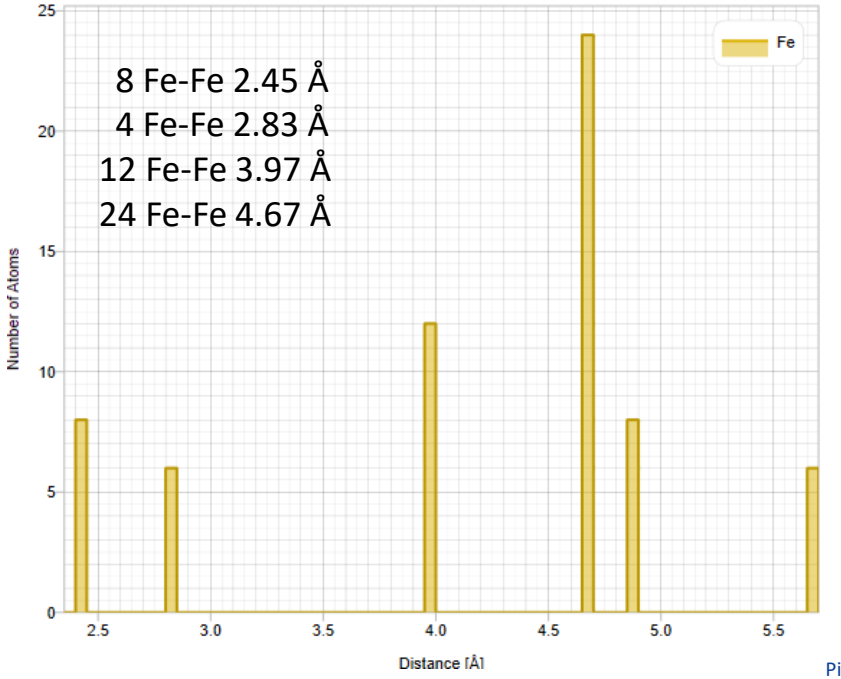

EXAFS examples: Fe bcc vs Fe in Goethite

8 Fe-Fe 2.45 Å
4 Fe-Fe 2.83 Å
12 Fe-Fe 3.97 Å
24 Fe-Fe 4.67 Å

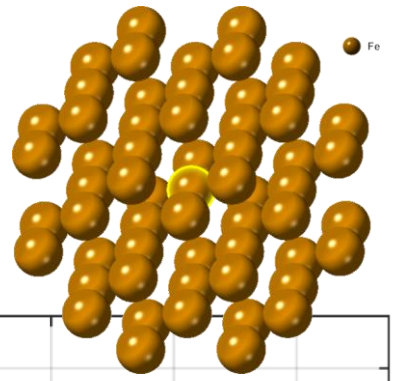

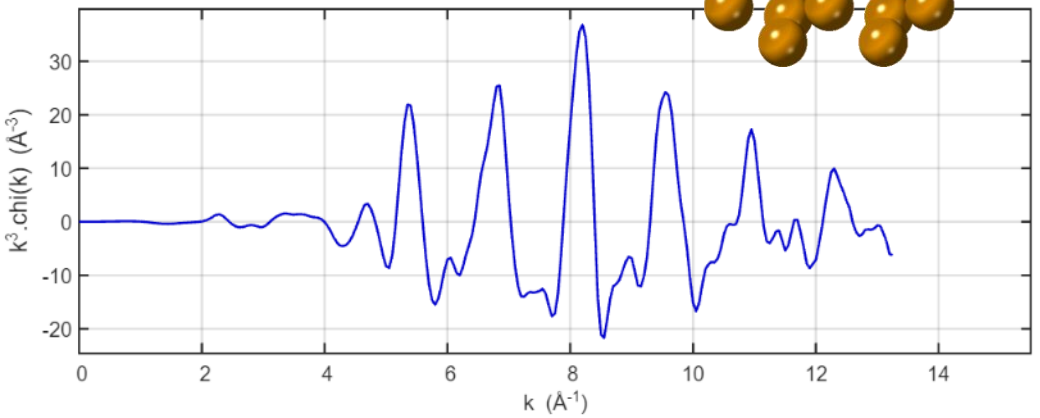

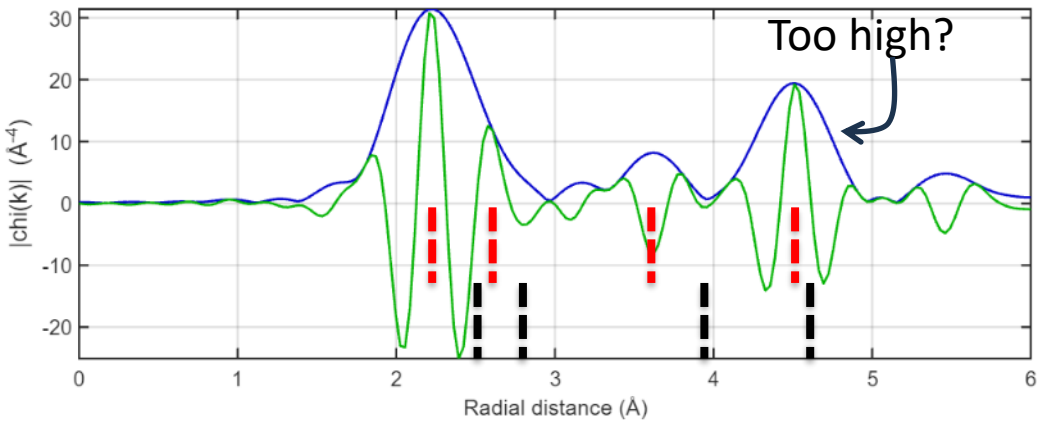

3 Fe-O 1.96 Å
3 Fe-O 2.11 Å
2 Fe-Fe 3.02 Å
1 Fe-O 3.21 Å
2 Fe-Fe 3.31 Å
4 Fe-Fe 3.44 Å

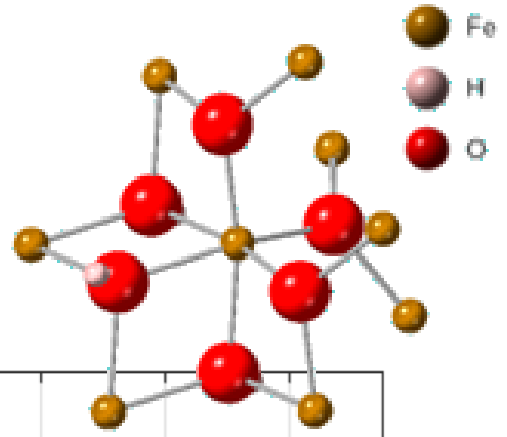

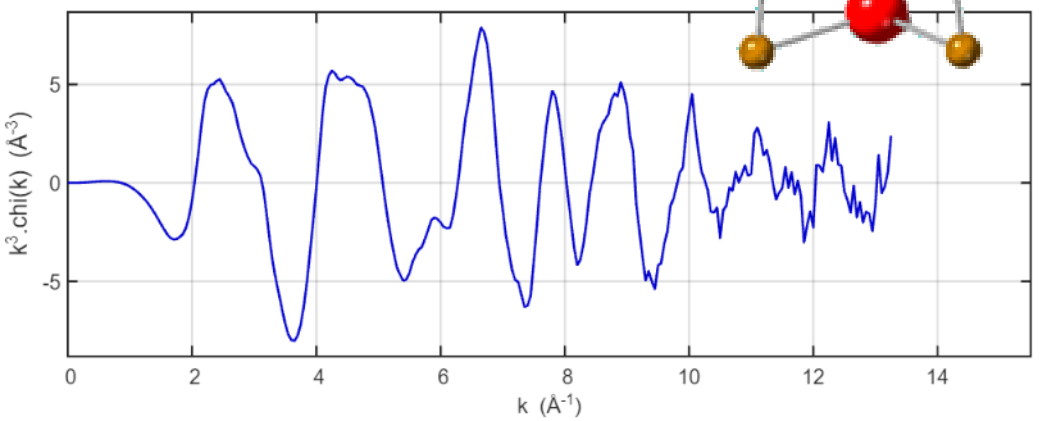

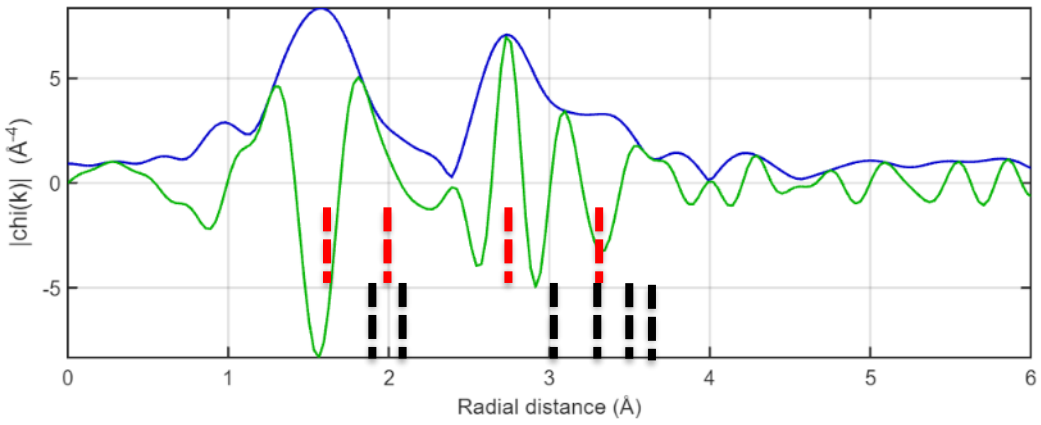

FT: a <u>pseudo</u> radial distribution representation

Multiple scattering the bcc-Fe case

8 Fe-Fe 2.45 Å
4 Fe-Fe 2.83 Å
12 Fe-Fe 3.97 Å
24 Fe-Fe 4.67 Å

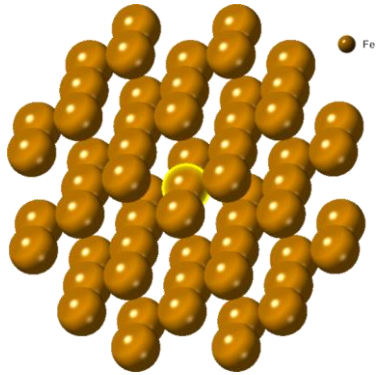

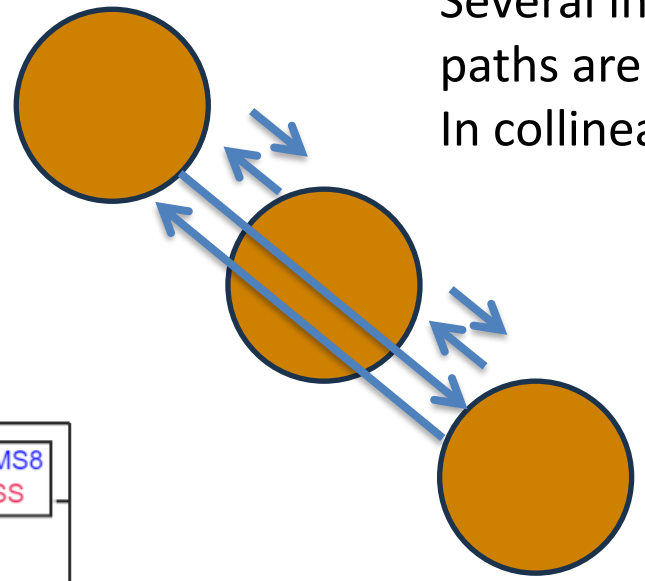

Several intense MS paths are possible
In collinear geometry

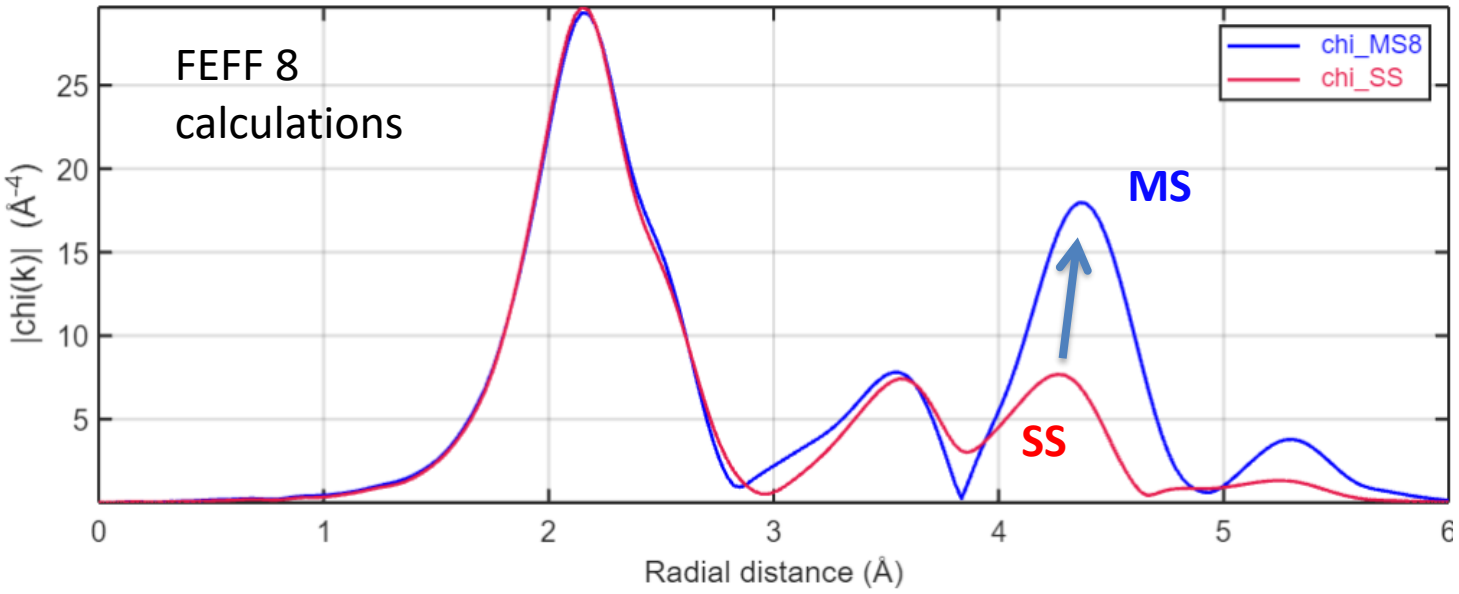

MS <u>requires</u> and <u>provides</u>
Geometrical information

EXAFS take away messages

Information provided by EXAFS and advantages

- Interatomic distances
- Coordination numbers
- Nature of atomic neighbors (for quite different Z)
- Disorder/thermal effects via Debye Waller

- It can be simulated via direct analytical methods
- We can stop simulations to first coordination shell

- Beamlines are getting better and better to provide high S/N
- Many good simulation codes are freely available

Disadvantages

- Signal is weak and thermal/structural disorders reduce it even more
- Resolution depends on k space = length of EXAFS
- Limited information versus complex structures in many cases

EXAFS data analysis in a nutshell

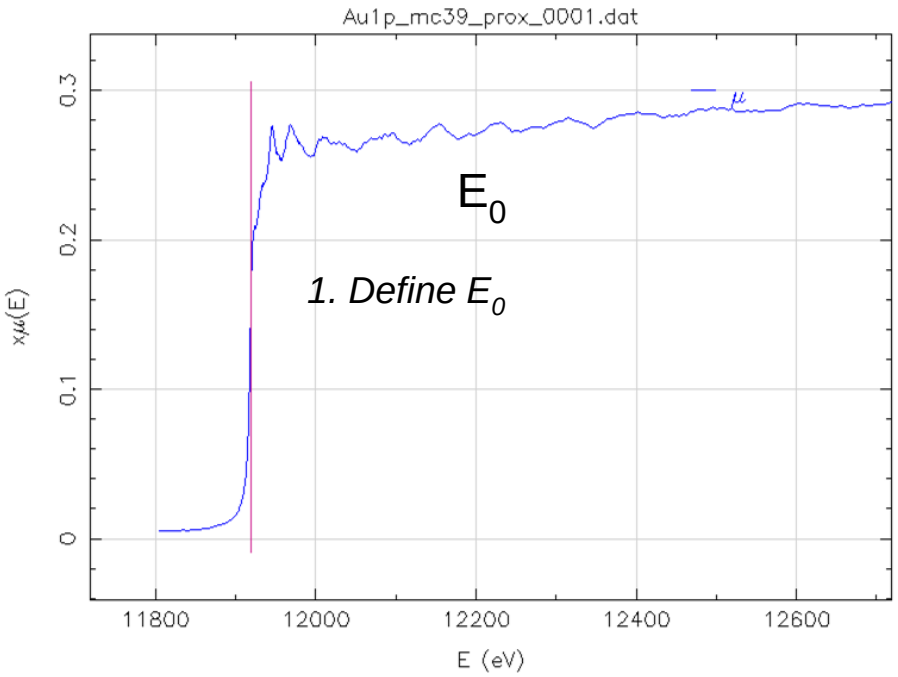

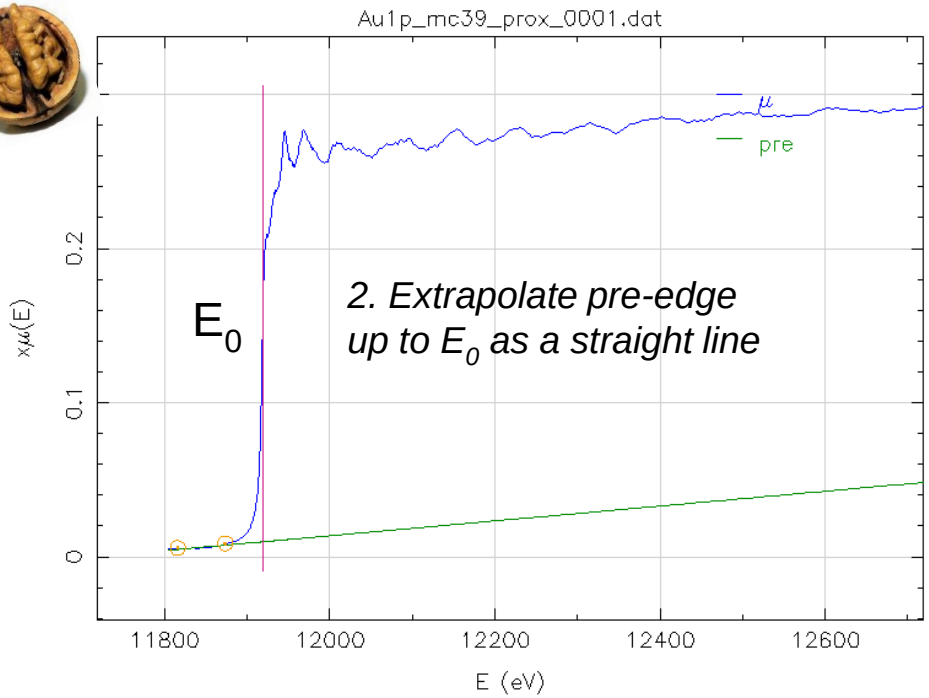

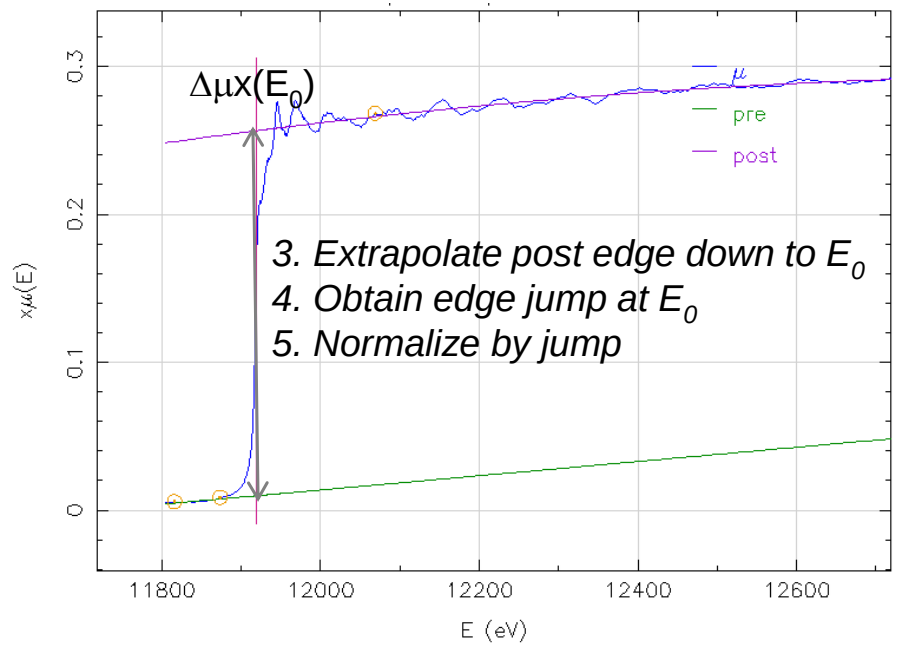

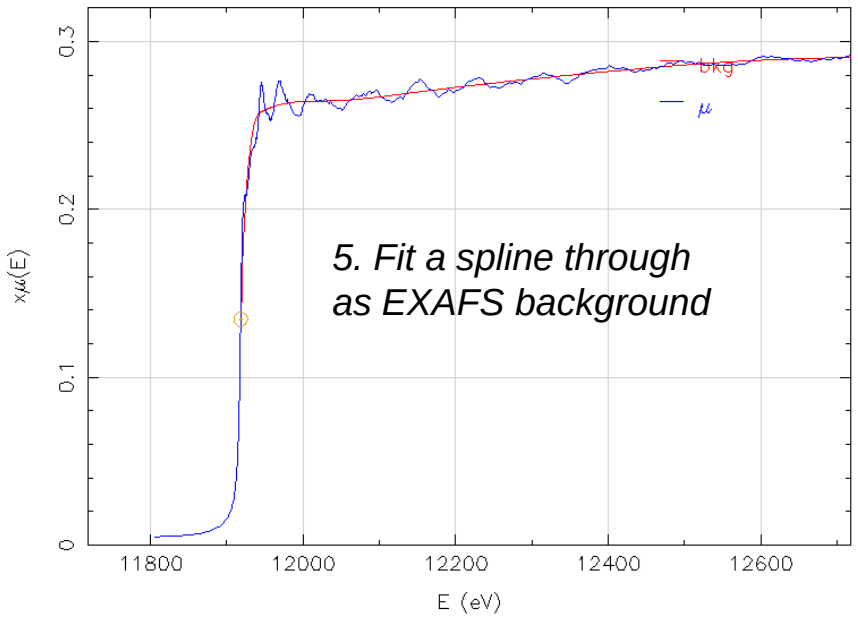

EXAFS data analysis in a nutshell

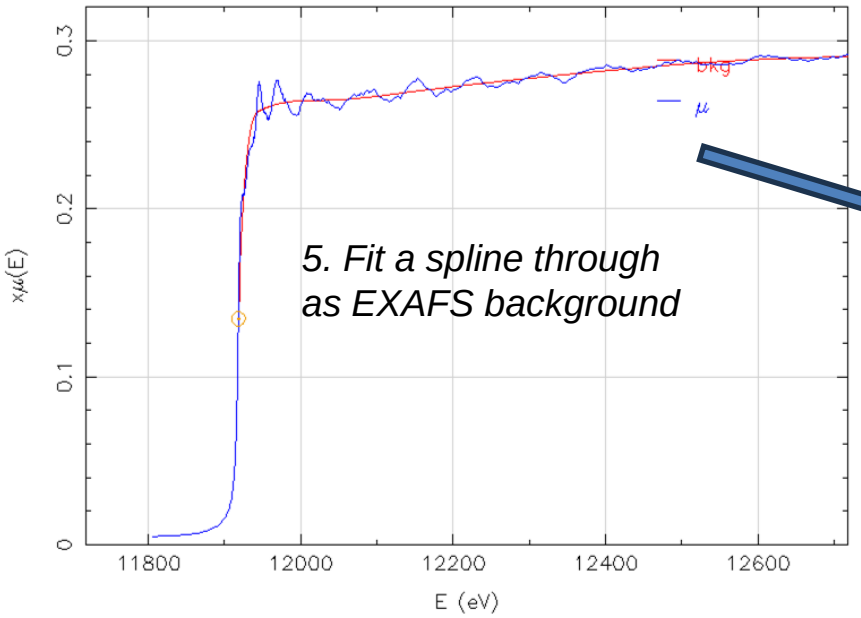

5. Fit a spline through as EXAFS background

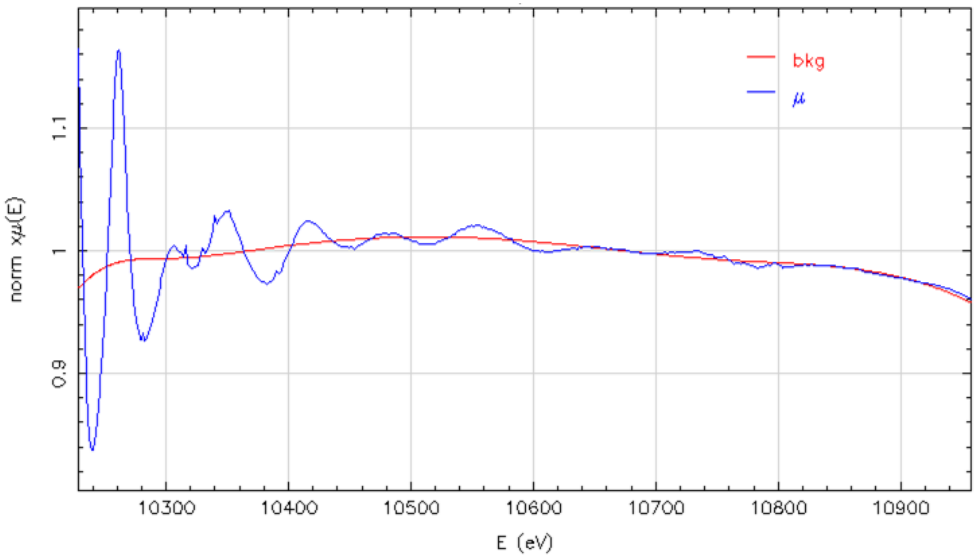

$$k \approx \sqrt{0.2625(E - E_0)}$$

EXAFS $\chi(k)$

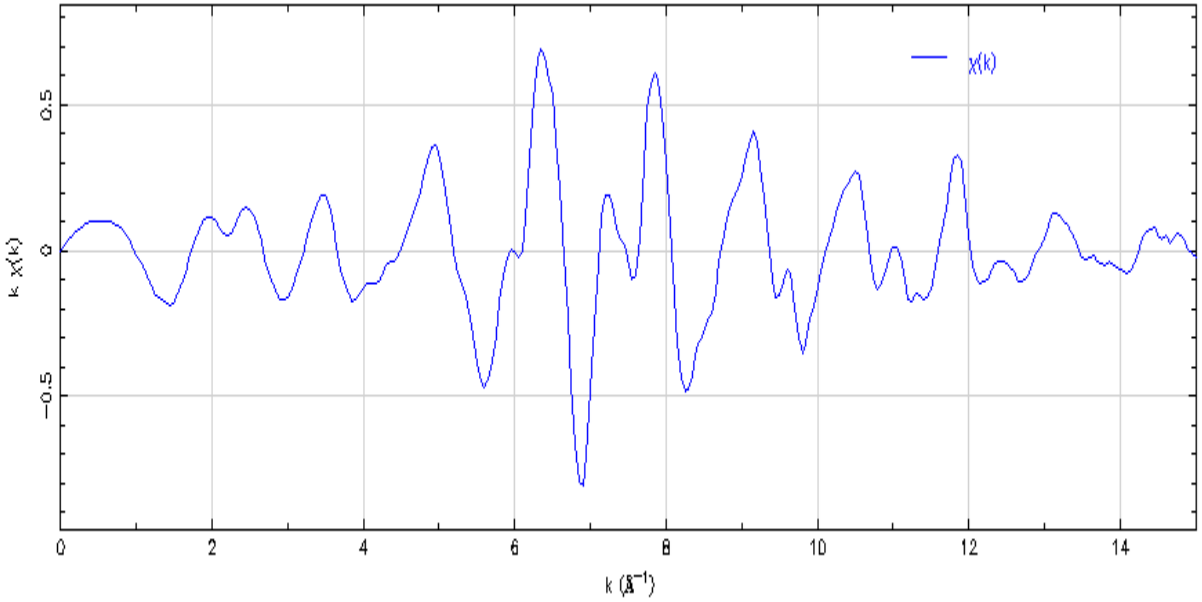

EXAFS data analysis in a nutshell

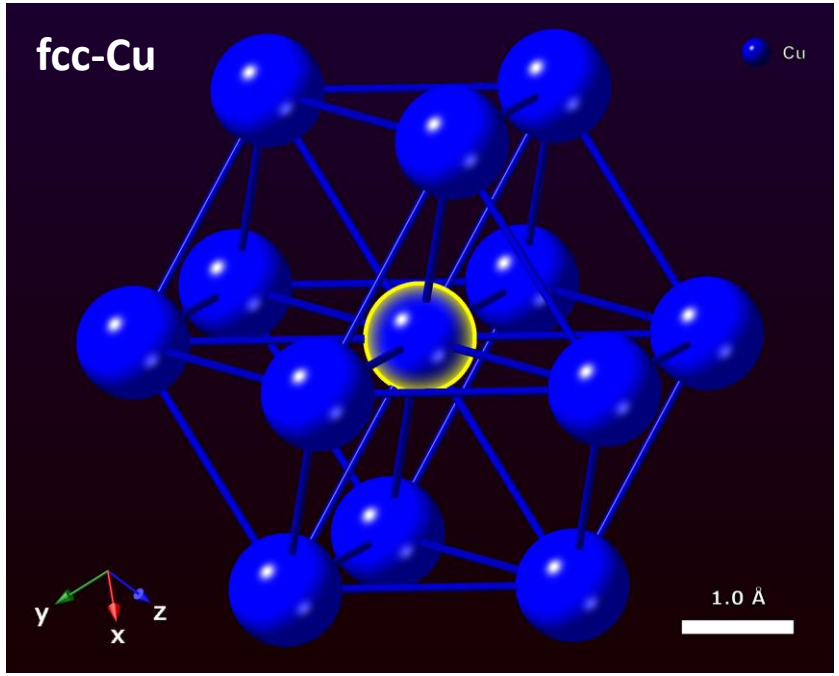

Radial distribution function contains too much information versus EXAFS.

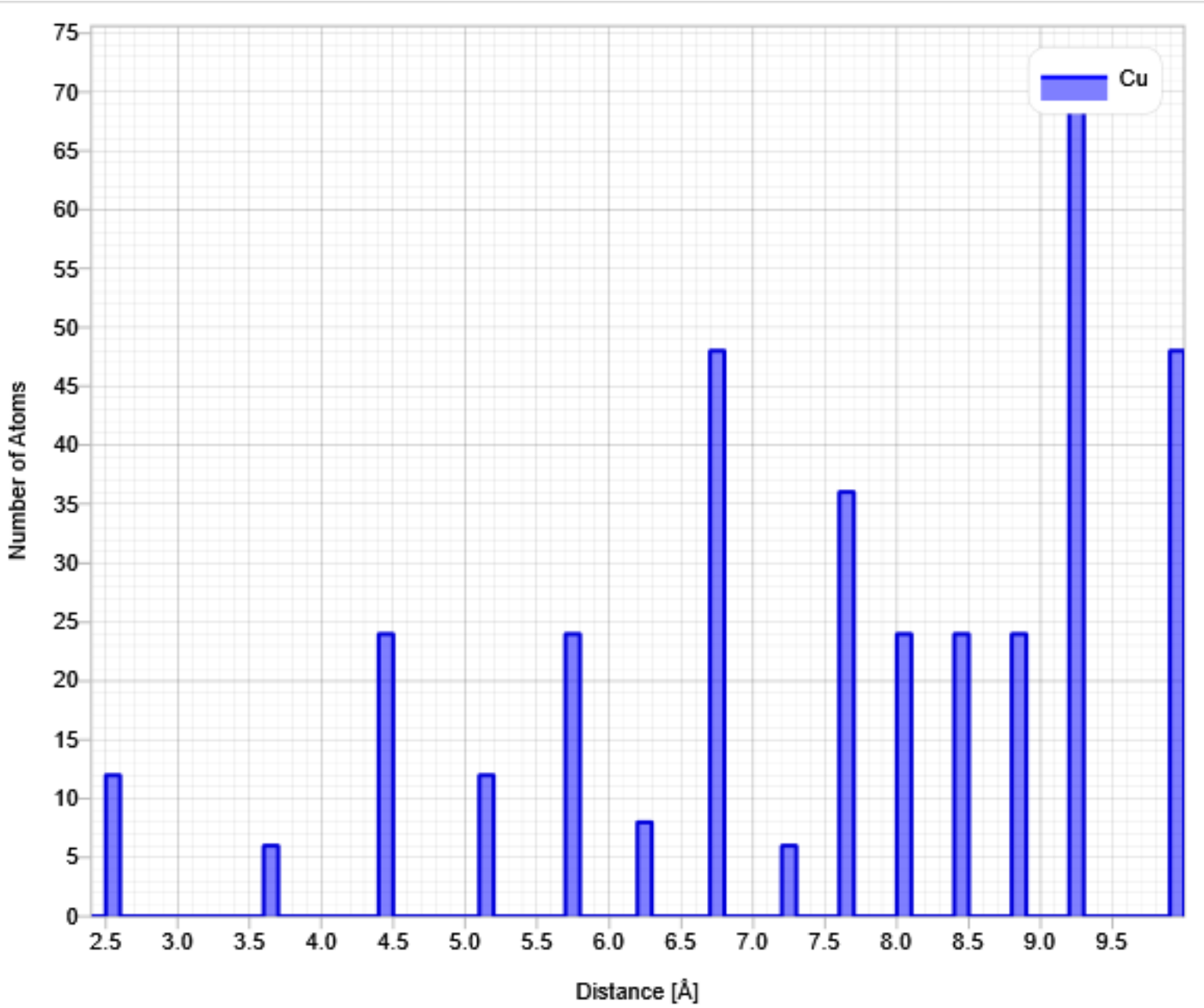

EXAFS data analysis in a nutshell

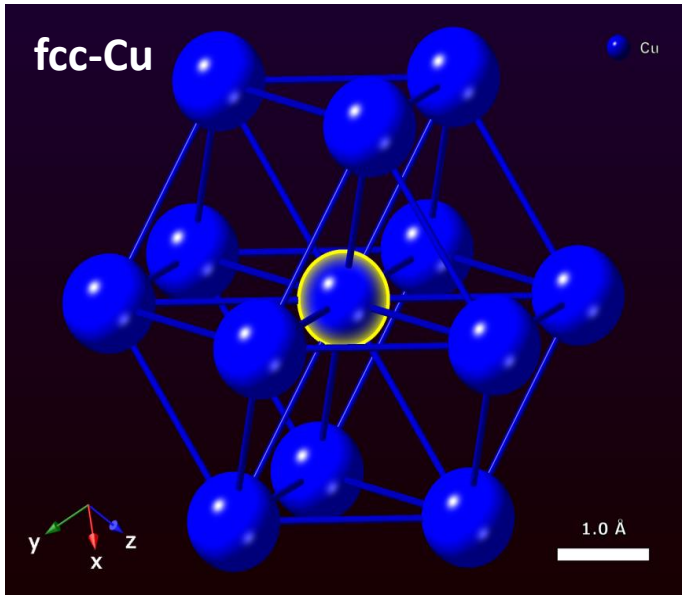

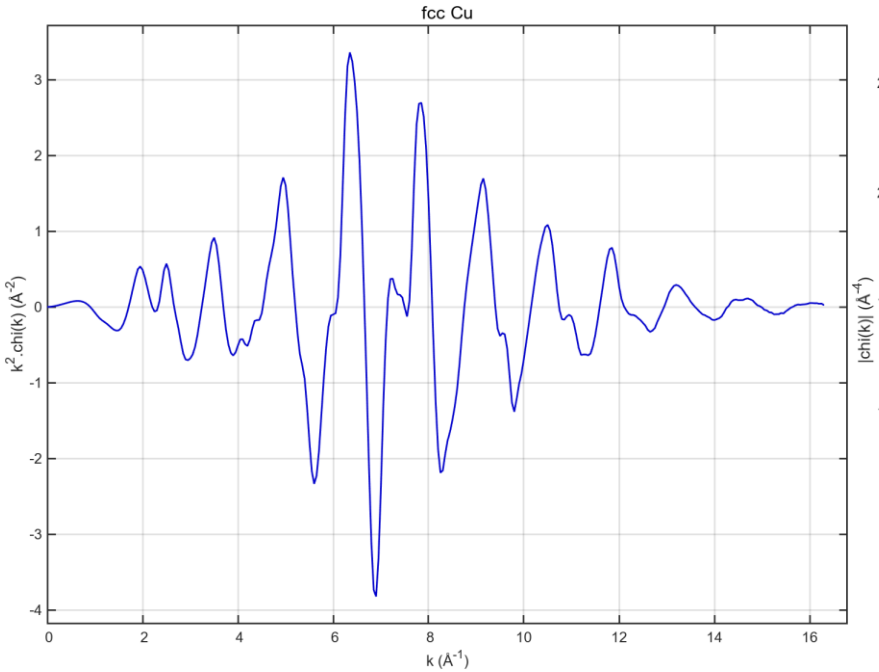

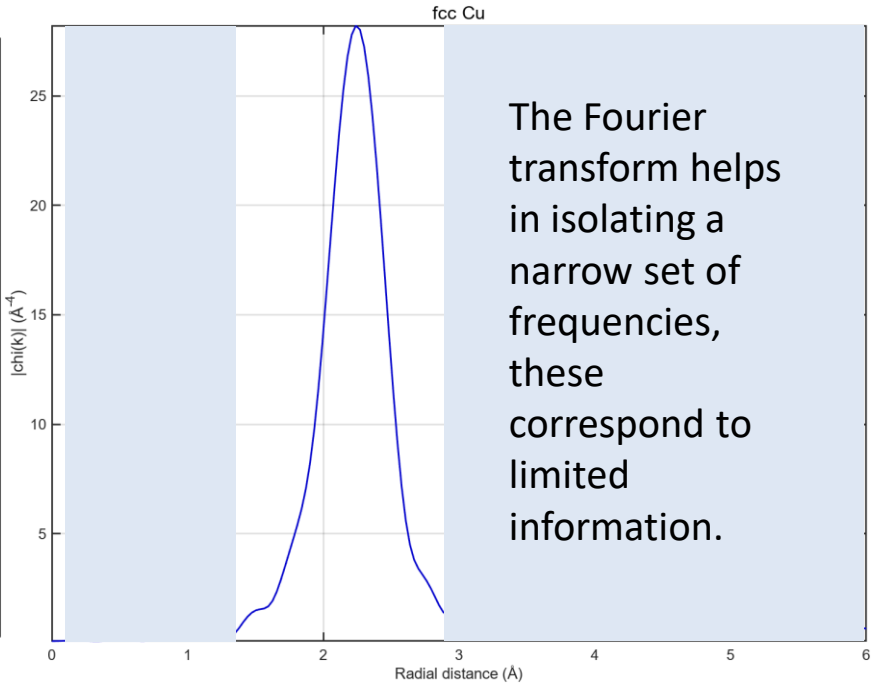

The Fourier transform helps in isolating a narrow set of frequencies, these correspond to limited information.

Δk ΔR

$$N_{idp} = \frac{2\Delta k \Delta R}{\pi} + (2)$$

Nyquist Shannon Theorem applied to EXAFS

Simulating the EXAFS signal implies:

- Making a structural hypothesis
- Fit a number of parameters $N_{par} < N_{idp}$

EXAFS data analysis in a nutshell

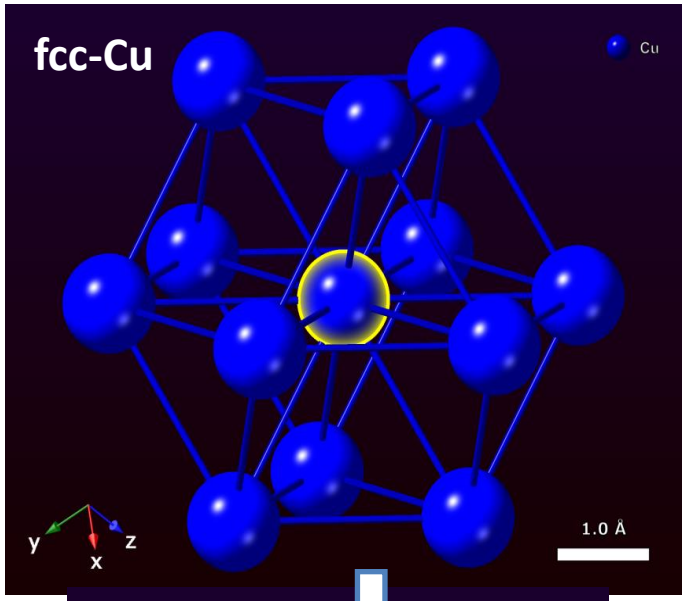

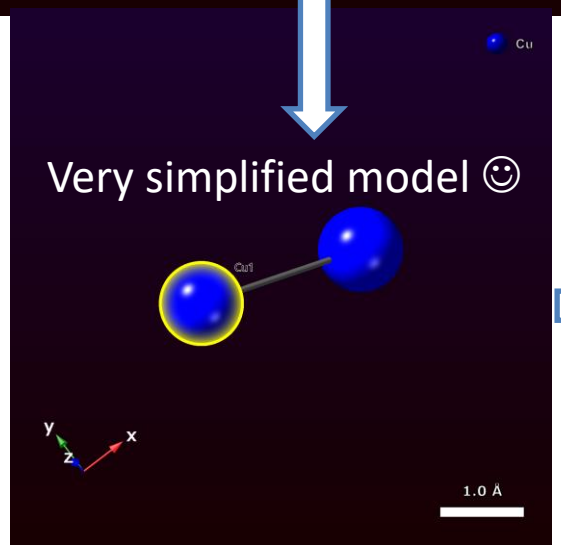

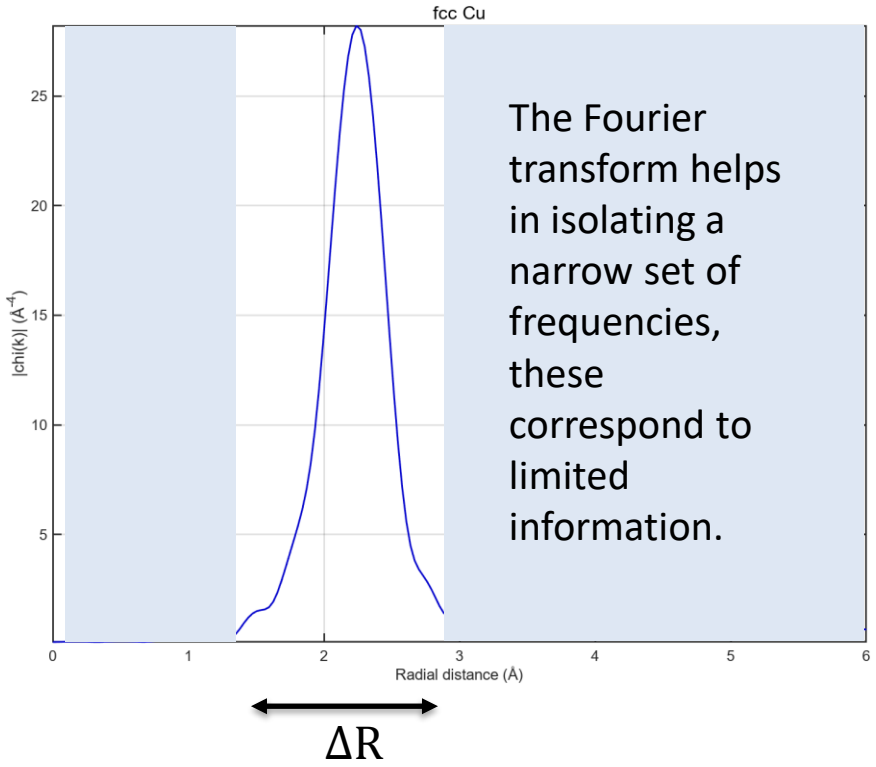

The Fourier transform helps in isolating a narrow set of frequencies, these correspond to limited information.

$$N_{idp} = \frac{2\Delta k \Delta R}{\pi} + (2)$$

Simplified Theoretical Calculation

$$k\chi(k) = N\frac{|f(k,\pi)|}{R^2}e^{-2\sigma^2 k^2}\sin(2Rk + \Phi(k))$$

Fitting parameters

EXAFS data analysis in a nutshell

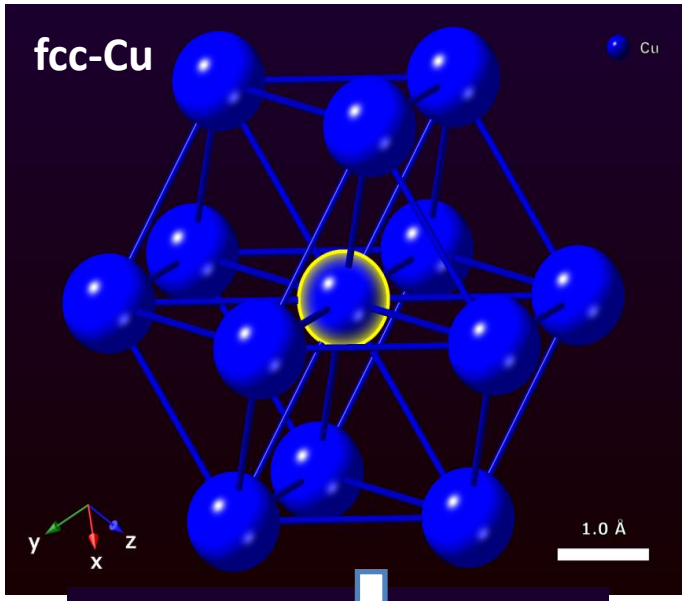

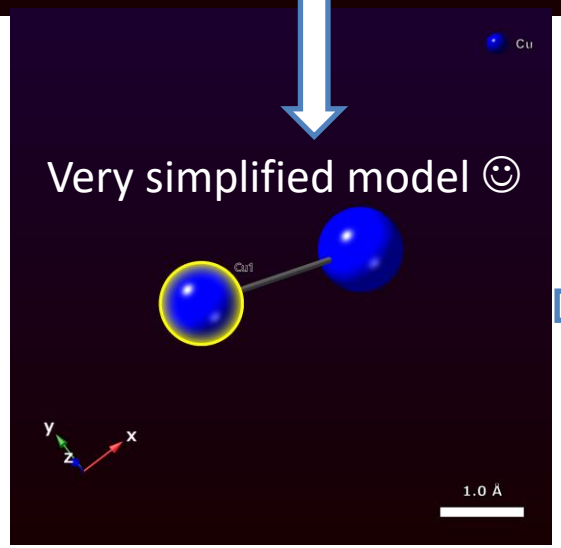

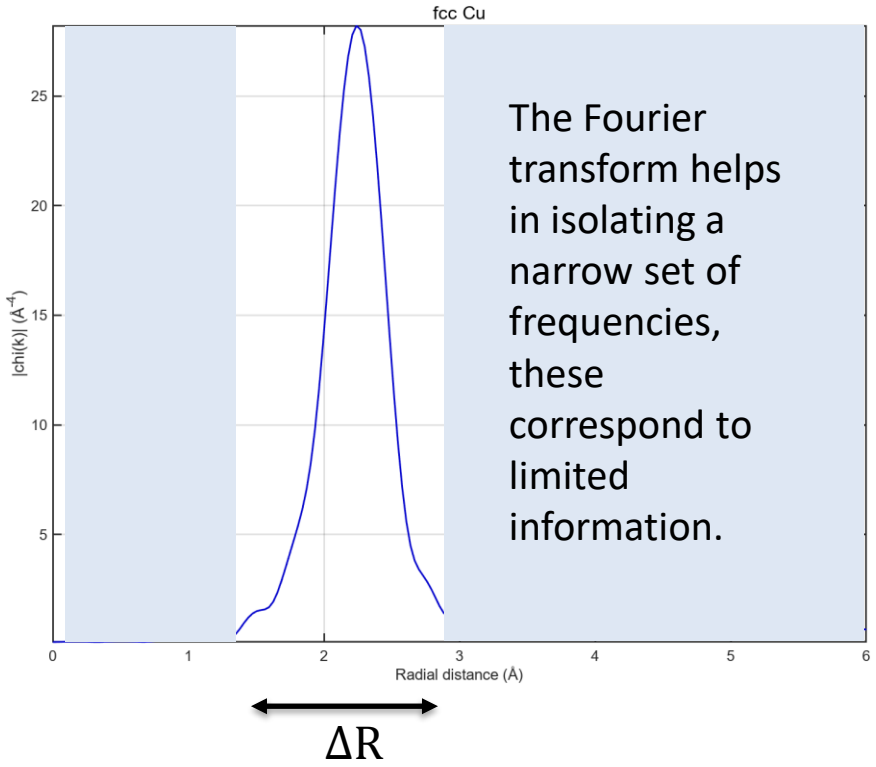

The Fourier transform helps in isolating a narrow set of frequencies, these correspond to limited information.

$$N_{idp} = \frac{2\Delta k \Delta R}{\pi} + (2)$$

Simplified Theoretical Calculation

$$k\chi(k) = N\frac{|f(k,\pi)|}{R^2}e^{-2\sigma^2 k^2}\sin(2Rk + \Phi(k))$$

Fitting parameters

EXAFS data analysis in a nutshell

A two step procedure to model signal:

- Create model

$$k\chi(k) = N\frac{|f(k,\pi)|}{R^2}e^{-2\sigma^2k^2}\sin(2Rk + \Phi(k))$$

Fastosh - Quick EXAFS Modelling & Fitting

Options

Model creation

New shell modelled by FEFF:

* req

Atom type of absorber	Cu	
Atom type of scatterer	Cu	
Absorber-scatterer distance	2.5	Å
Edge	K	
σ2	0.003	
N (SO2 fixed at 0.8)	12	
ΔE0	0	

Get your simulation over the first shell range

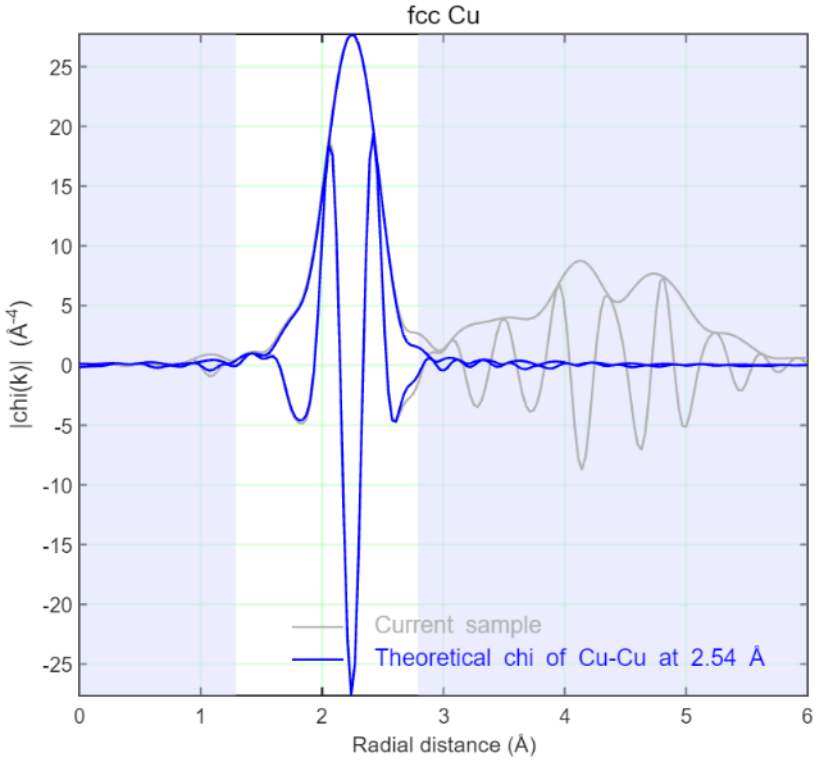

- Variate parameters to fit experiment

Fit parameters | Fit results | Hamilton Test

	Abs.	Scat.	Edge	R theo	R + ΔR	σ2	Δe0	N
					Float	Float	Float	Float
Float	Cu	Cu	K	2.50	2.54	0.0082	3.43	12.00

XAFS for studying the local structure of doping elements

Stepwise photoassisted decomposition of carbohydrates to H2.

*"**C–C bond first**" strategy of photoassisted splitting of biomass carbons into C_1 liquid hydrogen carriers*

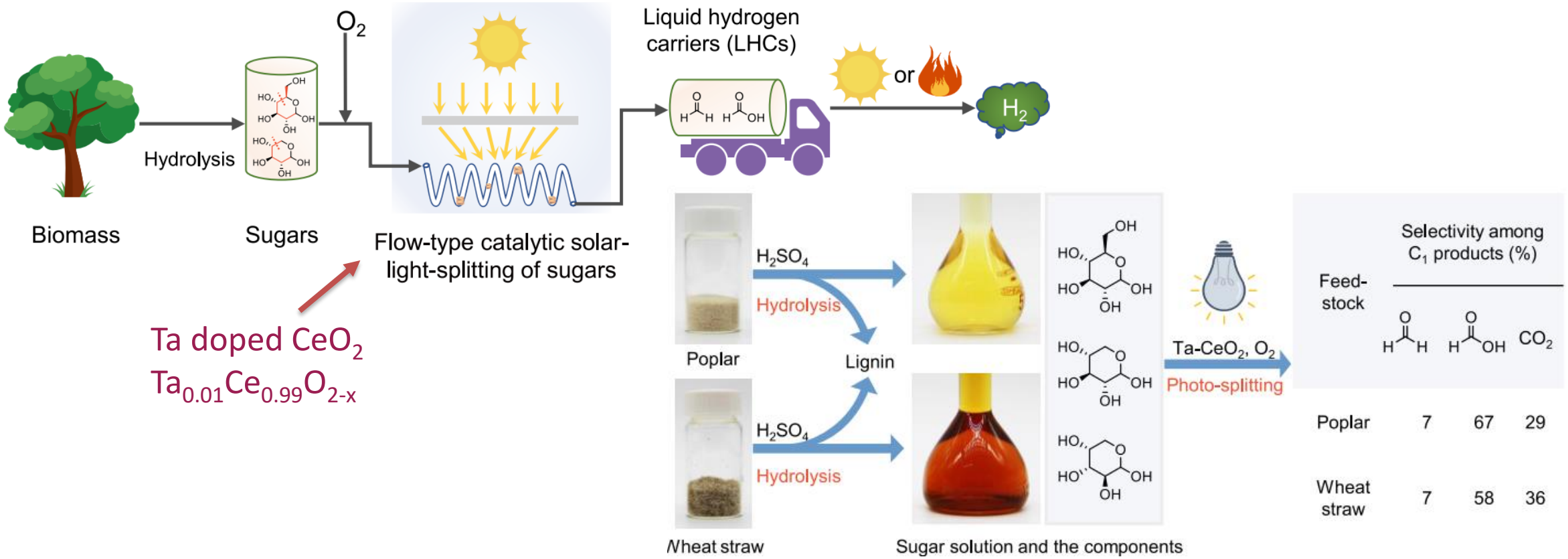

Feed-stock	Selectivity among C_1 products (%)		
	HCHO	HCOOH	CO_2
Poplar	7	67	29
Wheat straw	7	58	36

Ren, P., Z. Gao, T. Montini, Z. Zhao, N. Ta, Y. Huang, N. Luo, E. Fonda, P. Fornasiero and F. Wang (2023). Joule **7**(2): 333-349.

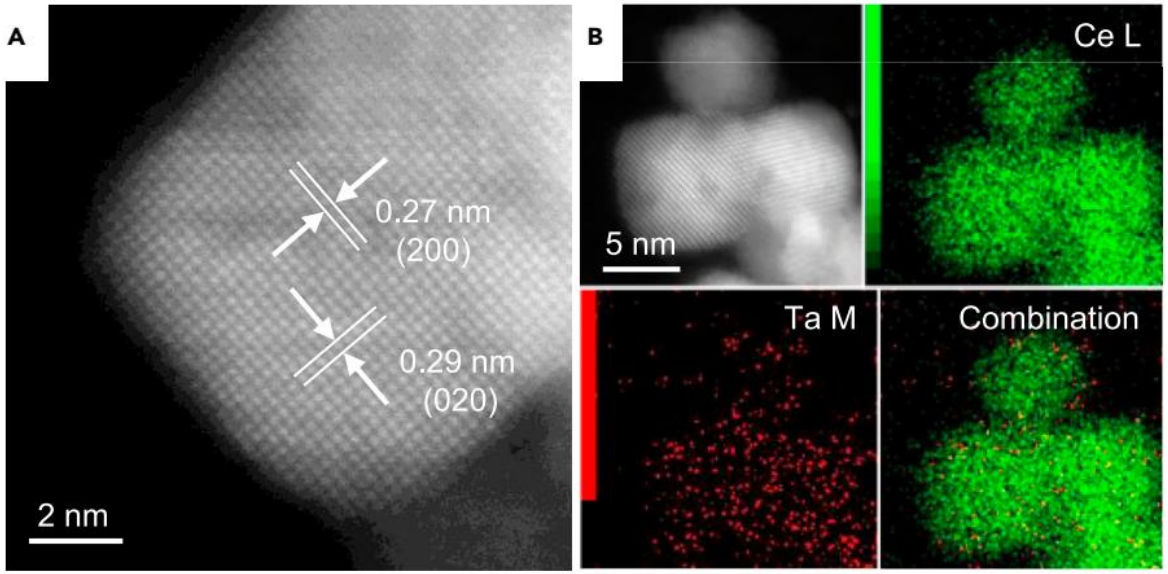

HAADF STEM EDX

- Dispersion of Ta in/over CeO_2 *(hydrothermal synthesis)*
- XRD/HAADF: unchanged lattice / increased disorder
- *Band gap is reduced from 2.6eV to 2.37eV by Ta doping*
- *Ce3+ detected by Raman*

➔Ta oxidation state / localisation ?

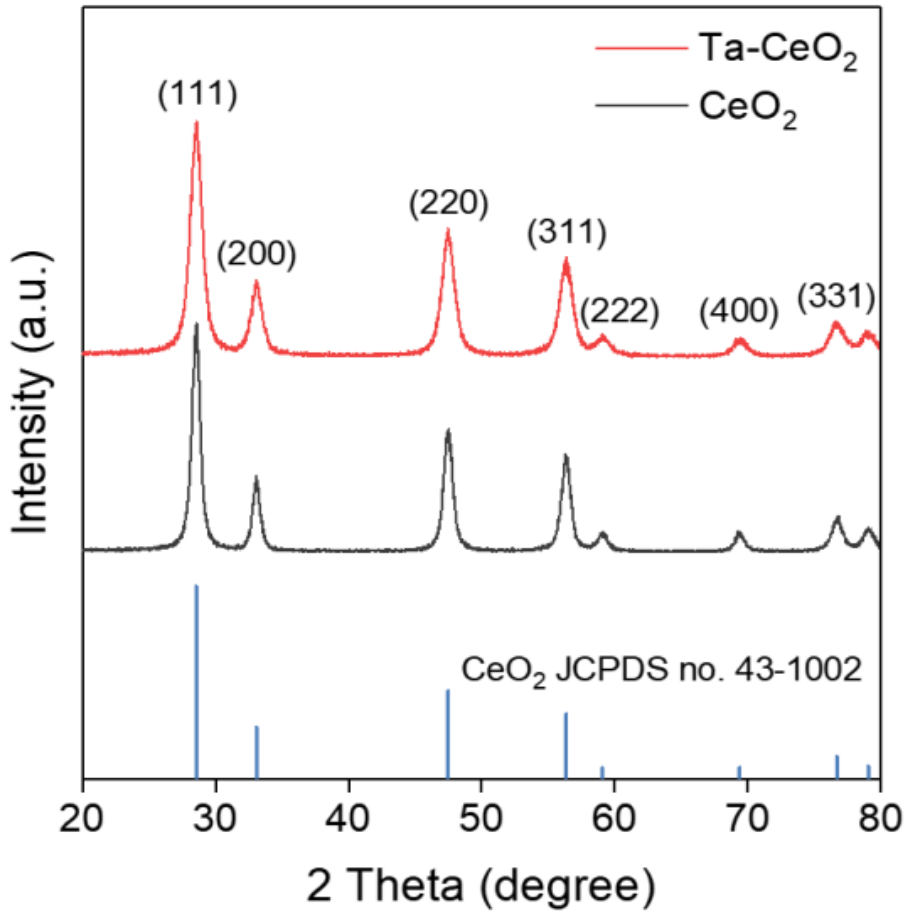

XANES: oxidation state

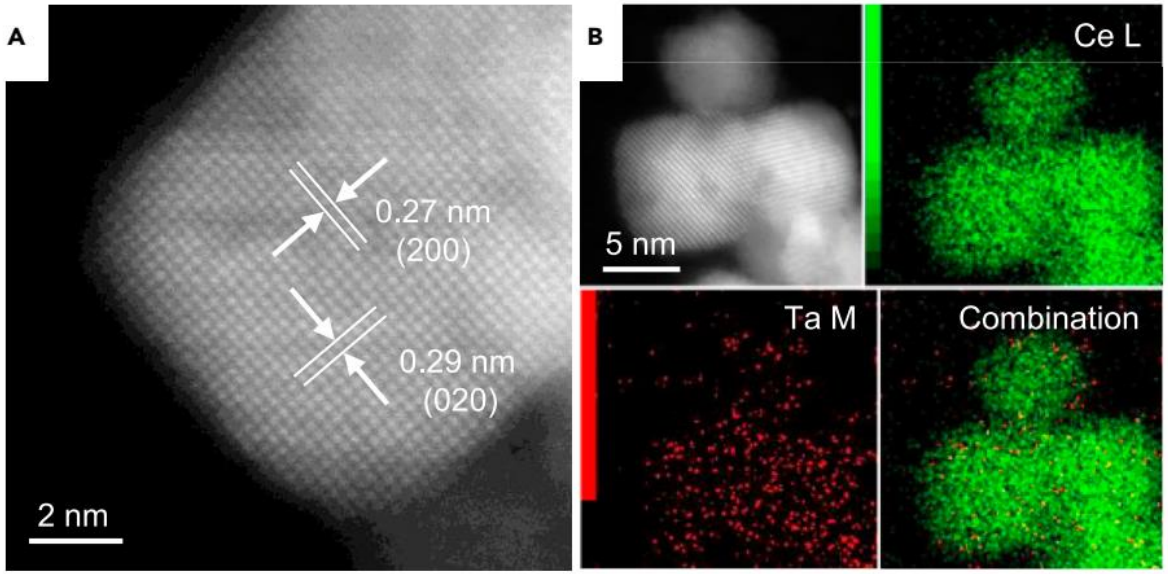

HAADF STEM EDX

- Dispersion of Ta in/over CeO_2 *(hydrothermal synthesis)*
- XRD/HAADF: unchanged lattice / increased disorder
- *Band gap is reduced from 2.6eV to 2.37eV by Ta doping*
- *Ce3+ detected by Raman*

➔Ta oxidation state / localisation ?

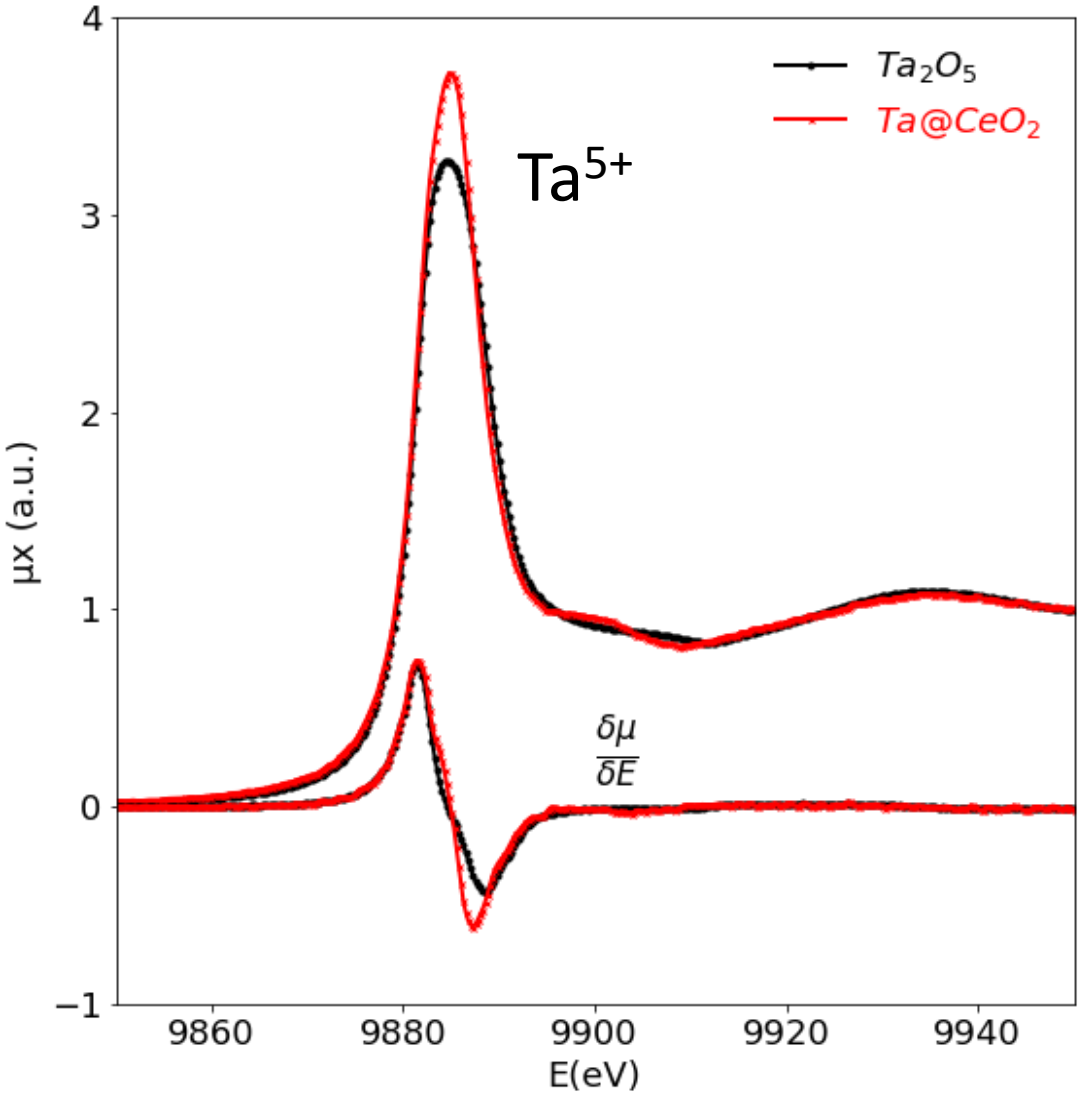

Ta very close to 5+ state

EXAFS: local structure

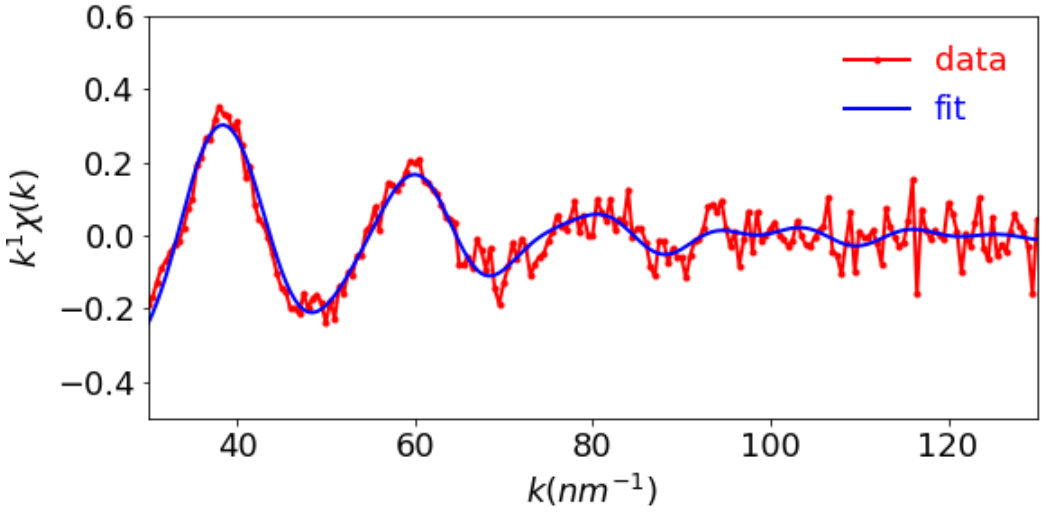

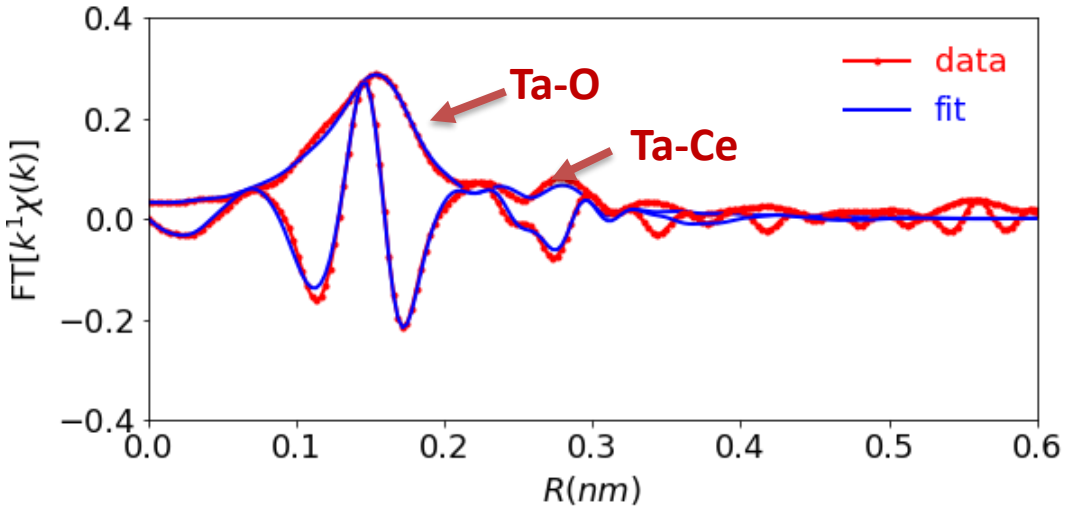

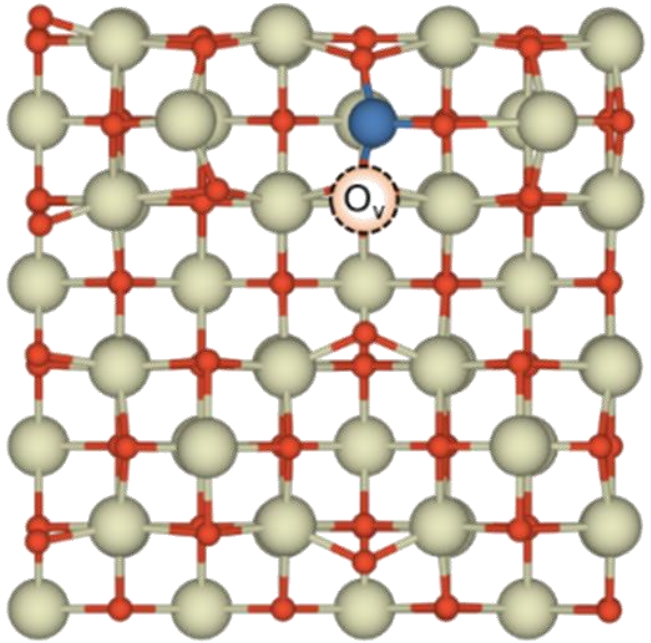

DFT model

r (Ta^{5+}) = 0.97 Å << r (Ce^{4+}) = 1.14 Å

Distance	N	R (nm)	S^2 (10^{-5} nm^2)
Ta–O	5.6 ± 0.9	0.194 ± 0.002	
Ta–O	1.4 ± 0.8	0.242 ± 0.003	5 ± 2
Ta–Ce	2.1 ± 0.7	0.312 ± 0.003	

Ta – O shell highly deformed
Ta – Ce shorter and only 2 detected
Ta is in the Ce^{4+} site

Ce^{3+} and O_V must compensate Ta^{5+}
Ce^{3+} lowers the band gap of CeO_2

Conclusions

XANES

Ta oxidation state is close to 5+

➔Charge compensation is necessary: Ce^{3+}

EXAFS

Ta – O : 7 oxygens (instead of 8 over a cube in CeO_2)

Ta – Ce : 2 detected at a much shorter distance than Ce-Ce (0.379 nm)

➔distorted geometry into CeO_2

Suggests

➔ proximal oxygen vacancy

➔Ce^{3+} localised nearby

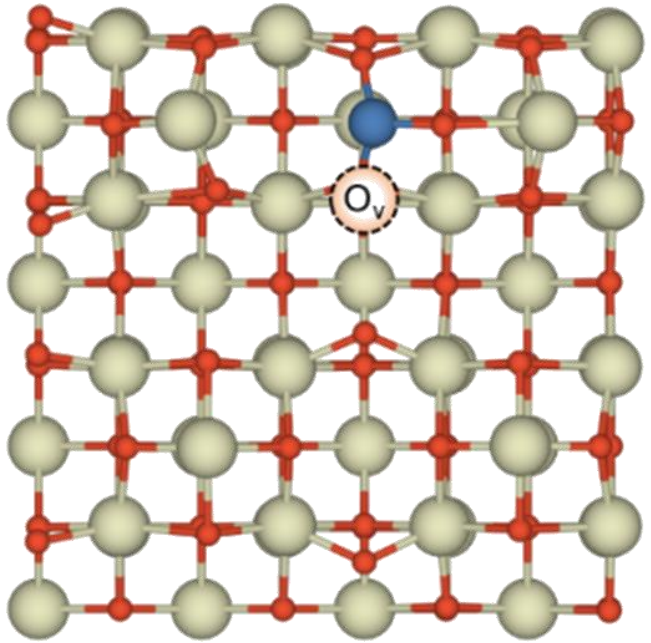

DFT model

Distance	N	R (nm)	S^2 (10^{-5} nm^2)
Ta–O	5.6 ± 0.9	0.194 ± 0.002	
Ta–O	1.4 ± 0.8	0.242 ± 0.003	5 ± 2
Ta–Ce	2.1 ± 0.7	0.312 ± 0.003	

Applications to nano objects: finite size effect on CN

Surface atoms have a diminished coordination number.

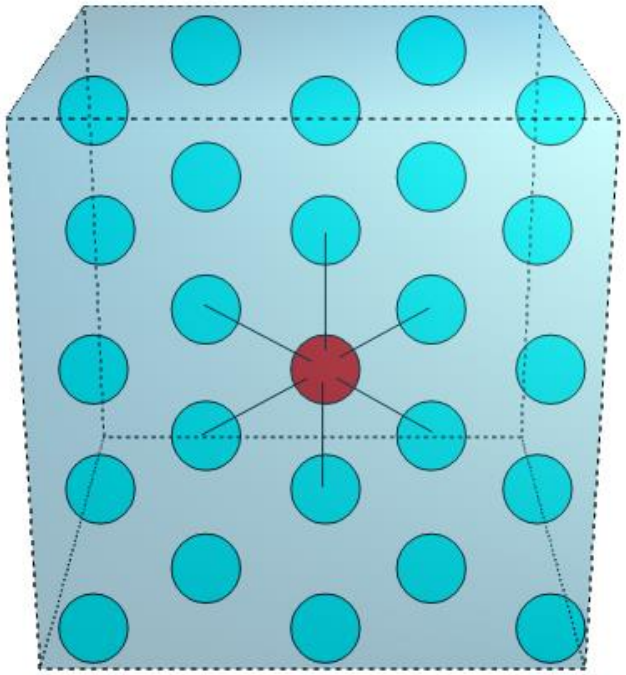

Diminishing size
N^* diminishes

$N_{surface}/N_{bulk}$ increases

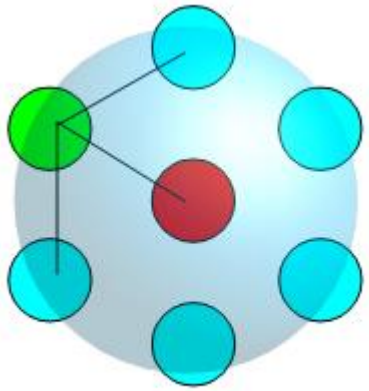

An average particle size may be deduced from N.
(Size is weighted by size dispersion).

EXAFS coordination number is the weighted average of the coordination numbers of all absorbers.

$$N^* = \frac{\sum_{i=1}^{n_{tot}} N_i}{n_{tot}}$$

E.g. Ni (fcc) N vs D (Å)

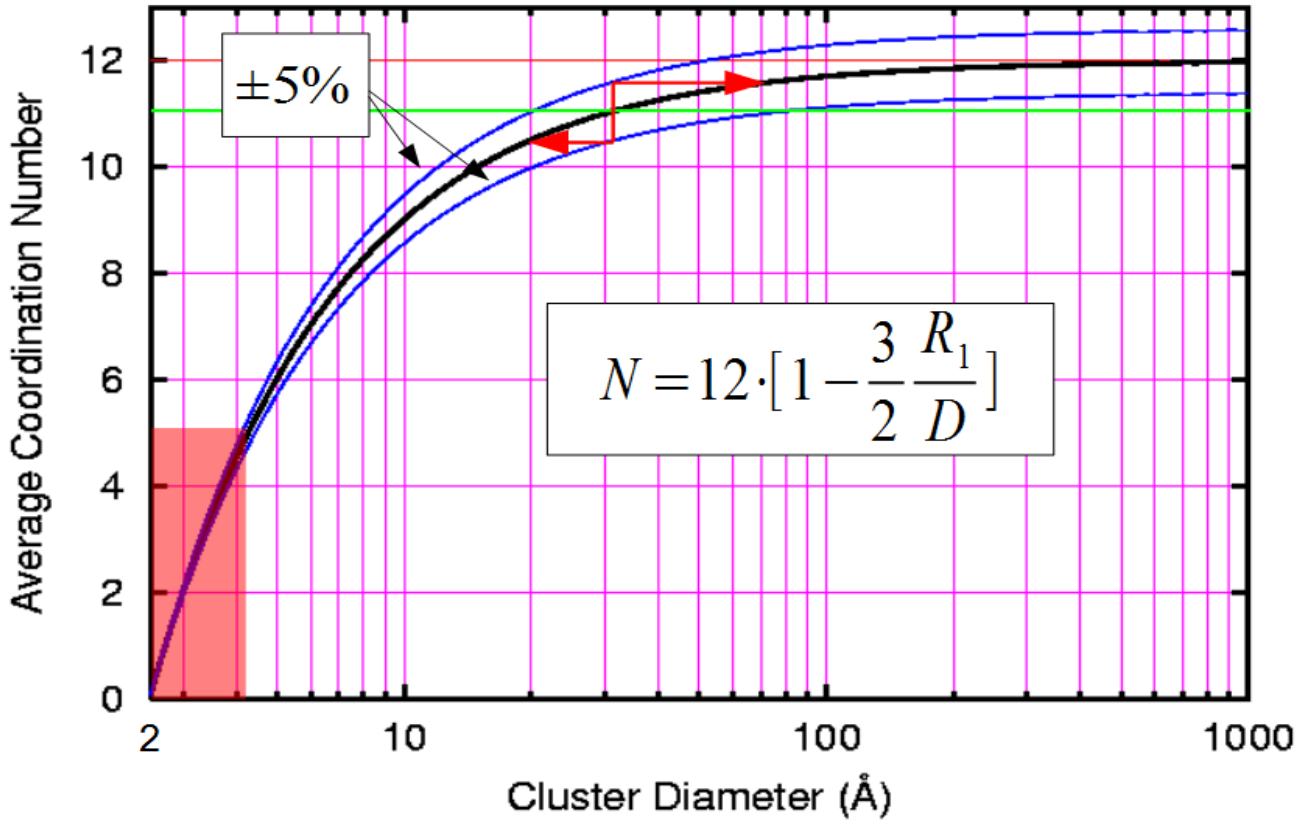

Pt-Pd Bimetallic nanoparticles for NH_4BH_3 hydrolysis

Renewable energy sources intermittently produce electricity

Other renewable sources

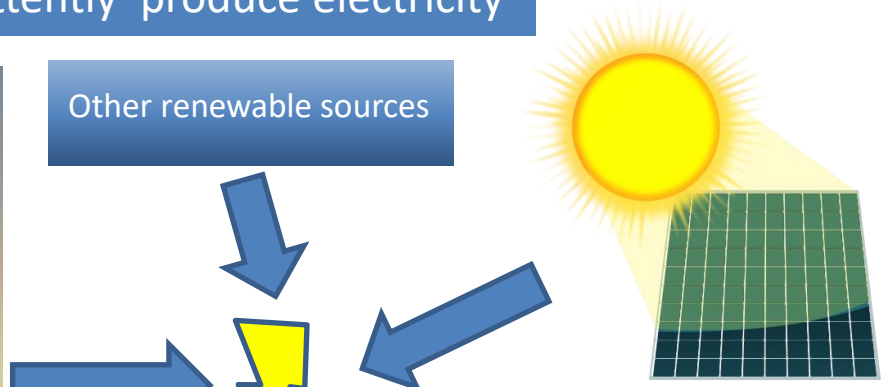

$H_{2(g)}$

H_2 Storage?

1 NH_4BH_3 solid

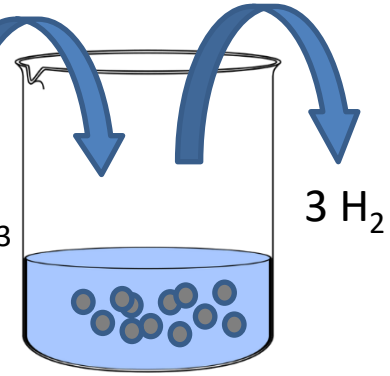

3 H_2

$$NH_3BH_{3\,(aq)} + 4H_2O_{(l)} \rightleftharpoons NH_4^+{}_{(aq)} + B(OH)_4^-{}_{(aq)} + 3H_{2\,(g)}$$

Monai et al., Appl. Catal. B-Environ., 2018, 236, 88-98

Pt-Pd Bimetallic nanoparticles

PreRed nanoparticles

K_2PdCl_4 + Pt NPs + MUA + $NaBH_4$ $\xrightarrow{H_2O/Acetone}$

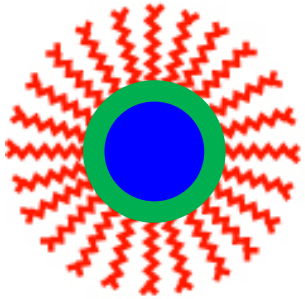

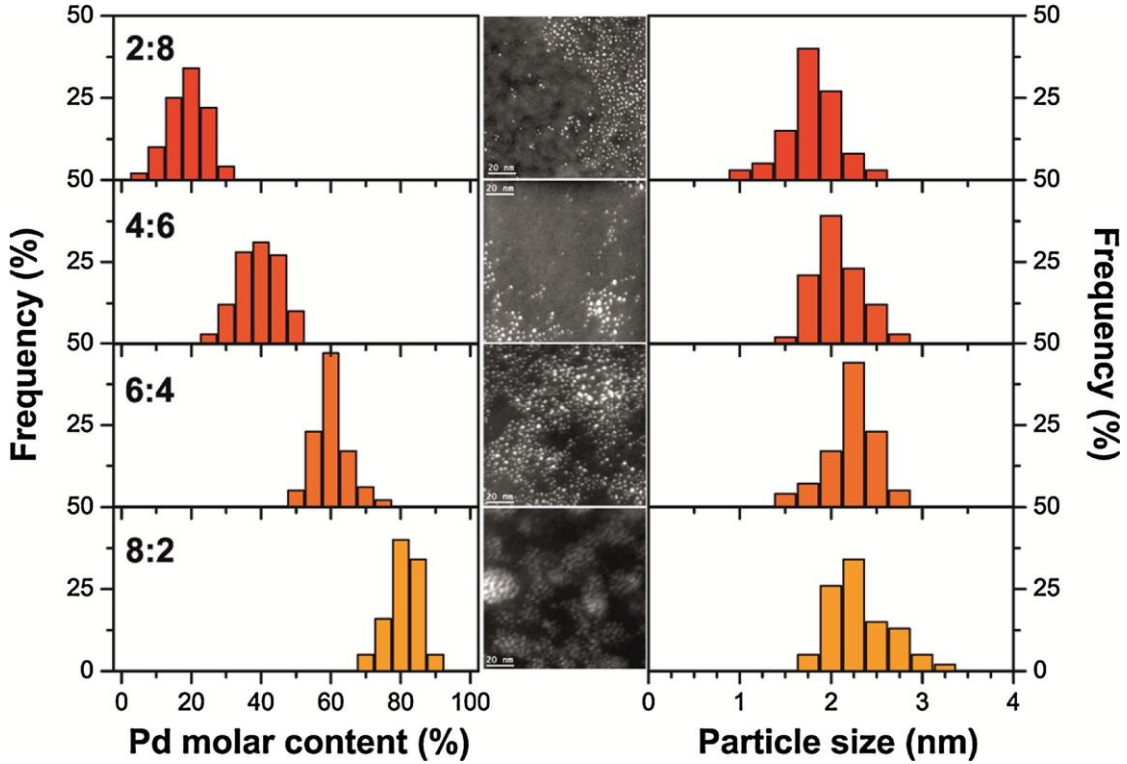

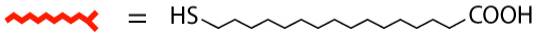

11-Mercaptoundecanoic acid

Monai et al., Appl. Catal. B-Environ., 2018, 236, 88-98

PreRed	
%Pd	N(Pt-Pt)
20	5.1(4)
40	6.1(9)
60	4.2(4)
80	5.6(5)
Average	5.3

CubeOctahedron

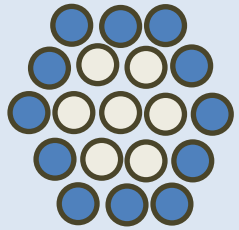

Pt (grey) => CN = 5.4 (Pt-Pt)
Pd (blue) => fully cover Pt

Pd/Pt = 80%

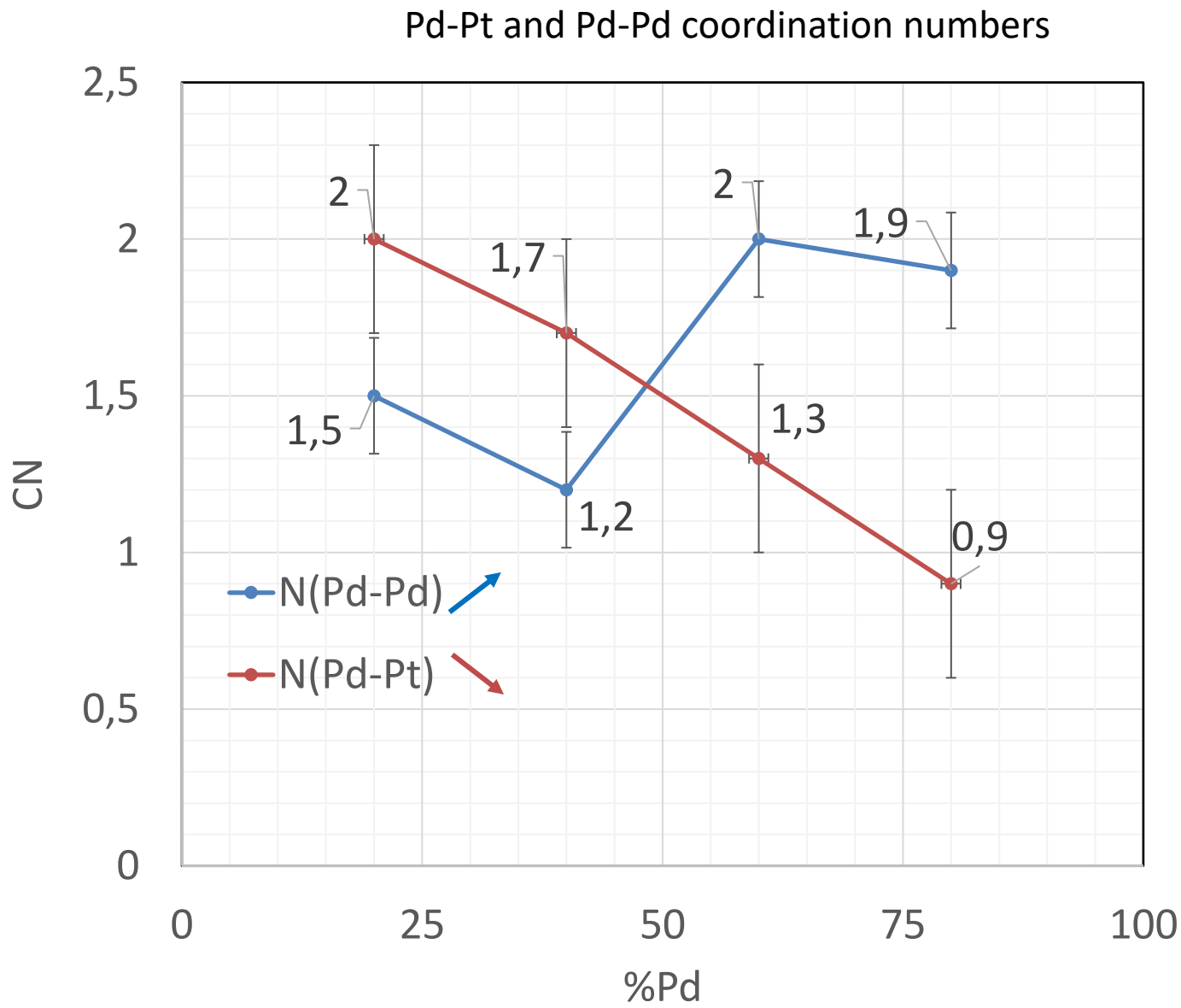

Activity structure relationship

CubeOctahedron

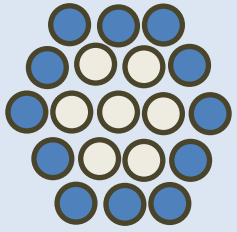

Pt (grey) => CN = 5.4 (Pt-Pt)
Pd (blue) => fully cover Pt

Pd/Pt = 80%

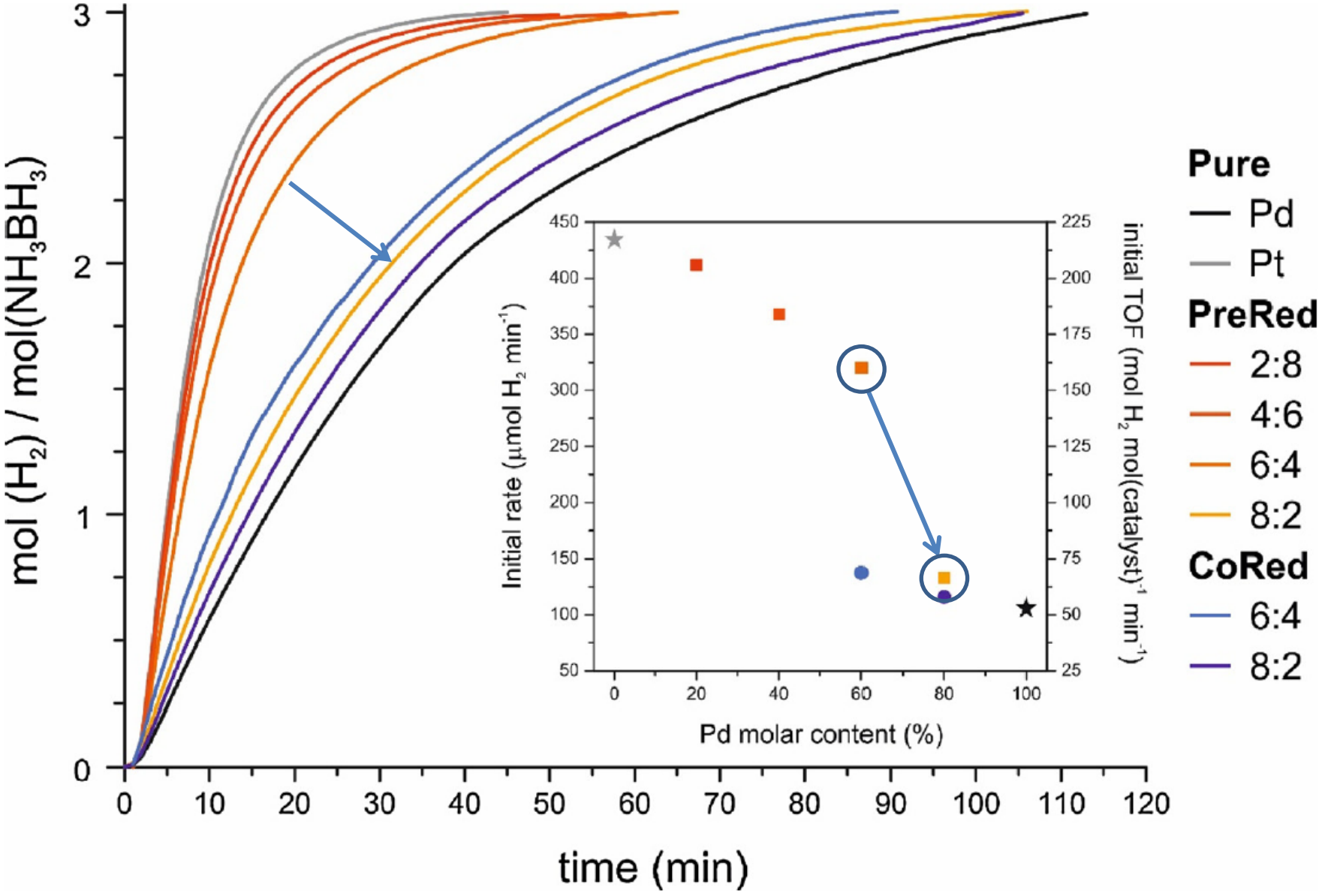

H_2 evolution at 20°C in NaOH 100mM Catalyst/AB=0.001

To be SAC or not to be ?

CO_2 reduction over atomically dispersed Me-N-C

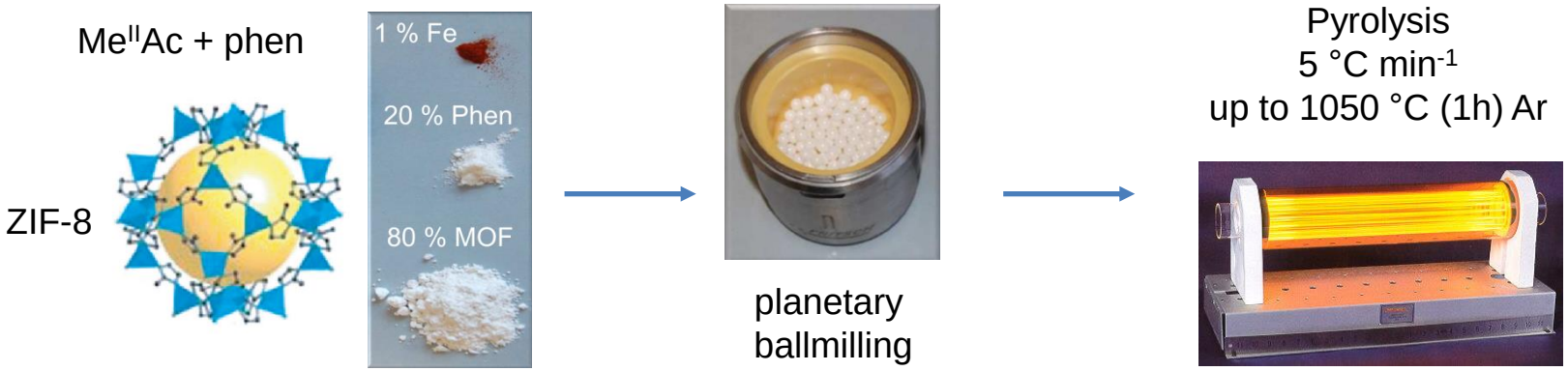

As prepared

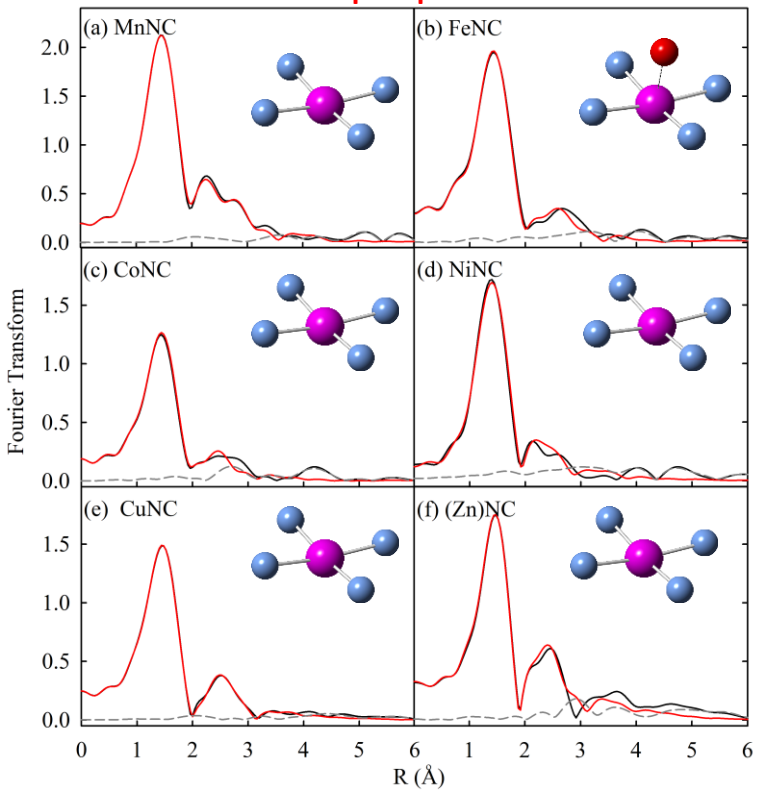

Synthesis may be more generalized

EXAFS analysis confirms the atomically-dispersed nature of Me-N-C :

- First shell peak at ~ 1.5 Å assigned to Me-N(C,O)
- Second shell peaks at 2-3 Å assigned to Me-C(N,O)
- Absence of metal signal due to metal clusters

CO_2 reduction over atomically dispersed Cu-N-C

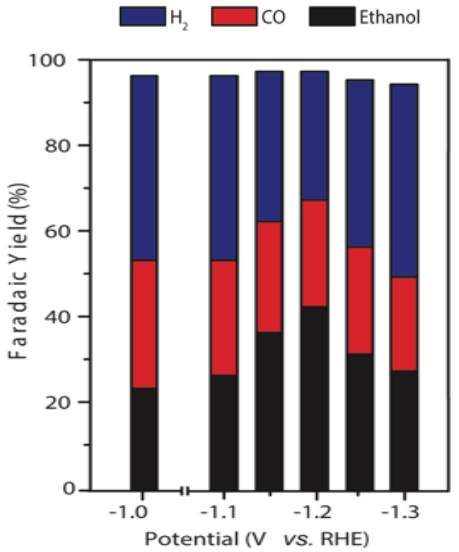

Faradaic yields in 0.1 M CsHCO3

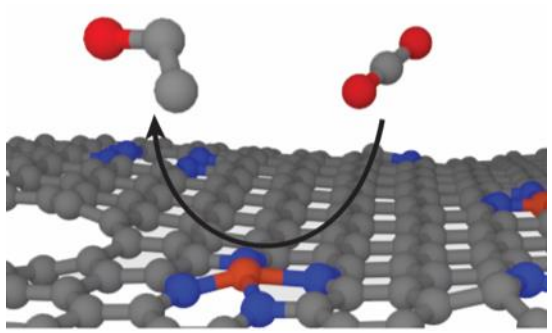

CO_2 electroreduction to ethanol

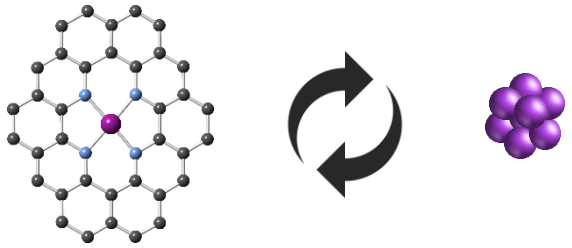

Pre-electrolysis -1.2V

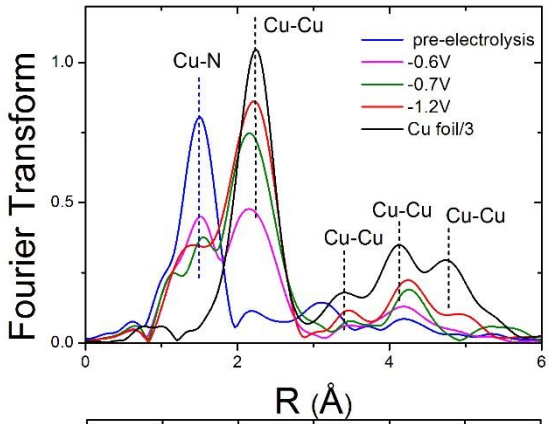

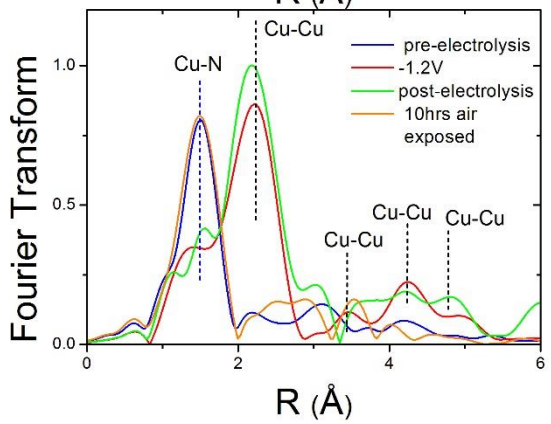

Reversible switching between CuN_4 sites and Cu nanoparticles, that are likely to be the catalytically active species at low potential

D. Karapinar […] Andrea Zitolo, F. Jaouen, V. Mougel, M. Fontecave *Angewandte Chemie Int. Ed*. **2019**, 58(42), 15098-15103

CO_2 reduction over atomically dispersed Cu-N-C

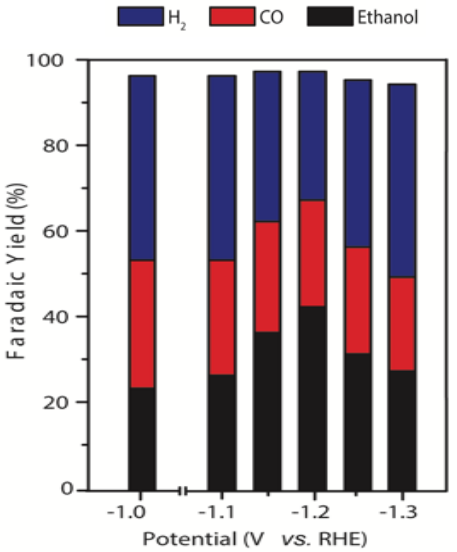

Faradaic yields in 0.1 M CsHCO3

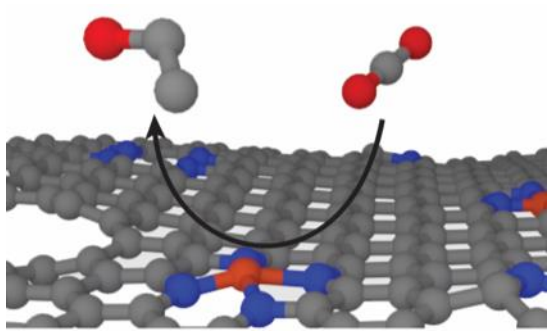

CO_2 electroreduction to ethanol

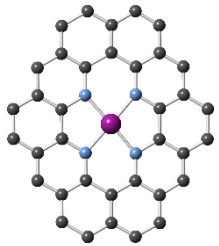

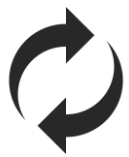

Active phase

Pre-electrolysis -1.2V

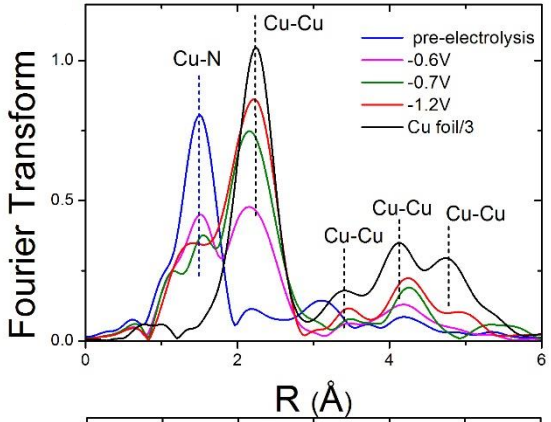

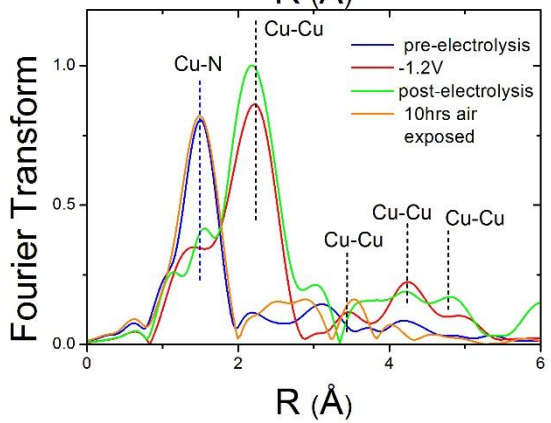

Estimated* NPs size: 0.47±0.04 nm

*Borowski equation (*J. Phys. IV France.* **1997**, *7*, C2-259--C252-260)

Conclusion: Only in situ measurements may provide an answer.

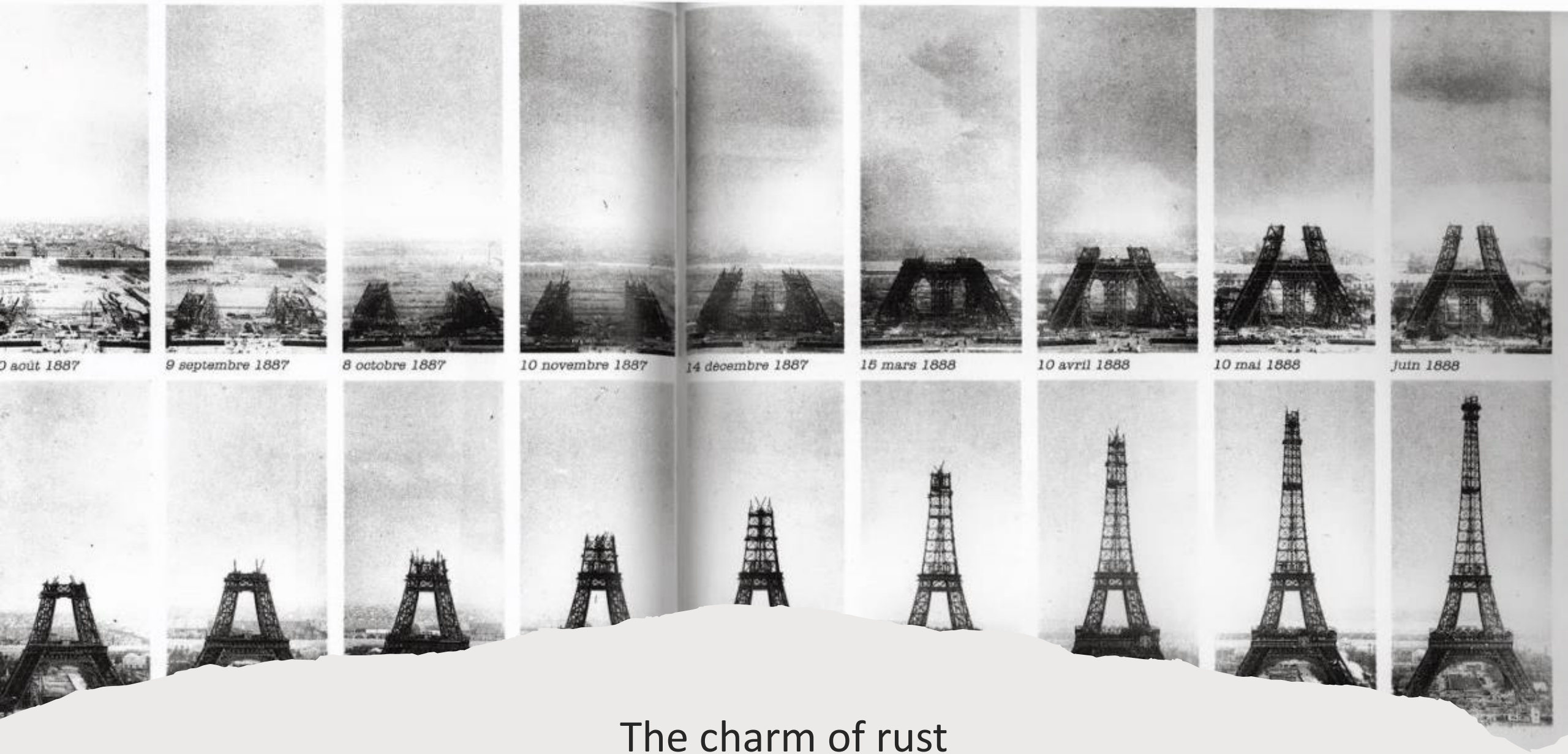

The charm of rust

High-Density Metal Ions in N-Doped Carbon Networks: Powering Fe–N–C Catalyst Efficiency in the Oxygen Reduction Reaction.

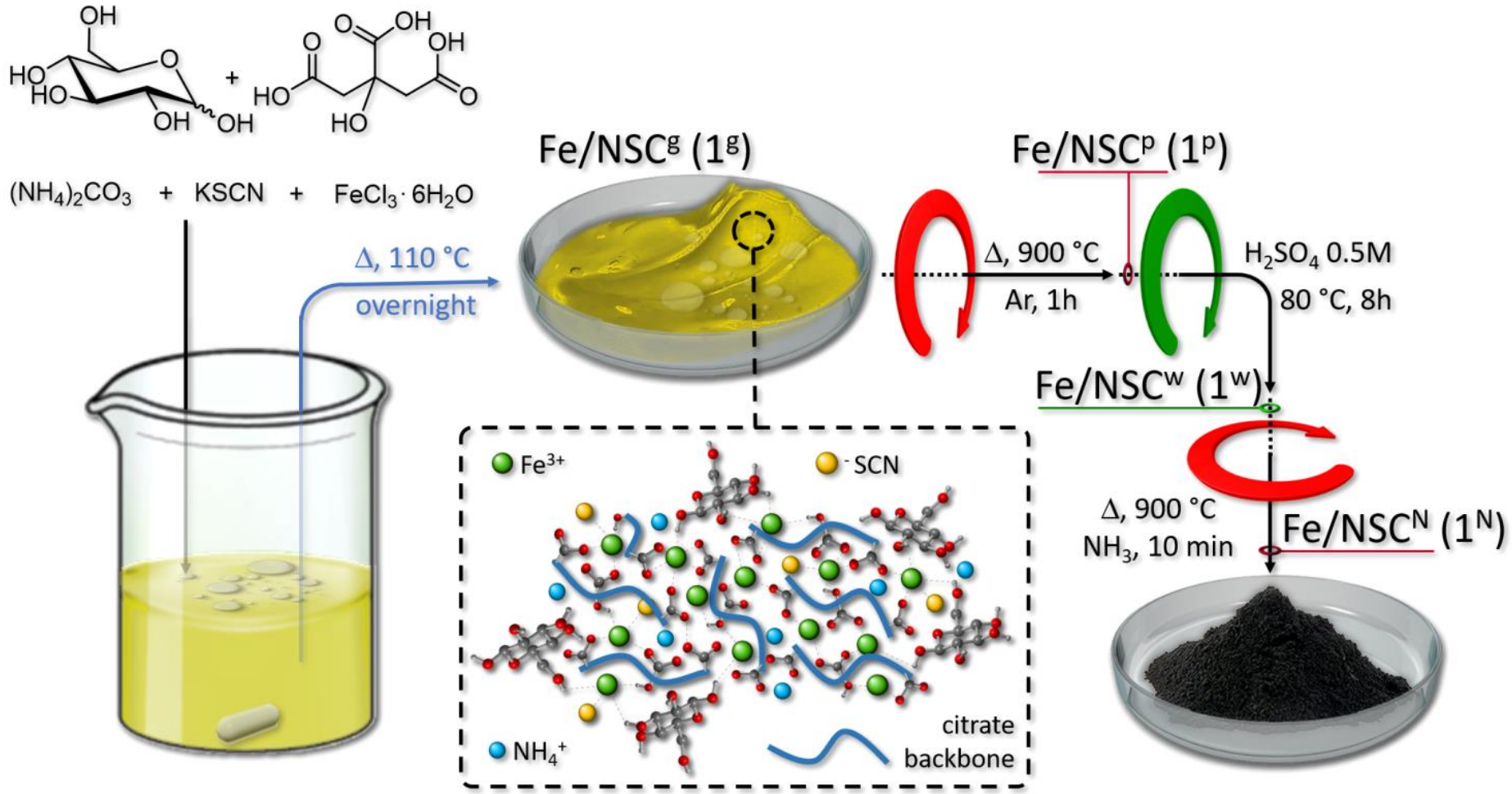

Zhang, X., L. Truong-Phuoc, X. Liao, G. Tuci, E. Fonda, V. Papaefthymiou, S. Zafeiratos, G. Giambastiani, S. Pronkin and C. Pham-Huu (2021). ACS Catalysis **11**(14): 8915-8928.

Ar annealed

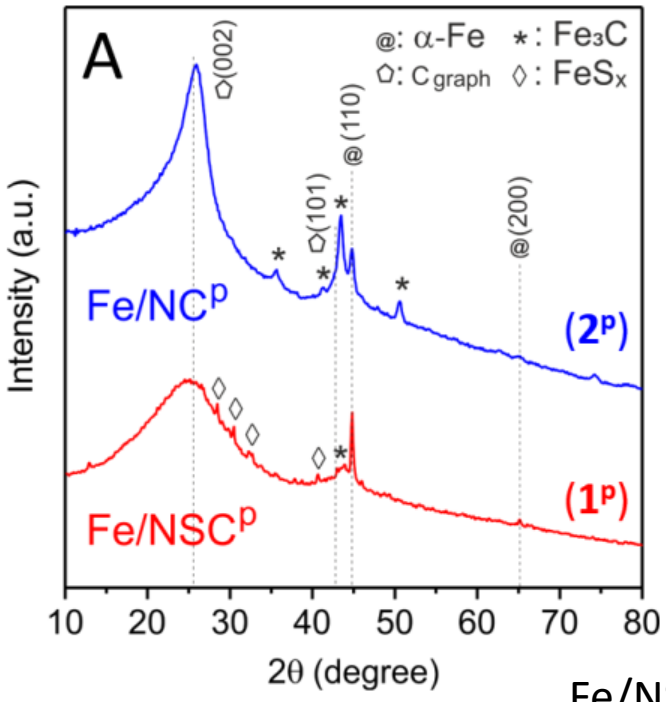

Acid washed

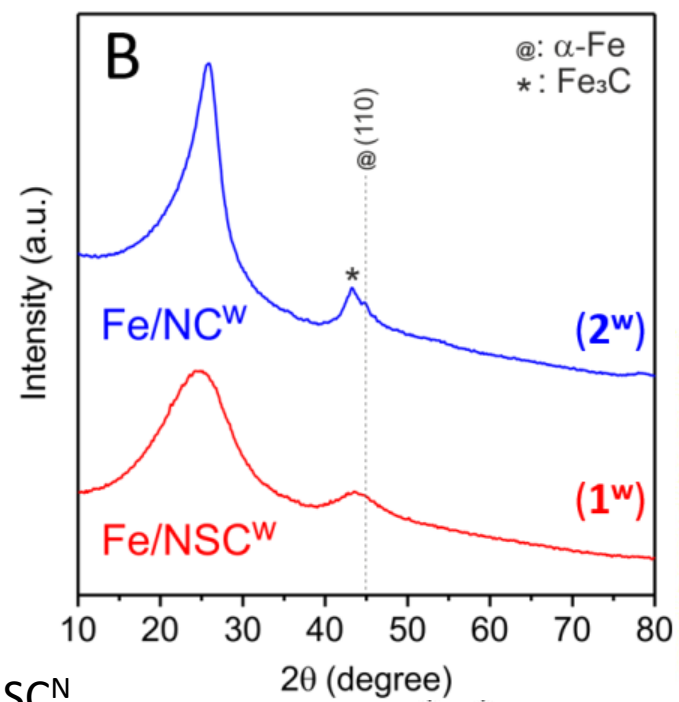

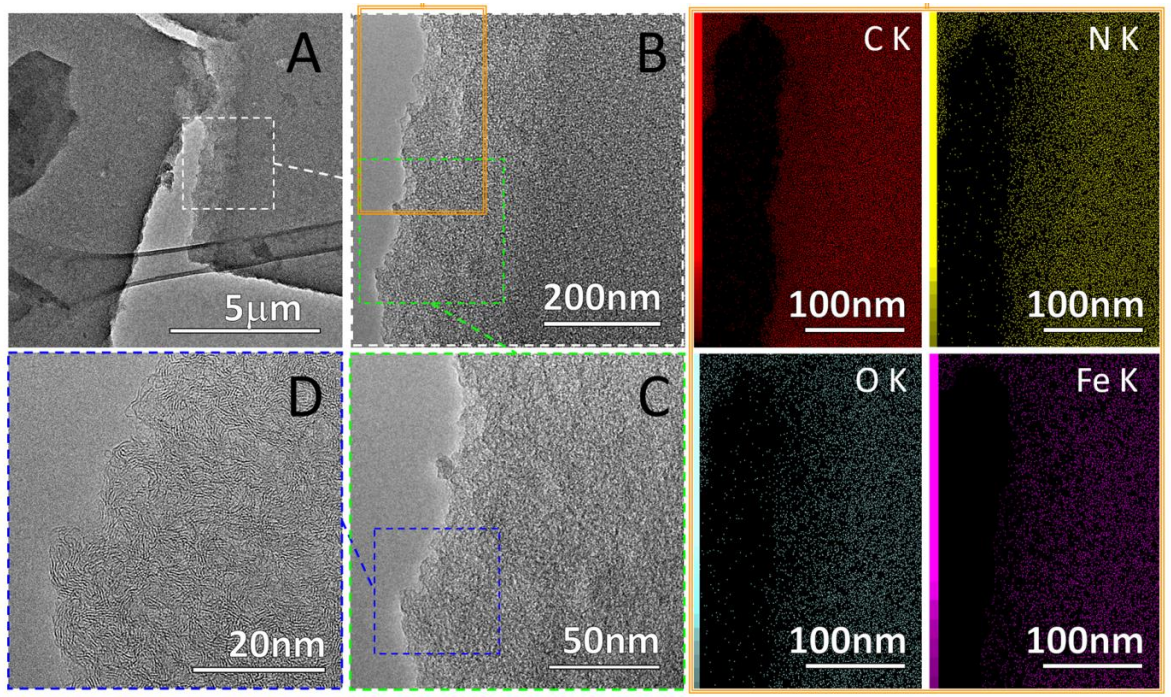

Fe/NSC^{N}

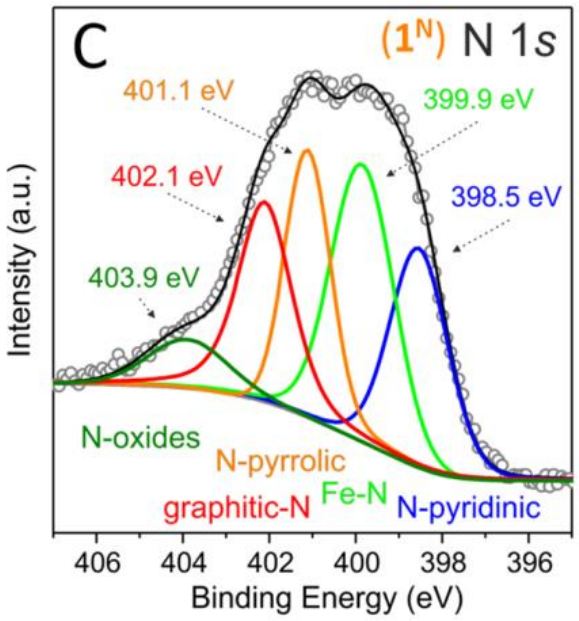

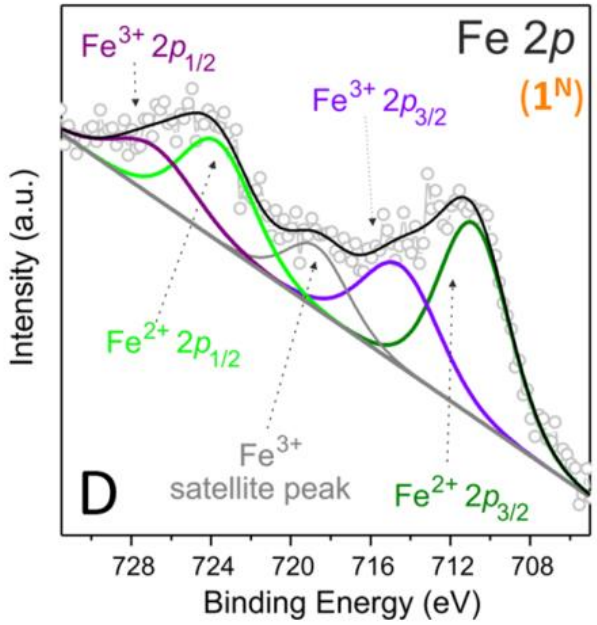

XRD: adding KSCN less particles are formed remaining are all washed out.

HR-TEM : no particles detected in Fe/NSC^{Washed}

XPS:

→ Fe2+ and Fe3+ detected

→Fe-N detected

So far so good… but is it a SAC ?

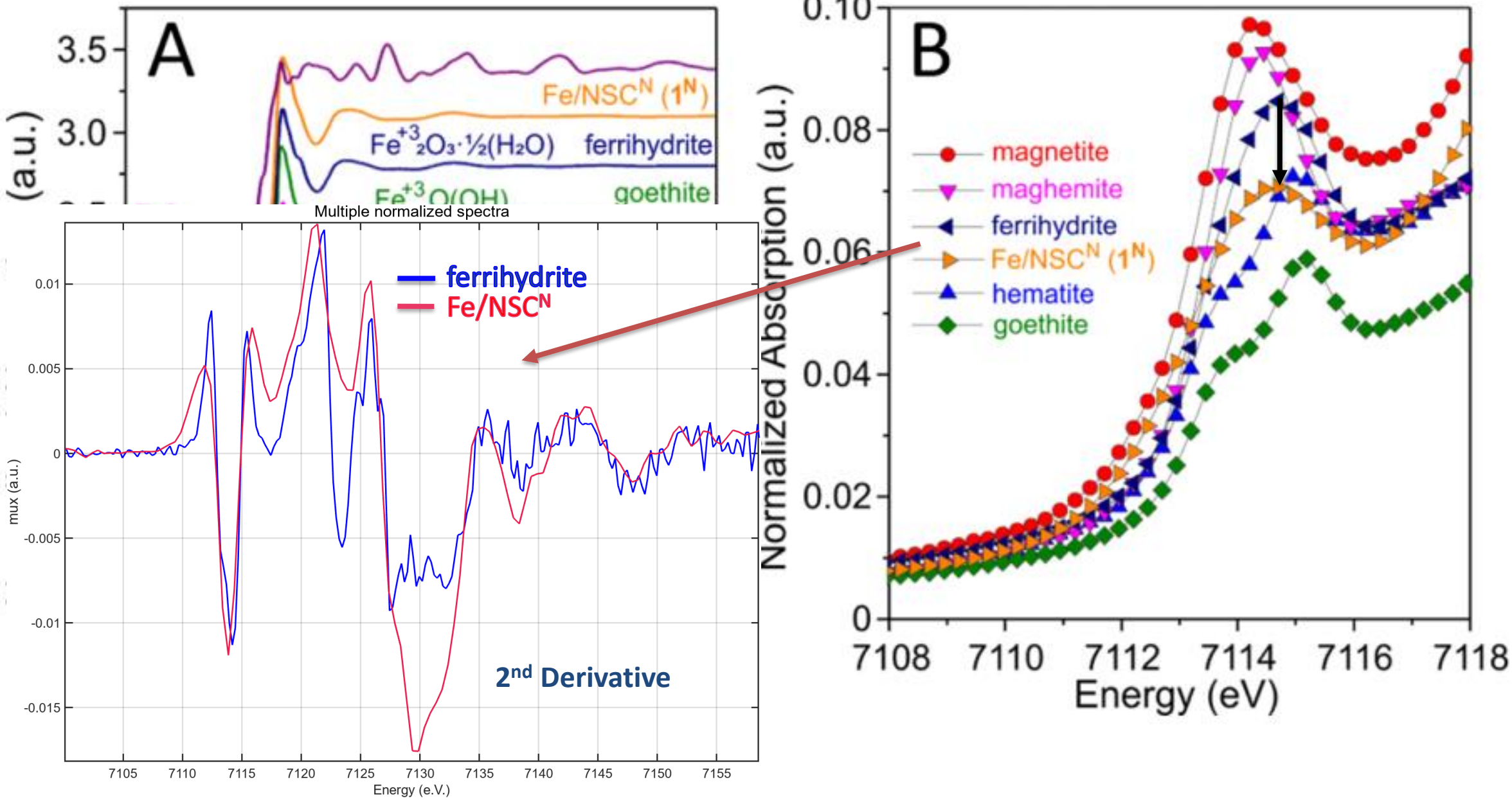
A
3.5
3.0
(a.u.)
Fe/NSC^{N} (1^{N})
$Fe^{+3}_2O_3 \cdot ½(H_2O)$ ferrihydrite
$Fe^{+3}O(OH)$ goethite
Multiple normalized spectra
ferrihydrite
Fe/NSC^{N}
2nd Derivative
mux (a.u.)
0.01
0.005
0
-0.005
-0.01
-0.015
7105
7110
7115
7120
7125
7130
7135
7140
7145
7150
7155
Energy (e.V.)
B
Normalized Absorption (a.u.)
0.10
0.08
0.06
0.04
0.02
0
magnetite
maghemite
ferrihydrite
Fe/NSC^{N} (1^{N})
hematite
goethite
7108
7110
7112
7114
7116
7118
Energy (eV)

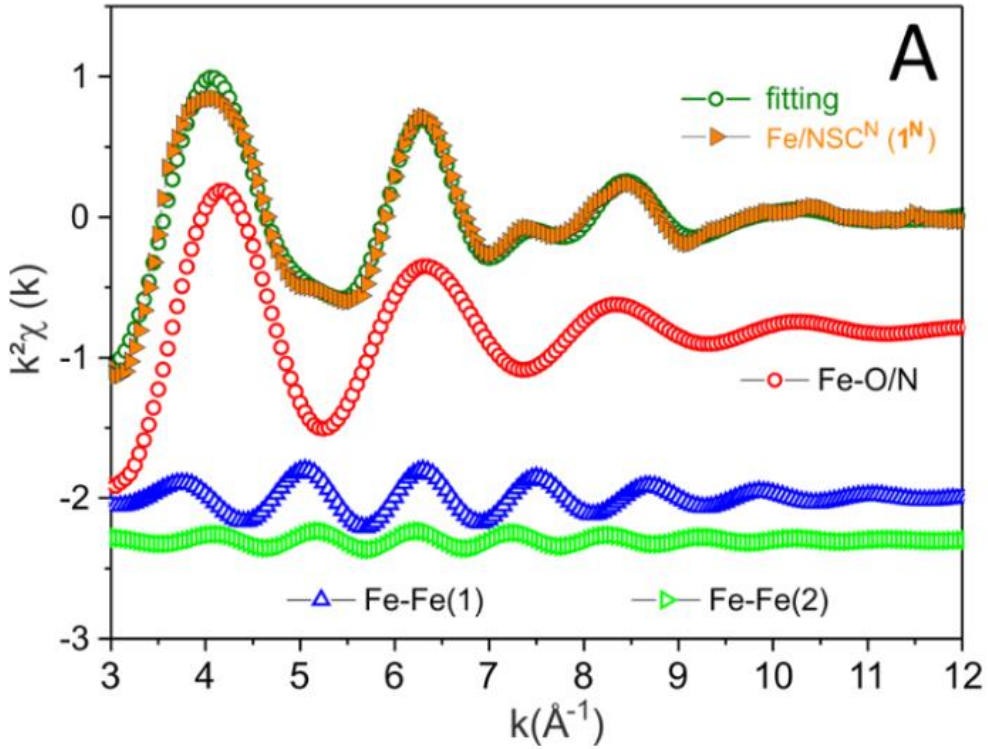

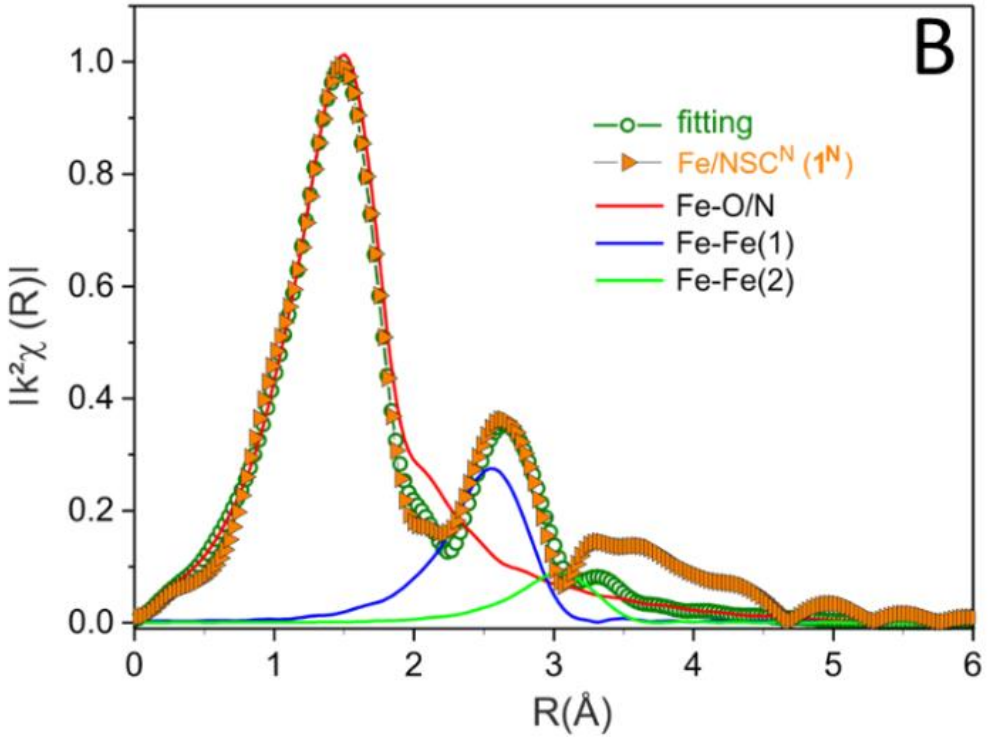

path	coord. numb.	R (Å)[a]	σ^2 (10^{-2} Å^2)[b]	ΔE_0 (eV)[c]	R-factor[d]
Fe–O(N)	6.2 (6)	1.957 (7)	1.2 (1)	−5 (1)	0.007
Fe–Fe (1)	1.3 (3)	3.00 (1)			
Fe–Fe (2)	1.6 (4)	3.45 (2)			

→ SAC anymore ?

An inspiring comparison:

Operando spectroscopy study of the carbon dioxide electro-reduction by iron species on nitrogen-doped carbon.

EXAFS
XPS
HAADF STEM

Validate Fe-N interaction

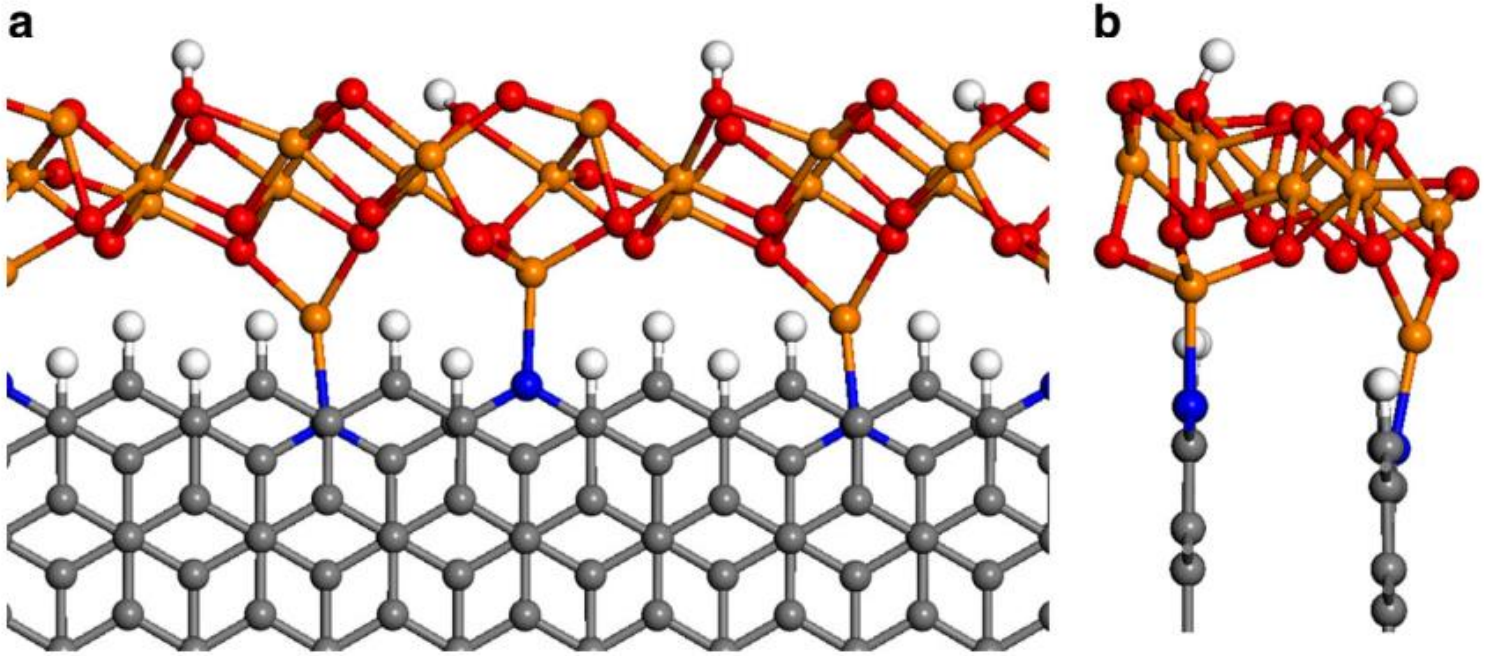

Fig. 5 Model of the *Fh*-FeOOH/N-C interface. **a** Top and **b** lateral views of the DFT + U-relaxed geometry of ferrihydrite nanostructures decorating the N-doped graphitic zigzag edges. Color code: C = gray, H = white, N = blue, Fe = orange, O = red

Genovese, C., M. E. Schuster, E. K. Gibson, D. Gianolio, V. Posligua, R. Grau-Crespo, G. Cibin, P. P. Wells, D. Garai, V. Solokha, S. Krick Calderon, J. J. Velasco-Velez, C. Ampelli, S. Perathoner, G. Held, G. Centi and R. Arrigo (2018). Nature Communications **9**(1): 935.

Summary

XAS ➔ Fe in Fh FeOOH

XPS ➔Fe-N

TEM ➔undetected Fh flakes

XRD/XPS➔KSCN inihibits FexC growth

Fh FeOOH are highly stable (cycles)

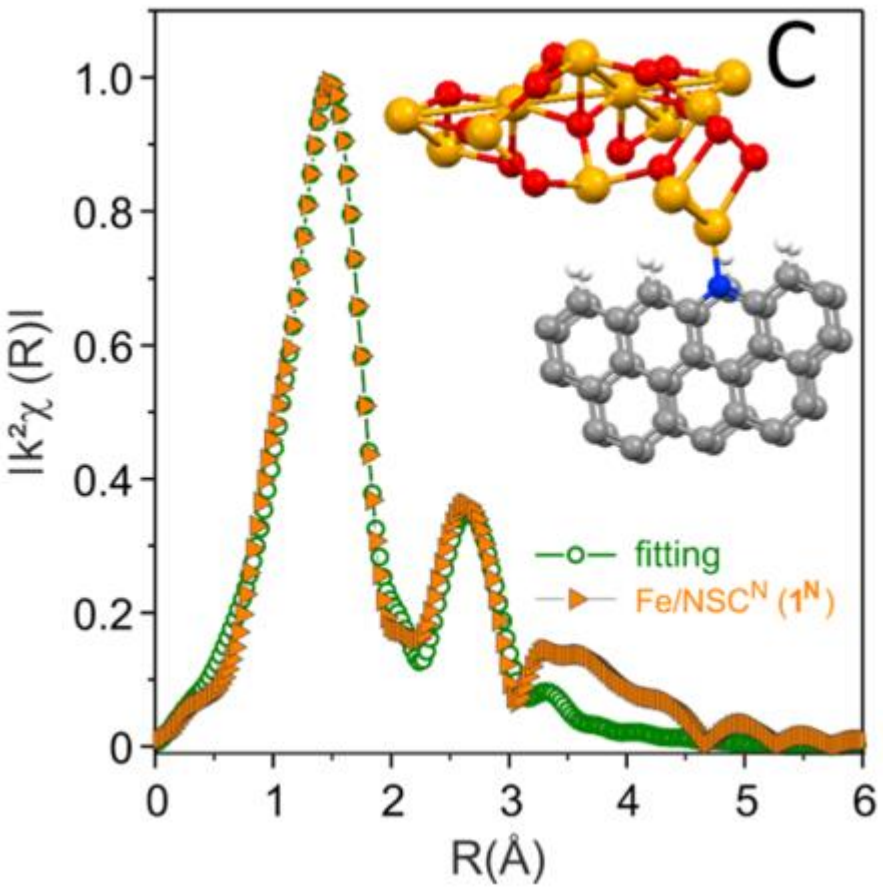

Conclusions

Most abundant Fe(III) species dominates XAFS signal

Anchoring and activities may be related to Fe-N in Fe/NSC^{N} only by a plethora of techniques and indirect evidences.

Without XAFS Fh FeOOH could pass undetected

Acknowledgments

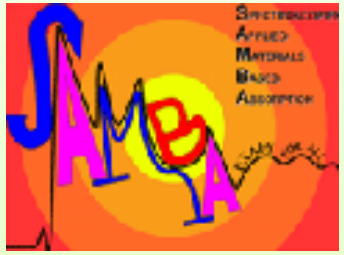

Andrea Zitolo
Guillaume Alizon
Anastassiya Khan
Gautier Landrot

Stephanie Blanchandin
Karine Chaouchi

SOLEIL SYNCHROTRON

anr agence nationale de la recherche

mee

Prof. Paolo Fornasiero
Prof. Tiziano Montini

ICGM Institut Charles Gerhardt Montpellier

Frédéric Jaouen
Tzonka Mineva
Lorenzo Stievano
Moulay-Thar Sougrati

iCCOM Istituto di Chimica dei Composti Organometallici
Consiglio Nazionale delle Ricerche

Dr. Giuliano Giambastiani